arXiv:hep-ph/0409317v2 9 Dec 2004

BNL-HET-04/17
December, 2004

Final State Interactions in Hadronic B Decays

Hai-Yang Cheng,[1] **Chun-Khiang Chua**[1] **and Amarjit Soni**[2]

[1] Institute of Physics, Academia Sinica
Taipei, Taiwan 115, Republic of China

[2] Physics Department, Brookhaven National Laboratory
Upton, New York 11973

Abstract

There exist many experimental indications that final-state interactions (FSIs) may play a prominent role not only in charmful B decays but also in charmless B ones. We examine the final-state rescattering effects on the hadronic B decay rates and their impact on direct CP violation. The color-suppressed neutral modes such as $B^0 \to D^0\pi^0, \pi^0\pi^0, \rho^0\pi^0, K^0\pi^0$ can be substantially enhanced by long-distance rescattering effects. The direct CP-violating partial rate asymmetries in charmless B decays to $\pi\pi/\pi K$ and $\rho\pi$ are significantly affected by final-state rescattering and their signs are generally different from that predicted by the short-distance approach. For example, direct CP asymmetry in $B^0 \to \rho^0\pi^0$ is increased to around 60% due to final state rescattering effects whereas the short-distance picture gives about 1%. Evidence of direct CP violation in the decay $\overline{B}^0 \to K^-\pi^+$ is now established, while the combined BaBar and Belle measurements of $\overline{B}^0 \to \rho^\pm\pi^\mp$ imply a 3.6σ direct CP asymmetry in the $\rho^+\pi^-$ mode. Our predictions for CP violation agree with experiment in both magnitude and sign, whereas the QCD factorization predictions (especially for $\rho^+\pi^-$) seem to have some difficulty with the data. Direct CP violation in the decay $B^- \to \pi^-\pi^0$ is very small ($\lesssim 1\%$) in the Standard Model even after the inclusion of FSIs. Its measurement will provide a nice way to search for New Physics as in the Standard Model QCD penguins cannot contribute (except by isospin violation). Current data on πK modes seem to violate the isospin sum rule relation, suggesting the presence of electroweak penguin contributions. We have also investigated whether a large transverse polarization in $B \to \phi K^*$ can arise from the final-state rescattering of $D^{(*)}\bar{D}_s^{(*)}$ into ϕK^*. While the longitudinal polarization fraction can be reduced significantly from short-distance predictions due to such FSI effects, no sizable perpendicular polarization is found owing mainly to the large cancellations occurring in the processes $\overline{B} \to D_s^*\bar{D} \to \phi\overline{K}^*$ and $\overline{B} \to D_s\bar{D}^* \to \phi\overline{K}^*$ and this can be understood as a consequence of CP and SU(3) [CPS] symmetry. To fully account for the polarization anomaly (especially the perpendicular polarization) observed in $B \to \phi K^*$, FSI from other states or other mechanism, e.g. the penguin-induced annihilation, may have to be invoked. Our conclusion is that the small value of the longitudinal polarization in VV modes cannot be regarded as a clean signal for New Physics.

I. INTRODUCTION

The importance of final-state interactions (FSIs) has long been recognized in hadronic charm decays since some resonances are known to exist at energies close to the mass of the charmed meson. As for hadronic B decays, the general folklore is that FSIs are expected to play only a minor role there as the energy release in the energetic B decay is so large that the final-state particles are moving fast and hence they do not have adequate time for getting involved in final-state rescattering. However, from the data accumulated at B factories and at CLEO, there are growing indications that soft final-state rescattering effects do play an essential role in B physics.

Some possible hints at FSIs in the B sector are:

1. There exist some decays that do not receive any factorizable contributions, for example $B \to K\chi_{0c}$, owing to the vanishing matrix element of the $(V-A)$ current, $\langle \chi_{0c}|\bar{c}\gamma_\mu(1-\gamma_5)c|0\rangle = 0$. Experimentally, it was reported by both Belle [1] and BaBar [2] that this decay mode has a sizable branching ratio, of order $(2 \sim 6) \times 10^{-4}$. This implies that the nonfactorizable correction is important and/or the rescattering effect is sizable. Studies based on the light-cone sum rule approach indicate that nonfactorizable contributions to $B \to \chi_{c0}K$ due to soft gluon exchanges is too small to accommodate the data [3, 4]. In contrast, it has been shown that the rescattering effect from the intermediate charmed mesons is able to reproduce the observed large branching ratio [5].

2. The color-suppressed modes $\overline{B}^0 \to D^{(*)0}\pi^0$ have been measured by Belle [6], CLEO [7] and BaBar [8]. Their branching ratios are all significantly larger than theoretical expectations based on naive factorization. When combined with the color-allowed $\overline{B} \to D^{(*)}\pi$ decays, it indicates non-vanishing relative strong phases among various $\overline{B} \to D^{(*)}\pi$ decay amplitudes. Denoting $\mathcal{T}$ and $\mathcal{C}$ as the color-allowed tree amplitude and color-suppressed W-emission amplitude, respectively, it is found that $\mathcal{C}/\mathcal{T} \sim 0.45\exp(\pm i60^\circ)$ (see e.g. [9]), showing a non-trivial relative strong phase between $\mathcal{C}$ and $\mathcal{T}$ amplitudes. The large magnitude and phase of $\mathcal{C}/\mathcal{T}$ compared to naive expectation implies the importance of long-distance FSI contributions to the color-suppressed internal W-emission via final-state rescattering of the color-allowed tree amplitude.

3. A model independent analysis of charmless B decay data based on the topological quark diagrammatic approach yields a larger value of $|\mathcal{C}/\mathcal{T}|$ and a large strong relative phase between the $\mathcal{C}$ and $\mathcal{T}$ amplitudes [10]. For example, one of the fits in [10] leads to $\mathcal{C}/\mathcal{T} = (0.46^{+0.43}_{-0.30})\exp([-i(94^{+43}_{-52})]^\circ$, which is indeed consistent with the result inferred from $B \to D\pi$ decays. This means that FSIs in charmless B decays are as important as in $B \to D\pi$ ones. The presence of a large color-suppressed amplitude is somewhat a surprise from the current model calculations such as those in the QCD factorization approach and most likely indicates a prominent role for final-state rescattering.

4. Both BaBar [11] and Belle [12] have reported a sizable branching ratio of order 2×10^{-6} for the decay $B^0 \to \pi^0\pi^0$. This cannot be explained by either QCD factorization or the PQCD

approach and it again calls for a possible rescattering effect to induce $\pi^0\pi^0$. Likewise, the color-suppressed decay $B^0 \to \rho^0\pi^0$ with the branching ratio $(1.9 \pm 1.2) \times 10^{-6}$ averaged from the Belle and BaBar measurements (see Table V) is substantially higher than the prediction based on PQCD [13] or the short-distance approach. Clearly, FSI is one of the prominent candidates responsible for this huge enhancement.

5. Direct CP violation in the decay $B^0 \to K^+\pi^-$ with the magnitude $\mathcal{A}_{K\pi} = -0.133 \pm 0.030 \pm 0.009$ at 4.2σ was recently announced by BaBar [14], which agrees with the previous Belle measurement of $\mathcal{A}_{K\pi} = -0.088 \pm 0.035 \pm 0.013$ at 2.4σ based on a $140\,\text{fb}^{-1}$ data sample [15]. A further evidence of this direct CP violation at 3.9σ was just reported by Belle with $253\,\text{fb}^{-1}$ of data [16]. In the calculation of QCD factorization [17, 18], the predicted CP asymmetry $\mathcal{A}_{K\pi} = (4.5^{+9.1}_{-9.9})\%$ is apparently in conflict with experiment. It is conceivable that FSIs via rescattering will modify the prediction based on the short-distance interactions. Likewise, a large direct CP asymmetry in the decay $B^0 \to \pi^+\pi^-$ was reported by Belle [19], but it has not been confirmed by BaBar [20]. The weighted average of Belle and BaBar gives $\mathcal{A}_{\pi\pi} = 0.31 \pm 0.24$ [21] with the PDG scale factor of $S = 2.2$ on the error. Again, the central value of the QCD factorization prediction [18] has a sign opposite to the world average.

6. Under the factorization approach, the color-suppressed mode $\overline{B}^0 \to D_s^+K^-$ can only proceed via W-exchange. Its sizable branching ratio of order 4×10^{-5} observed by Belle [22] and BaBar [23] will need a large final-state rescattering contribution if the short-distance W-exchange effect is indeed small according to the existing model calculations.

7. The measured longitudinal fractions for $B \to \phi K^*$ by both BaBar [24] and Belle [25] are close to 50%. This is in sharp contrast to the general argument that factorizable amplitudes in B decays to light vector meson pairs give a longitudinal polarization satisfying the scaling law: $1 - f_L = \mathcal{O}(1/m_b^2)$. [1] This law remains formally true even when nonfactorizable graphs are included in QCD factorization. Therefore, in order to obtain a large transverse polarization in $B \to \phi K^*$, this scaling law valid at short-distance interactions must be violated. The effect of long-distance rescattering on this scaling law should be examined.

The presence of FSIs can have interesting impact on the direct CP violation phenomenology. As stressed in [28], traditional discussions have centered around the absorptive part of the penguin graph in $b \to s$ transitions [29] and as a result causes "simple" CP violation; long-distance final state rescattering effects, in general, will lead to a different pattern of CP violation, namely, "compound" CP violation. Predictions of simple CP violation are quite distinct from that of compound CP violation. The sizable CP asymmetry observed in $\overline{B}^0 \to K^-\pi^+$ decays is a strong indication for large direct CP violation driven by long-distance rescattering effects. Final state rescattering phases in B decays are unlikely to be small possibly causing large compound CP-violating partial rate asymmetries in these modes. As shown below, the sign of CP asymmetry can be easily flipped by long-distance rescattering effects. Hence, it is important to explore the compound CP violation.

---

[1] More recently Kagan has suggested that the penguin-induced annihilation can cause an appreciable deviation from this expectation numerically, though the scaling law is still respected *formally* [26, 27]. However, it is difficult to make a reliable estimation of this deviation.

Of course, it is notoriously difficult to study FSI effects in a systematic way as it is nonperturbative in nature. Nevertheless, we can gain some control on rescattering effects by studying them in a phenomenological way. More specifically, FSIs can be modelled as the soft rescattering of certain intermediate two-body hadronic channels, e.g. $B \to D\overline{D} \to \pi\pi$, so that they can be treated as the one-particle-exchange processes at the hadron level. That is, we shall study long-distance rescattering effects by considering one-particle-exchange graphs. As the exchanged particle is not on-shell, form factors must be introduced to render the whole calculation meaningful in the perturbative sense. This approach has been applied to the study of FSIs in charm decays for some time [30, 31]. In the context of B physics, the so-called "charming penguin" contributions to charmless hadronic B decays have been treated as long-distance effects manifesting in the rescattering processes such as $B \to D_s\bar{D} \to K\pi$ [32, 33, 34]. Likewise, the dynamics for final-state interactions is assumed to be dominated by the mixing of the final state with $D^{(*)}\bar{D}^{(*)}$ in [35, 36]. Final-state rescattering effects were also found in B to charmonium final states, e.g. $B^- \to K^-\chi_{c0}$, a process prohibited in the naive factorization approach [5]. Effects of final-state rescattering on $K\pi$ and $\pi\pi$ final states have been discussed extensively in the literature [28, 37, 38].

The approach of modelling FSIs as soft rescattering processes of intermediate two-body states has been criticized on several grounds [39]. First, there are many more intermediate multi-body channels in B decays and systematic cancellations among them are predicted to occur in the heavy quark limit. This effect of cancellation will be missed if only a few intermediate states are taken into account. Second, the hadronic dynamics of multi-body decays is very complicated and in general not under theoretical control. Moreover, the number of channels and the energy release in B decays are large. We wish to stress that the b quark mass ($\sim$ 4.5 GeV) is not very large and far from infinity in reality. The aforementioned cancellation may not occur or may not be very effective for the finite B mass. For intermediate two-body states, we always consider those channels that are quark-mixing-angle most favored so that they give the dominant long-distance contributions. Whether there exist cancellations between two-body and multi-body channels is not known. Following [40], we may assume that two-body $\rightleftharpoons$ n-body rescatterings are negligible either justified from the $1/N_c$ argument [41] or suppressed by large cancellations. We view our treatment of the two-body hadronic model for FSIs as a working tool. We work out the consequences of this tool to see if it is empirically working. If it turns out to be successful, then it will imply the possible dominance of intermediate two-body contributions. In other approaches such as QCD factorization [17], the complicated hadronic B decays in principle can be treated systematically as $1/m_b$ power corrections which vanish in the heavy quark limit. However, one should recognize that unless the coefficients of power corrections are known or calculable in a model independent manner, the short-distance picture without a control of the $1/m_b$ coefficients and without being able to include the effects of FSIs have their limitation as well. When the short-distance scenario is tested against experiment and failings occur such as the many examples mentioned before, then it does not necessarily mean that New Physics has been discovered and an examination of rescattering effects can be helpful.

The layout of the present paper is as follows. In Sec. II we give an overview of the role played by the final-state interactions in hadronic B decays. As a warm-up, we begin in Sec. III with a study of final-state rescattering contributions to $B \to D\pi$ decays which proceed only through tree diagrams. We then proceed to the penguin-dominated $B \to K\pi$ decays in Sec. IV, tree-dominated $B \to \pi\pi$ decays in Sec. V and $B \to \rho\pi$ decays in Sec. VI. Effects of FSIs on the branching ratios and direct CP asymmetries are studied. Sec. VII is devoted to the polarization anomaly discovered recently in $B \to \phi K^*$ decays. Conclusion and discussion are given in Sec. VIII. Appendix A gives some useful formula for the phase-space integration, while the theoretical input parameters employed in the present paper are summarized in Appendix B.

II. FINAL-STATE INTERACTIONS

In the diagrammatic approach, all two-body nonleptonic weak decays of heavy mesons can be expressed in terms of six distinct quark diagrams [42, 43, 44]: $\mathcal{T}$, the color-allowed external W-emission tree diagram; $\mathcal{C}$, the color-suppressed internal W-emission diagram; $\mathcal{E}$, the W-exchange diagram; $\mathcal{A}$, the W-annihilation diagram; $\mathcal{P}$, the penguin diagram; and $\mathcal{V}$, the vertical W-loop diagram. It should be stressed that these quark diagrams are classified according to the topologies of weak interactions with all strong interaction effects included and hence they are *not* Feynman graphs. All quark graphs used in this approach are topological with all the strong interactions included, i.e. gluon lines are included in all possible ways.

As stressed above, topological graphs can provide information on final-state interactions (FSIs). In general, there are several different forms of FSIs: elastic scattering and inelastic scattering such as quark exchange, resonance formation,$\cdots$, etc. Take the decay $\overline{B}^0 \to D^0\pi^0$ as an illustration. The topological amplitudes $\mathcal{C}$, $\mathcal{E}$, $\mathcal{A}$ can receive contributions from the tree amplitude $\mathcal{T}$ of e.g. $\overline{B}^0 \to D^+\pi^-$ via final-state rescattering, as illustrated in Fig. 1: Fig. 1(a) has the same topology as W-exchange, while 1(b) and 1(c) mimic the internal W-emission amplitude $\mathcal{C}$. Therefore, even if the short-distance W-exchange vanishes, a long-distance W-exchange can be induced via inelastic FSIs. Historically, it was first pointed out in [45] that rescattering effects required by unitarity can produce the reaction $D^0 \to \overline{K}^0\phi$, for example, even in the absence of the W-exchange diagram. Then it was shown in [42] that this rescattering diagram belongs to the generic W-exchange topology.

Since FSIs are nonperturbative in nature, in principle it is extremely difficult to calculate their effects. It is customary to evaluate the long-distance W-exchange contribution, Fig. 1(a), at the hadron level manifested as Fig. 2 [30, 31, 46]. Fig. 2(a) shows the resonant amplitude coming from $\overline{B}^0 \to D^+\pi^-$ followed by a s-channel $J^P = 0^+$ particle exchange with the quark content $(c\bar{u})$, which couples to $\overline{D}^0\pi^0$ and $D^+\pi^-$. Fig. 2(b) corresponds to the t-channel contribution with a ρ particle exchange. The relative phase between $\mathcal{T}$ and $\mathcal{C}$ indicates some final-state interactions responsible for this. Figs. 1(b) and 1(c) show that final-state rescattering via quark exchange has the same topology as the color-suppressed internal W-emission amplitude. At the hadron level,

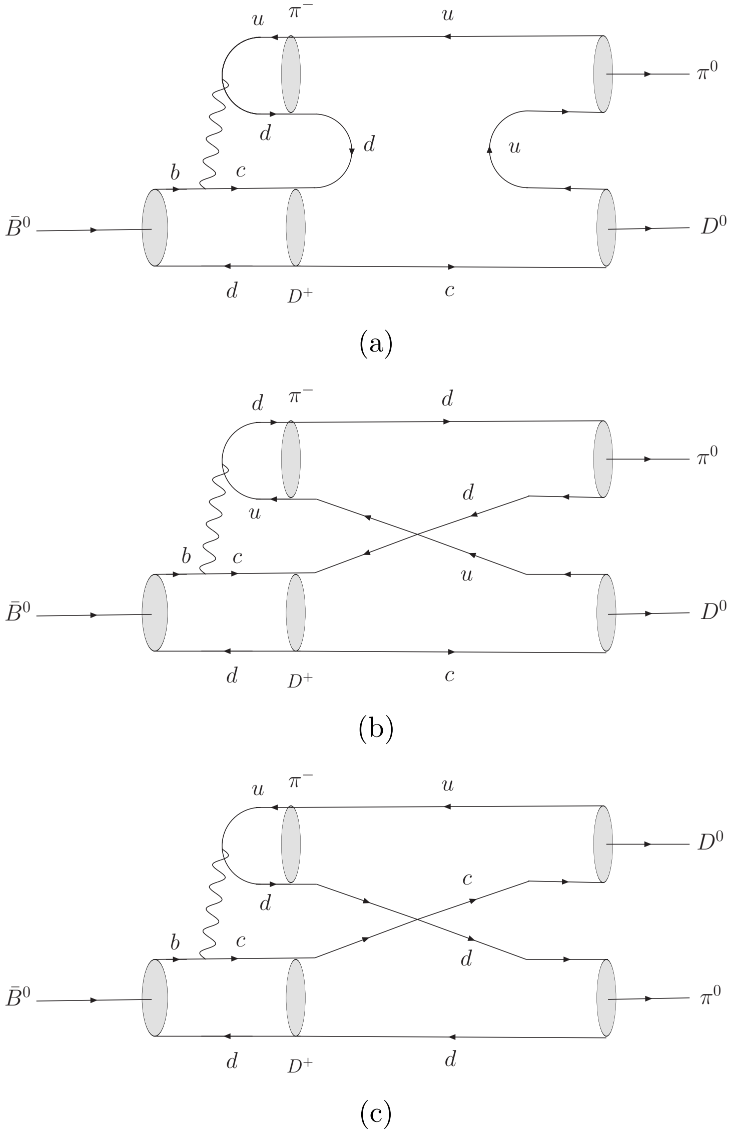

FIG. 1: Contributions to $\overline{B}^0 \to D^0\pi^0$ from the color-allowed weak decay $\overline{B}^0 \to D^+\pi^-$ followed by a resonant-like rescattering (a) and quark exchange (b) and (c). While (a) has the same topology as the W-exchange graph, (b) and (c) mimic the color-suppressed internal W-emission graph.

Figs. 1(b) and 1(c) are manifested in the rescattering processes with one particle exchange in the t channel [30] (see Fig. 3). Note that Figs. 3(a) and 2(b) are the same at the meson level even though at the quark level they correspond to different processes, namely, annihilation and quark exchange, respectively. In contrast, Fig. 3(b) is different than Fig. 3(a) in the context of the t-channel exchanged particle.

For charm decays, it is expected that the long-distance W-exchange is dominated by resonant FSIs as shown in Fig. 2(a). That is, the resonance formation of FSI via $q\bar{q}$ resonances is probably the most important one due to the fact that an abundant spectrum of resonances is known to exist at energies close to the mass of the charmed meson. However, a direct calculation of this diagram

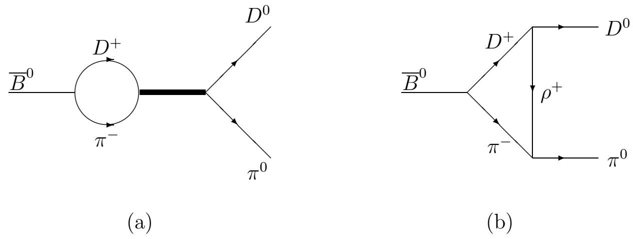

(a) (b)

FIG. 2: Manifestation of Fig. 1(a) as the long-distance s- and t-channel contributions to the W-exchange amplitude in $\overline{B}^0 \to D^0\pi^0$. The thick line in (a) represents a resonance.

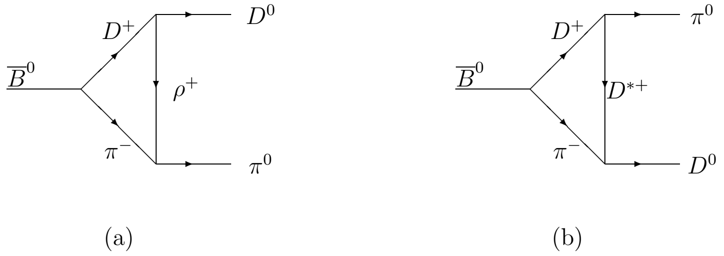

(a) (b)

FIG. 3: Manifestation of Figs. 1(b) and 1(c) as the long-distance t-channel contributions to the color-suppressed internal W-emission amplitude in $\overline{B}^0 \to D^0\pi^0$.

is subject to many theoretical uncertainties. For example, the coupling of the resonance to $D\pi$ states is unknown and the off-shell effects in the chiral loop should be properly addressed [46]. Nevertheless, as emphasized in [47, 48], most of the properties of resonances follow from unitarity alone, without regard to the dynamical mechanism that produces the resonance. Consequently, as shown in [47, 49], the effect of resonance-induced FSIs [Fig. 2(a)] can be described in a model-independent manner in terms of the mass and width of the nearby resonances. It is found that the $\mathcal{E}$ amplitude is modified by resonant FSIs by (see e.g. [49])

$$\mathcal{E} = e + (e^{2i\delta_r} - 1)\left(e + \frac{\mathcal{T}}{3}\right), \tag{2.1}$$

with

$$e^{2i\delta_r} = 1 - i\,\frac{\Gamma}{m_D - m_R + i\Gamma/2}, \tag{2.2}$$

where the reduced W-exchange amplitude $\mathcal{E}$ before resonant FSIs is denoted by e. Therefore, resonance-induced FSIs amount to modifying the W-exchange amplitude and leaving the other quark-diagram amplitudes $\mathcal{T}$ and $\mathcal{C}$ intact. We thus see that even if the short-distance W-exchange vanishes (i.e. $e = 0$), as commonly asserted, a long-distance W-exchange contribution still can be induced from the tree amplitude $\mathcal{T}$ via FSI rescattering in resonance formation.

In B decays, in contrast to D decays, the resonant FSIs will be expected to be suppressed relative to the rescattering effect arising from quark exchange owing to the lack of the existence of resonances at energies close to the B meson mass. This means that one can neglect the s-channel contribution from Fig. 2(a).

As stressed before, the calculation of the meson level Feynman diagrams in Fig. 2 or Fig. 3 involves many theoretical uncertainties. If one naively calculates the diagram, one obtains an answer which does not make sense in the context of perturbation theory since the contributions become so large that perturbation theory is no longer trustworthy. For example, consider the loop contribution to $B^0 \to \pi^+\pi^-$ via the rescattering process $D^+D^- \to \pi^+\pi^-$. Since $B^0 \to \pi^+\pi^-$ is CKM suppressed relative to $B^0 \to D^+D^-$, the loop contribution is larger than the initial $B \to \pi\pi$ amplitude. Because the t-channel exchanged particle is not on-shell, as we shall see later, a form-factor cutoff must be introduced to the vertex to render the whole calculation meaningful.

III. $B \to D\pi$ DECAYS

The color-suppressed decays of $\overline{B}^0$ into $D^{(*)0}\pi^0, D^0\eta, D^0\omega$ and $D^0\rho^0$ have been observed by Belle [6] and $\overline{B}^0$ decays into $D^{(*)0}\pi^0$ have been measured by CLEO [7]. Recently, BaBar [8] has presented the measurements of $\overline{B}^0$ decays into $D^{(*)0}(\pi^0,\eta,\omega)$ and $D^0\eta'$. All measured color-suppressed decays have similar branching ratios with central values between 1.7×10^{-4} and 4.2×10^{-4}. They are all significantly larger than theoretical expectations based on naive factorization. For example, the measurement $\mathcal{B}(\overline{B}^0 \to D^0\pi^0) = 2.5\times10^{-4}$ (see below) is larger than the theoretical prediction, $(0.58 \sim 1.13) \times 10^{-4}$ [9], by a factor of $2 \sim 4$. Moreover, the three $B \to D\pi$ amplitudes form a non-flat triangle, indicating nontrivial relative strong phases between them. In this section we will focus on $B \to D\pi$ decays and illustrate the importance of final-state rescattering effects.

In terms of the quark-diagram topologies $\mathcal{T}$, $\mathcal{C}$ and $\mathcal{E}$, where $\mathcal{T}$ is the color-allowed external W-emission tree amplitude, $\mathcal{C}$, $\mathcal{E}$ are color-suppressed internal W-emission and W-exchange amplitudes, respectively, the $\overline{B} \to D\pi$ amplitudes can be expressed as

$$\begin{aligned} A(\overline{B}^0 \to D^+\pi^-) &= \mathcal{T}+\mathcal{E}, \\ A(B^- \to D^0\pi^-) &= \mathcal{T}+\mathcal{C}, \\ A(\overline{B}^0 \to D^0\pi^0) &= \frac{1}{\sqrt{2}}(-\mathcal{C}+\mathcal{E}), \end{aligned} \tag{3.1}$$

and they satisfy the isospin triangle relation

$$A(\overline{B}^0 \to D^+\pi^-) = \sqrt{2}A(\overline{B}^0 \to D^0\pi^0) + A(B^- \to D^0\pi^-). \tag{3.2}$$

Using the data [50]

$$\begin{aligned} \mathcal{B}(\overline{B}^0 \to D^+\pi^-) &= (2.76 \pm 0.25) \times 10^{-3}, \\ \mathcal{B}(B^- \to D^0\pi^-) &= (4.98 \pm 0.29) \times 10^{-3}, \end{aligned} \tag{3.3}$$

and the world average $\mathcal{B}(\overline{B}^0 \to D^0\pi^0) = (2.5 \pm 0.2) \times 10^{-4}$ from the measurements

$$\mathcal{B}(\overline{B}^0 \to D^0\pi^0) = \begin{cases} (2.9 \pm 0.2 \pm 0.3) \times 10^{-4}, & \text{BaBar [8]} \\ (2.31 \pm 0.12 \pm 0.23) \times 10^{-4}, & \text{Belle [6]} \\ (2.74^{+0.36}_{-0.32} \pm 0.55) \times 10^{-4}, & \text{CLEO [7]} \end{cases} \tag{3.4}$$

we find (only the central values for phase angles are shown here)

$$\left.\frac{\mathcal{C}-\mathcal{E}}{\mathcal{T}+\mathcal{E}}\right|_{D\pi}=(0.41\pm 0.05)\,e^{\pm i53^\circ}, \qquad \left.\frac{\mathcal{C}-\mathcal{E}}{\mathcal{T}+\mathcal{C}}\right|_{D\pi}=(0.29\pm 0.03)\,e^{\pm i38^\circ}, \tag{3.5}$$

where we have used the relation, for example,

$$\cos\theta_{\{\mathcal{C}-\mathcal{E},\mathcal{T}+\mathcal{E}\}}=\frac{\mathcal{B}(\overline{B}^0\to D^+\pi^-)+2\mathcal{B}(\overline{B}^0\to D^0\pi^0)-\frac{\tau(B^0)}{\tau(B^+)}\mathcal{B}(B^-\to D^0\pi^-)}{2\sqrt{\mathcal{B}(\overline{B}^0\to D^+\pi^-)}\sqrt{2\mathcal{B}(\overline{B}^0\to D^0\pi^0)}} \tag{3.6}$$

to extract the strong phases. For the numerical results in Eq. (3.5), we have employed the B meson lifetimes $\tau(B^0)=(1.536\pm 0.014)\times 10^{-12}s$ and $\tau(B^+)=(1.671\pm 0.018)\times 10^{-12}s$ [50].

It is known that in Cabibbo-allowed $D\to PP$ decays, the topological amplitudes $\mathcal{T},\mathcal{C},\mathcal{E}$ can be *individually* extracted from the data with the results [52]

$$\left.\frac{\mathcal{C}}{\mathcal{T}}\right|_{D\to PP}=(0.73\pm 0.05)\,e^{-i152^\circ}, \qquad \left.\frac{\mathcal{E}}{\mathcal{T}}\right|_{D\to PP}=(0.59\pm 0.05)\,e^{i114^\circ}. \tag{3.7}$$

Therefore, in charm decays the color-suppressed amplitude $\mathcal{C}$ is not color suppressed and the W-exchanged amplitude is quite sizable ! The large phase of $\mathcal{E}$ is suggestive of nearby resonance effects. The three amplitudes $\mathcal{T},\mathcal{C}$ and $\mathcal{E}$ in $B\to D\pi$ decays can be individually determined from the measurements of $D\pi$ in conjunction with the data of $D_s^+K^-$ and $D^0\eta$ [51].

In the factorization approach, the short-distance factorizable amplitudes read

$$\begin{aligned}
\mathcal{T}_{\rm SD} &= i\frac{G_F}{\sqrt{2}}\,V_{cb}V_{ud}^*\,a_1(D\pi)(m_B^2-m_D^2)f_\pi F_0^{BD}(m_\pi^2),\\
\mathcal{C}_{\rm SD} &= i\frac{G_F}{\sqrt{2}}\,V_{cb}V_{ud}^*\,a_2(D\pi)(m_B^2-m_\pi^2)f_D F_0^{B\pi}(m_D^2),\\
\mathcal{E}_{\rm SD} &= i\frac{G_F}{\sqrt{2}}\,V_{cb}V_{ud}^*\,a_2(D\pi)(m_D^2-m_\pi^2)f_B F_0^{0\to D\pi}(m_B^2),
\end{aligned} \tag{3.8}$$

where $a_{1,2}$ are the parameters related to the Wilson coefficients and some calculable short-distance nonfactorizable effects. The annihilation form factor $F_0^{0\to D\pi}(m_B^2)$ is expected to be suppressed at large momentum transfer, $q^2=m_B^2$, corresponding to the conventional helicity suppression. Based on the argument of helicity and color suppression, one may therefore neglect short-distance (hard) W-exchange contributions. In the QCD factorization approach, contrary to the parameter $a_1(D\pi)$, $a_2(D\pi)$ is not calculable owing to the presence of infrared divergence caused by the gluon exchange between the emitted D^0 meson and the $(\overline{B}^0\pi^0)$ system. In other words, the nonfactorizable contribution to a_2 is dominated by nonperturbative effects. For charmless B decays, a typical value of $a_2\approx 0.22\exp(-i30^\circ)$ is obtained in the QCD factorization approach [17]. Recall that the experimental value for $B\to J/\psi K$ is $|a_2(J/\psi K)|=0.26\pm 0.02$ [53]. However, neglecting the W-exchange contribution, a direct fit to the $D\pi$ data requires that $a_2/a_1\approx(0.45-0.65)e^{\pm i60^\circ}$ [9, 54, 55, 56]. The question is then why the magnitude and phase of a_2/a_1 are so different from the model expectation. To resolve this difficulty, we next turn to long-distance rescattering effects. An early effort along this direction is based on a quasi-elastic scattering model [57]. For a recent study of the color-suppressed $B\to D^{(*)0}M$ decays in the perturbative QCD approach based on k_T factorization theorem and in soft-collinear effective theory, see [58] and [59] respectively.

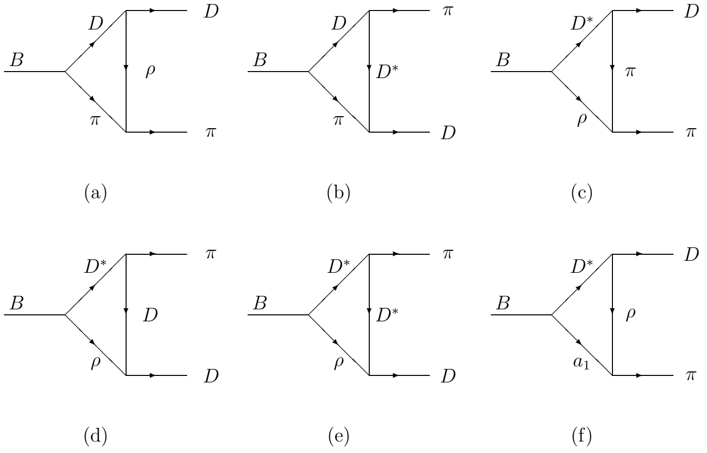

FIG. 4: Long-distance t-channel rescattering contributions to $B \to D\pi$.

A. Long-distance contributions to $B \to D\pi$

Some possible leading long-distance FSI contributions to $B \to D\pi$ are depicted in Fig. 4. Apart from the $D\pi$ intermediate state contributions as shown in Figs. 2 and 3, here we have also included rescattering contributions from the $D^*\rho$ and D^*a_1 intermediate states. As noted in passing, the s-channel contribution is presumably negligible owing to the absence of nearby resonances. Hence, we will focus only on the t-channel long-distance contributions. For each diagram in Fig. 4, one should consider all the possible isospin structure and draw all the possible sub-diagrams at the quark level [31]. While all the six diagrams contribute to $B^- \to D^0\pi^-$, only the diagrams 4(a), 4(c) and 4(f) contribute to $\overline{B}^0 \to D^+\pi^-$ and 4(b), 4(d) and 4(e) to $\overline{B}^0 \to D^0\pi^0$. To see this, we consider the contribution of Fig. 4(a) to $\overline{B}^0 \to D^0\pi^0$ as an example. The corresponding diagrams of Fig. 4(a) at the quark level are Figs. 1(a) and 1(b). At the meson level, Fig. 4(a) contains Figs. 2(b) and 3(a). Owing to the wave function $\pi^0 = (\bar{u}u - \bar{d}d)/\sqrt{2}$, Fig. 1(a) and hence Fig. 2(b) has an isospin factor of $1/\sqrt{2}$, while Fig. 1(b) and hence Fig. 3(a) has a factor of $-1/\sqrt{2}$. Consequently, there is a cancellation between Figs. 2(b) and 3(a). Another way for understanding this cancellation is to note that Fig. 2(b) contributes to $\mathcal{E}$, while Fig. 3(a) to $\mathcal{C}$. From Eq. (3.1), it is clear that there is a cancellation between them.

Given the weak Hamiltonian in the form $H_{\rm W} = \sum_i \lambda_i Q_i$, where λ_i is the combination of the quark mixing matrix elements and Q_i is a T-even local operator (T: time reversal), the absorptive part of Fig. 4 can be obtained by using the optical theorem and time-reversal invariant weak decay operator Q_i. From the time reversal invariance of Q $(= U_T Q^* U_T^\dagger)$, it follows that

$$\langle i;{\rm out}|Q|B;{\rm in}\rangle^* = \sum_j S^*_{ji}\langle j;{\rm out}|Q|B;{\rm in}\rangle, \tag{3.9}$$

where $S_{ij} \equiv \langle i;{\rm out}|\,j;{\rm in}\rangle$ is the strong interaction S-matrix element, and we have used

$U_T|\mathrm{out\,(in)}\rangle^* = |\mathrm{in\,(out)}\rangle$ to fix the phase convention.[2] Eq. (3.9) implies an identity related to the optical theorem. Noting that $S = 1 + iT$, we find

$$2\,\mathcal{A}bs\,\langle i;\mathrm{out}|Q|B;\mathrm{in}\rangle = \sum_j T^*_{ji}\langle j;\mathrm{out}|Q|B;\mathrm{in}\rangle, \tag{3.10}$$

where use of the unitarity of the S-matrix has been made. Specifically, for two-body B decays, we have

$$\begin{aligned}\mathcal{A}bs\,M(p_B\to p_1p_2) &= \frac{1}{2}\sum_j\left(\Pi^j_{k=1}\int\frac{d^3\vec{q}_k}{(2\pi)^3 2E_k}\right)(2\pi)^4 \\ &\quad\times\ \delta^4(p_1+p_2-\sum_{k=1}^{j}q_k)M(p_B\to\{q_k\})T^*(p_1p_2\to\{q_k\}).\end{aligned} \tag{3.11}$$

Thus the optical theorem relates the absorptive part of the two-body decay amplitude to the sum over all possible B decay final states $\{q_k\}$, followed by strong $\{q_k\}\to p_1p_2$ rescattering.

Neglecting the dispersive parts for the moment, the FSI corrections to the topological amplitudes are

$$\begin{aligned}\mathcal{T} &= \mathcal{T}_{\rm SD}, \\ \mathcal{C} &= \mathcal{C}_{\rm SD} + i\mathcal{A}bs\,(4a+4b+4c+4d+4e+4f), \\ \mathcal{E} &= \mathcal{E}_{\rm SD} + i\mathcal{A}bs\,(4a+4c+4f).\end{aligned} \tag{3.12}$$

The color-allowed amplitude $\mathcal{T}$ does receive contributions from, for example, the s-channel $\overline{B}^0 \to D^+\pi^- \to D^+\pi^-$ and the t-channel rescattering process $\overline{B}^0 \to D^0\pi^0 \to D^+\pi^-$. However, they are both suppressed: The first one is subject to $\mathcal{O}(1/m_b^2)$ suppression while the weak decay in the second process is color suppressed. Therefore, it is safe to neglect long-distance corrections to $\mathcal{T}$. As a result,

$$\begin{aligned}A(\overline{B}^0\to D^+\pi^-) &= \mathcal{T}_{\rm SD}+\mathcal{E}_{\rm SD}+i\mathcal{A}bs\,(4a+4c+4f), \\ A(B^-\to D^0\pi^-) &= \mathcal{T}_{\rm SD}+\mathcal{C}_{\rm SD}+i\mathcal{A}bs\,(4a+4b+4c+4d+4e+4f), \\ A(\overline{B}^0\to D^0\pi^0) &= \frac{1}{\sqrt{2}}(-\mathcal{C}+\mathcal{E})_{\rm SD}-\frac{i}{\sqrt{2}}\mathcal{A}bs\,(4b+4d+4e).\end{aligned} \tag{3.13}$$

Note that the isospin relation (3.2) is still respected, as it should be.

To proceed we write down the relevant Lagrangian [60, 61][3]

$$\mathcal{L} = -ig_{\rho\pi\pi}\Big(\rho^+_\mu\pi^0\overleftrightarrow{\partial}^\mu\pi^- + \rho^-_\mu\pi^+\overleftrightarrow{\partial}^\mu\pi^0 + \rho^0_\mu\pi^-\overleftrightarrow{\partial}^\mu\pi^+\Big)$$

---

[2] Note that in the usual phase convention we have $T|P(\vec{p})\rangle = -|P(-\vec{p})\rangle$, $T|V(\vec{p},\lambda)\rangle = -(-)^\lambda|V(-\vec{p},\lambda)\rangle$ with λ being the helicity of the vector meson. For the $B\to PP, VP, VV$ decays followed by two-particle to two-particle rescatterings, the $|PP\rangle$ and S,D-wave $|VV\rangle$ states satisfy the $U_T|\mathrm{out\,(in)}\rangle^* = |\mathrm{in\,(out)}\rangle$ relation readily, while for $|B\rangle$ and P-wave $|VV\rangle$ as well as $|VP\rangle$ states we may assign them an additional phase i to satisfy the above relation. We shall return to the usual phase convention once the optical theorem for final-state rescattering, namely, Eq. (3.10), is obtained.

[3] In the chiral and heavy quark limits, the effective Lagrangian of (3.15) can be recast compactly in terms

$$
\begin{aligned}
&- \; i g_{D^*DP}(D^i\partial^\mu P_{ij}D^{*j\dagger}_\mu - D^{*i}_\mu \partial^\mu P_{ij}D^{j\dagger}) + \frac{1}{2} g_{D^*D^*P}\varepsilon_{\mu\nu\alpha\beta}\, D^{*\mu}_i \partial^\nu P^{ij} \overleftrightarrow{\partial}{}^\alpha D^{*\beta\dagger}_j \\
&- \; i g_{DDV} D^\dagger_i \overleftrightarrow{\partial}_\mu D^j (V^\mu)^i_j - 2 f_{D^*DV}\epsilon_{\mu\nu\alpha\beta}(\partial^\mu V^\nu)^i_j (D^\dagger_i \overleftrightarrow{\partial}{}^\alpha D^{*\beta j} - D^{*\beta\dagger}_i \overleftrightarrow{\partial}{}^\alpha D^j) \\
&+ \; i g_{D^*D^*V} D^{*\nu\dagger}_i \overleftrightarrow{\partial}_\mu D^{*j}_\nu (V^\mu)^i_j + 4 i f_{D^*D^*V} D^{*\dagger}_{i\mu}(\partial^\mu V^\nu - \partial^\nu V^\mu)^i_j D^{*j}_\nu,
\end{aligned}
\tag{3.15}
$$

with the convention $\varepsilon^{0123} = 1$, where P and V_μ are 3×3 matrices for the octet pseudoscalar and nonet vector mesons, respectively

$$
P = \begin{pmatrix} \frac{\pi^0}{\sqrt{2}} + \frac{\eta}{\sqrt{6}} & \pi^+ & K^+ \\ \pi^- & -\frac{\pi^0}{\sqrt{2}} + \frac{\eta}{\sqrt{6}} & K^0 \\ K^- & \overline{K}^0 & -\sqrt{\frac{2}{3}}\eta \end{pmatrix}, \quad V = \begin{pmatrix} \frac{\rho^0}{\sqrt{2}} + \frac{\omega}{\sqrt{2}} & \rho^+ & K^{*+} \\ \rho^- & -\frac{\rho^0}{\sqrt{2}} + \frac{\omega}{\sqrt{2}} & K^{*0} \\ K^{*-} & \overline{K}^{*0} & \phi \end{pmatrix}. \tag{3.16}
$$

Note that our phase convention on fields is fixed by

$$
\langle 0|A_\mu|P\rangle = i f_P p_\mu, \qquad \langle 0|V_\mu|V\rangle = m_V \varepsilon_\mu, \tag{3.17}
$$

and is different from [60]. In the chiral and heavy quark limits, we have [60]

$$
g_{D^*D^*\pi} = \frac{g_{D^*D\pi}}{\sqrt{m_D m_{D^*}}} = \frac{2}{f_\pi} g, \quad g_{DDV} = g_{D^*D^*V} = \frac{\beta g_V}{\sqrt{2}}, \quad f_{D^*DV} = \frac{f_{D^*D^*V}}{m_{D^*}} = \frac{\lambda g_V}{\sqrt{2}}, \tag{3.18}
$$

with $f_\pi = 132$ MeV. The parameters g_V, β and λ thus enter into the effective chiral Lagrangian describing the interactions of heavy mesons with low momentum light vector mesons (see e.g. [60]). The parameter g_V respects the relation $g_V = m_\rho/f_\pi$ [60]. We shall follow [34] to use $\beta = 0.9$ and $\lambda = 0.56$ GeV^{-1}. Instead of writing down the Feynman rules for the vertices, we work out the corresponding matrix elements:

$$
\begin{aligned}
\langle \rho^+(\varepsilon)\pi^-(p_2)|i\mathcal{L}|\pi^0(p_1)\rangle &= -i g_{\rho\pi\pi}\varepsilon\cdot(p_1+p_2), \\
\langle D(p_2)\pi(q)|i\mathcal{L}|D^*(\varepsilon,p_1)\rangle &= -i g_{D^*D\pi}\,\varepsilon\cdot q, \\
\langle D^*(\varepsilon_2,p_2)\pi(q)|i\mathcal{L}|D^*(\varepsilon_1,p_1)\rangle &= -i g_{D^*D^*\pi}\epsilon_{\mu\nu\alpha\beta}\varepsilon_1^\mu\varepsilon_2^{*\nu}q^\alpha p_1^\beta, \\
\langle D(p_2)\rho(\varepsilon)|i\mathcal{L}|D(p_1)\rangle &= -\frac{i}{\sqrt{2}}\,\beta g_V\,\varepsilon\cdot(p_1+p_2), \\
\langle D^*(\varepsilon_2,p_2)\rho(\varepsilon_\rho,q)|i\mathcal{L}|D(p_1)\rangle &= -i2\sqrt{2}\lambda\, g_V\,\epsilon_{\mu\nu\alpha\beta}\varepsilon^\mu_\rho\varepsilon^{*\nu}_{D^*}p_1^\alpha q^\beta.
\end{aligned}
\tag{3.19}
$$

Figs. 4(a) and 4(b) arise from the weak decay $B \to D\pi$ followed by the rescattering of $D\pi$ to $D\pi$. Denoting the momenta by $B(p_B) \to D(p_1)\pi(p_2) \to D(p_3)\pi(p_4)$, it follows that the absorptive part of 4(a) is given by [4]

$$
\mathcal{A}bs\,(4a) = \frac{1}{2}\int \frac{d^3\vec{p}_1}{(2\pi)^3 2E_1}\frac{d^3\vec{p}_2}{(2\pi)^3 2E_2}(2\pi)^4\delta^4(p_B - p_1 - p_2)A(\overline{B}^0 \to D^+\pi^-)
$$

---

of superfields [60]

$$
\begin{aligned}
\mathcal{L} = \; & i\langle H_b v^\mu \mathcal{D}_{\mu ba}\overline{H}_a\rangle + i g\langle H_b\gamma_\mu\gamma_5 A^\mu_{ba}\overline{H}_a\rangle \\
& + i\beta\langle H_b v^\mu (V_\mu - \rho_\mu)_{ba}\overline{H}_a\rangle + i\lambda\langle H_b\sigma^{\mu\nu}F_{\mu\nu}(\rho)_{ba}\overline{H}_a\rangle,
\end{aligned}
\tag{3.14}
$$

where the superfield H is given by $H = \frac{1+\not{v}}{2}(D^{*\mu}\gamma_\mu - i\gamma_5 D)$, and $(V_\mu)_{ba}$ and $(A_\mu)_{ba}$ are the matrix elements of vector and axial currents, respectively, constructed from Goldstone bosons.

[4] As noticed in [31], the isospin factor of $1/\sqrt{2}$ or $-1/\sqrt{2}$ should be dropped for the intermediate state ρ^0 or π^0.

$$
\begin{aligned}
&\times\ i\frac{1}{\sqrt{2}}\beta g_V\,\frac{F^2(t,m_\rho)}{t-m_\rho^2+im_\rho\Gamma_\rho}\,(-i)g_{\rho\pi\pi}\,(p_1+p_3)^\mu(p_2+p_4)^\nu\left(-g_{\mu\nu}+\frac{k_\mu k_\nu}{m_\rho^2}\right)\\
&=\int_{-1}^{1}\frac{|\vec{p}_1|d\cos\theta}{16\pi m_B}\frac{1}{\sqrt{2}}\,g_Vg_{\rho\pi\pi}\beta\,A(\overline{B}^0\to D^+\pi^-)\frac{F^2(t,m_\rho)}{t-m_\rho^2+im_\rho\Gamma_\rho}H_1,
\end{aligned}
\tag{3.20}
$$

where θ is the angle between $\vec{p}_1$ and $\vec{p}_3$, k is the momentum of the exchanged ρ meson ($k^2=t$), and

$$
\begin{aligned}
t &\equiv (p_1-p_3)^2=m_1^2+m_3^2-2E_1E_3+2|\vec{p}_1||\vec{p}_3|\cos\theta,\\
H_1 &= -(p_1\cdot p_2+p_3\cdot p_4+p_1\cdot p_4+p_2\cdot p_3)-\frac{(m_1^2-m_3^2)(m_2^2-m_4^2)}{m_\rho^2}.
\end{aligned}
\tag{3.21}
$$

The form factor $F(t,m)$ in Eq. (3.20) takes care of the off-shell effect of the exchanged particle, which is usually parametrized as

$$
F(t,m)=\left(\frac{\Lambda^2-m^2}{\Lambda^2-t}\right)^n,
\tag{3.22}
$$

normalized to unity at $t=m^2$. The monopole behavior of the form factor (i.e. $n=1$) is preferred as it is consistent with the QCD sum rule expectation [62]. However, we shall return back to this point when discussing the FSI effects in $B\to\phi K^*$ decays (see Sec. VII.C).

Likewise, the absorptive part of 4(b) is given by

$$
\begin{aligned}
\mathcal{A}bs\,(4b) &= \frac{1}{2}\int\frac{d^3\vec{p}_1}{(2\pi)^32E_1}\,\frac{d^3\vec{p}_2}{(2\pi)^32E_2}\,(2\pi)^4\delta^4(p_B-p_1-p_2)A(\overline{B}^0\to D^+\pi^-)\\
&\times\ ig_{D^*D\pi}p_4^\mu\,\frac{F^2(t,m_{D^*})}{t-m_{D^*}^2}\,(-i)g_{D^*D\pi}(-p_2^\nu)\left(-g_{\mu\nu}+\frac{k_\mu k_\nu}{m_{D^*}^2}\right)\\
&= -\int_{-1}^{1}\frac{|\vec{p}_1|d\cos\theta}{16\pi m_B}g_{D^*D\pi}^2\,A(\overline{B}^0\to D^+\pi^-)\,\frac{F^2(t,m_{D^*})}{t-m_{D^*}^2}\,H_2,
\end{aligned}
\tag{3.23}
$$

with

$$
H_2=-p_2\cdot p_4+\frac{(p_2\cdot p_3-m_2^2)(p_1\cdot p_4-m_4^2)}{m_{D^*}^2}.
\tag{3.24}
$$

Figs. 4(c)-4(e) come from the rescattering process $B\to D^*(p_1)\rho(p_2)\to D(p_3)\pi(p_4)$. The absorptive part of 4(c) reads

$$
\begin{aligned}
\mathcal{A}bs\,(4c) &= \frac{1}{2}\int\frac{d^3\vec{p}_1}{(2\pi)^32E_1}\,\frac{d^3\vec{p}_2}{(2\pi)^32E_2}\,(2\pi)^4\delta^4(p_B-p_1-p_2)\sum_{\lambda_1,\lambda_2}A(\overline{B}^0\to D^{*+}\rho^-)\\
&\times\ (-i)g_{D^*D\pi}\,\varepsilon_1\cdot(-p_3)\,\frac{F^2(t,m_\pi)}{t-m_\pi^2}\,(-i)g_{\rho\pi\pi}\,2\varepsilon_2\cdot p_4.
\end{aligned}
\tag{3.25}
$$

To proceed, we note that the factorizable amplitude of $B\to V_1V_2$ is given by

$$
\begin{aligned}
A(B\to V_1V_2) &= \frac{G_F}{\sqrt{2}}V_{\rm CKM}\langle V_2|(\bar{q}_2q_3)_{V-A}|0\rangle\langle V_1|(\bar{q}_1b)_{V-A}|\overline{B}\rangle\\
&= -if_{V_2}m_2\Bigg[(\varepsilon_1^*\cdot\varepsilon_2^*)(m_B+m_1)A_1^{BV_1}(m_2^2)-(\varepsilon_1^*\cdot p_{_B})(\varepsilon_2^*\cdot p_{_B})\frac{2A_2^{BV_1}(m_2^2)}{m_B+m_1}\\
&-\ i\epsilon_{\mu\nu\alpha\beta}\varepsilon_2^{*\mu}\varepsilon_1^{*\nu}p_{_B}^\alpha p_1^\beta\,\frac{2V^{BV_1}(m_2^2)}{m_B+m_1}\Bigg],
\end{aligned}
\tag{3.26}
$$

with $(\bar{q}_1 q_2)_{V-A} \equiv \bar{q}_1 \gamma_\mu (1-\gamma_5) q_2$. Therefore,

$$\begin{aligned}
\mathcal{A}bs\,(4c) \;&=\; -i2\int_{-1}^{1} \frac{|\vec{p}_1| d\cos\theta}{16\pi m_B}\, g_{D^*D\pi} g_{\rho\pi\pi}\, \frac{F^2(t,m_\pi)}{t-m_\pi^2} \\
&\times\; f_\rho m_\rho \Big[(m_B+m_{D^*})A_1^{BD^*}(m_\rho^2) H_3 - \frac{2A_2^{BD^*}(m_\rho^2)}{m_B+m_{D^*}} H_3'\Big],
\end{aligned} \tag{3.27}$$

where

$$\begin{aligned}
H_3 \;&=\; \left(p_3\cdot p_4 - \frac{(p_1\cdot p_3)(p_1\cdot p_4)}{m_1^2} - \frac{(p_2\cdot p_3)(p_2\cdot p_4)}{m_2^2} + \frac{(p_1\cdot p_2)(p_1\cdot p_3)(p_2\cdot p_4)}{m_1^2 m_2^2}\right), \\
H_3' \;&=\; \left(p_2\cdot p_3 - \frac{(p_1\cdot p_2)(p_1\cdot p_3)}{m_1^2}\right)\left(p_1\cdot p_4 - \frac{(p_1\cdot p_2)(p_2\cdot p_4)}{m_2^2}\right).
\end{aligned} \tag{3.28}$$

Likewise,

$$\begin{aligned}
\mathcal{A}bs\,(4d) \;&=\; \frac{1}{2}\int \frac{d^3\vec{p}_1}{(2\pi)^3 2E_1}\frac{d^3\vec{p}_2}{(2\pi)^3 2E_2}\,(2\pi)^4\delta^4(p_B-p_1-p_2)\sum_{\lambda_1,\lambda_2} A(\overline{B}^0 \to D^{*+}\rho^-) \\
&\times\; (-i) g_{D^*D\pi}\varepsilon_1\cdot p_4\,\frac{F^2(t,m_{D^*})}{t-m_{D^*}^2}(-i)\frac{\beta}{\sqrt{2}}\, g_V\, \varepsilon_2\cdot(k+p_3) \\
&=\; i\sqrt{2}\int_{-1}^{1}\frac{|\vec{p}_1| d\cos\theta}{16\pi m_B}\,\beta\, g_V\, g_{D^*D\pi}\,\frac{F^2(t,m_D)}{t-m_D^2} \\
&\times\; f_\rho m_\rho \Big[(m_B+m_{D^*})A_1^{BD^*}(m_\rho^2) H_4 - \frac{2A_2^{BD^*}(m_\rho^2)}{m_B+m_{D^*}} H_4'\Big],
\end{aligned} \tag{3.29}$$

where H_4 and H_4' can be obtained from H_3 and H_3', respectively, by interchanging p_3 and p_4, and

$$\begin{aligned}
\mathcal{A}bs\,(4e) \;&=\; \frac{1}{2}\int \frac{d^3\vec{p}_1}{(2\pi)^3 2E_1}\frac{d^3\vec{p}_2}{(2\pi)^3 2E_2}\,(2\pi)^4\delta^4(p_B-p_1-p_2)\sum_{\lambda_1,\lambda_2} A(\overline{B}^0 \to D^{*+}\rho^-) \\
&\times\; i g_{D^*D^*\pi}\,\epsilon_{\mu\nu\alpha\beta}\varepsilon_1^\mu\, p_4^\alpha p_1^\beta\,\frac{F^2(t,m_{D^*})}{t-m_{D^*}^2}\, i2\sqrt{2}\,\lambda\, g_V\, \epsilon_{\rho\sigma\xi\eta}\varepsilon_2^\rho p_3^\xi(-p_2)^\eta\left(-g^{\nu\sigma}+\frac{k^\nu k^\sigma}{m_{D^*}^2}\right) \\
&=\; i2\sqrt{2}\int_{-1}^{1}\frac{|\vec{p}_1| d\cos\theta}{16\pi m_B} g_V \lambda\, g_{D^*D^*\pi}\,\frac{F^2(t,m_{D^*})}{t-m_{D^*}^2} \\
&\times\; f_\rho m_\rho \Big[(m_B+m_{D^*})A_1^{BD^*}(m_\rho^2) H_5 - \frac{2A_2^{BD^*}(m_\rho^2)}{m_B+m_{D^*}} H_5'\Big],
\end{aligned} \tag{3.30}$$

where

$$\begin{aligned}
H_5 \;&=\; 2(p_1\cdot p_2)(p_3\cdot p_4) - 2(p_1\cdot p_3)(p_2\cdot p_4), \\
H_5' \;&=\; m_B^2\Big[(p_1\cdot p_2)(p_3\cdot p_4) - (p_1\cdot p_4)(p_2\cdot p_4)\Big] + (p_2\cdot p_B)(p_4\cdot p_B)(p_1\cdot p_3) \\
&+\; (p_1\cdot p_B)(p_3\cdot p_B)(p_2\cdot p_4) - (p_1\cdot p_B)(p_2\cdot p_B)(p_3\cdot p_4) - (p_3\cdot p_B)(p_4\cdot p_B)(p_1\cdot p_2).
\end{aligned} \tag{3.31}$$

Fig. 4(f) comes from the weak decay $\overline{B}^0 \to D^{*+}a_1^-$ followed by a strong scattering. We obtain

$$\mathcal{A}bs\,(4f) \;=\; \frac{1}{2}\int \frac{d^3\vec{p}_1}{(2\pi)^3 2E_1}\frac{d^3\vec{p}_2}{(2\pi)^3 2E_2}\,(2\pi)^4\delta^4(p_B-p_1-p_2)\sum_{\lambda_1,\lambda_2} A(\overline{B}^0 \to D^{*+}a_1^-) \tag{3.32}$$

$$\times\; i2\sqrt{2} g_V \lambda \epsilon_{\mu\nu\alpha\beta}\varepsilon_1^\mu\, p_3^\alpha k^\beta\,\frac{F^2(t,m_\rho)}{t-m_\rho^2+im_\rho\Gamma_\rho}\,(gG_{\rho\sigma}+\ell L_{\rho\sigma})\varepsilon_2^\rho\left(-g^{\nu\sigma}+\frac{k^\nu k^\sigma}{m_{D^*}^2}\right)$$

where

$$
\begin{aligned}
G^{\rho\sigma} &= \delta^{\rho\sigma} - \frac{1}{Y}\Big[m_2^2 k^\rho k^\sigma + k^2 p_2^\rho p_2^\sigma + p_2\cdot k(p_2^\rho k^\sigma + k^\rho p_2^\sigma)\Big] \\
L^{\rho\sigma} &= \frac{p_2\cdot k}{Y}\left(p_2^\rho + k^\rho \frac{m_2^2}{p_2\cdot k}\right)\left(k^\sigma + p_2^\sigma \frac{k^2}{p_2\cdot k}\right),
\end{aligned}
\tag{3.33}
$$

and $Y = (p_2\cdot k)^2 - k^2 m_2^2$. The parameters g and ℓ appearing in Eq. (3.32) also enter into the strong decay amplitude of $a_1 \to \rho\pi$ parametrized as

$$
A(a_1 \to \rho\pi) = (gG_{\mu\nu} + \ell L_{\mu\nu})\varepsilon_{a_1}^\mu \varepsilon_\rho^\nu
\tag{3.34}
$$

and hence they can determined from the measured decay rate and the ratio of D and S waves:

$$
\begin{aligned}
\Gamma(a_1 \to \rho\pi) &= \frac{p_c}{12\pi m_{a_1}^2}\left(2|g|^2 + \frac{m_{a_1}^2 m_\rho^2}{(p_{a_1}\cdot p_\rho)^2}|\ell|^2\right), \\
\frac{D}{S} &= -\sqrt{2}\,\frac{(E_\rho - m_\rho)g + p_c^2 m_{a_1} h}{(E_\rho + 2m_\rho)g + p_c^2 m_{a_1} h},
\end{aligned}
\tag{3.35}
$$

with p_c being the c.m. momentum of the ρ or π in the a_1 rest frame, and

$$
h = \frac{p_{a_1}\cdot p_\rho}{Y}\left(-g + \ell\frac{m_{a_1}^2 m_\rho^2}{(p_{a_1}\cdot p_\rho)^2}\right).
\tag{3.36}
$$

Hence, Eq. (3.32) can be recast to

$$
\mathcal{A}bs\,(4f) = i2\sqrt{2}\int_{-1}^{1}\frac{|\vec{p}_1|d\cos\theta}{16\pi m_B}\,g_V\lambda\,f_{a_1}m_{a_1}\,\frac{F^2(t,m_\rho)}{t - m_\rho^2 + im_\rho\Gamma_\rho}\,\frac{2V^{BD^*}(m_{a_1}^2)}{m_B + m_{D^*}}H_6,
\tag{3.37}
$$

with

$$
\begin{aligned}
H_6 &= \left(\frac{g}{Y}p_2\cdot k - \frac{\ell}{Y}\frac{m_2^2 k^2}{p_2\cdot k}\right)\Big[m_1^2(p_2\cdot p_4)(p_2\cdot p_3) + m_2^2(p_1\cdot p_3)(p_1\cdot p_4) + (p_1\cdot p_2)^2 p_3\cdot p_4 \\
&- m_1^2 m_2^2\, p_3\cdot p_4 - (p_2\cdot p_4)(p_1\cdot p_3)(p_1\cdot p_2) - (p_1\cdot p_2)(p_2\cdot p_3)(p_1\cdot p_4)\Big] \\
&- 2g\Big(m_1^2 p_2\cdot p_3 - (p_1\cdot p_2)(p_1\cdot p_3)\Big).
\end{aligned}
\tag{3.38}
$$

It should be emphasized that attention must be paid to the relative sign between $B \to PP$ and $B \to VV$ decay amplitudes when calculating long-distance contributions from various rescattering processes. For the one-body matrix element defined by $\langle 0|\bar{q}\gamma_\mu\gamma_5|P\rangle = if_P q_\mu$, the signs of $B \to PP$ and $B \to VV$ amplitudes, respectively, are fixed as in Eqs. (3.8) and (3.26). This can be checked explicitly via heavy quark symmetry (see e.g. [63]).

The dispersive part of the rescattering amplitude can be obtained from the absorptive part via the dispersion relation

$$
\mathcal{D}is\,A(m_B^2) = \frac{1}{\pi}\int_s^\infty \frac{\mathcal{A}bs\,A(s')}{s' - m_B^2}ds'.
\tag{3.39}
$$

Unlike the absorptive part, it is known that the dispersive contribution suffers from the large uncertainties due to some possible subtractions and the complication from integrations. For this reason, we will assume the dominance of the rescattering amplitude by the absorptive part and ignore the dispersive part in the present work except for the decays $B^0 \to \pi^+\pi^-$ and $B^0 \to \pi^0\pi^0$ where a dispersive contribution arising from $D\bar{D} \to \pi\pi$ and $\pi\pi \to \pi\pi$ rescattering via annihilation may play an essential role.

B. Numerical results

To estimate the contributions from rescattering amplitudes we need to specify various parameters entering into the vertices of Feynman diagrams. The on-shell strong coupling $g_{\rho\pi\pi}$ is determined from the $\rho \to \pi\pi$ rate to be $g_{\rho\pi\pi} = 6.05 \pm 0.02$. The coupling $g_{D^*D\pi}$ has been extracted by CLEO to be $17.9 \pm 0.3 \pm 1.9$ from the measured D^{*+} width [64]. The parameters relevant for the $D^*D^{(*)}\rho$ couplings are $g_V = 5.8$, $\beta = 0.9$ and $\lambda = 0.56\,\mathrm{GeV}^{-1}$.

For form factors we use the values determined from the covariant light-front model [63]. For the coefficients g and ℓ in Eq. (3.34), one can use the experimental results of $D/S = -0.1 \pm 0.028$ and $\Gamma(a_1 \to \rho\pi) = 250 - 600$ MeV [50] to fix them. Specifically, we use $D/S = -0.1$ and $\Gamma(a_1 \to \rho\pi) = 400$ MeV to obtain $g = 4.3$ and $\ell = 5.8$. For decay constants, we use $f_\pi = 132$ MeV, $f_D = 200$ MeV, $f_{D^*} = 230$ MeV and $f_{a_1} = -205$ MeV.[5]

Since the strong vertices are determined for physical particles and since the exchanged particle is not on-shell, it is necessary to introduce the form factor $F(t)$ to account for the off-shell effect of the t-channel exchanged particle. For the cutoff Λ in the form factor $F(t)$ [see Eq. (3.22)], Λ should be not far from the physical mass of the exchanged particle. To be specific, we write

$$\Lambda = m_{\mathrm{exc}} + \eta\Lambda_{\mathrm{QCD}}, \tag{3.40}$$

where the parameter η is expected to be of order unity and it depends not only on the exchanged particle but also on the external particles involved in the strong-interaction vertex. Since we do not have first-principles calculations of η, we will determine it from the measured branching ratios given in (3.3) and (3.4). Taking $\Lambda_{\mathrm{QCD}} = 220$ MeV, we find $\eta = 2.2$ for the exchanged particles D^* and D and $\eta = 1.1$ for ρ and π. As noted in passing, the loop corrections will be larger than the initial $B \to D\pi$ amplitudes if the off-shell effect is not considered. Although the strong couplings are large in the magnitude, the rescattering amplitude is suppressed by a factor of $F^2(t) \sim m^2\Lambda^2_{\mathrm{QCD}}/t^2$. Consequently, the off-shell effect will render the perturbative calculation meaningful.

Numerically, we obtain (in units of GeV)

$$\begin{aligned} A(\overline{B}^0 \to D^+\pi^-) &= i6.41 \times 10^{-7} - (0.90 + i0.09) \times 10^{-7}, \\ A(\overline{B}^0 \to D^0\pi^0) &= -i0.91 \times 10^{-7} - 1.56 \times 10^{-7}, \\ A(B^- \to D^0\pi^-) &= i7.69 \times 10^{-7} + (1.30 - i0.09) \times 10^{-7} \end{aligned} \tag{3.41}$$

for $a_1 = 0.90$ and $a_2 = 0.25$,[6] where the first term on the right hand side of each amplitude arises from the short-distance factorizable contribution and the second term comes from absorptive parts of the final-state rescattering processes. Note that the absorptive part of $\overline{B}^0 \to D^+\pi^-$ and $B^- \to D^0\pi^-$ decay amplitudes are complex owing to a non-vanishing ρ width. To calculate the branching ratios, we will take into account the uncertainty from the $\Lambda_{\rm QCD}$ scale. Recall that $\Lambda_{\rm QCD} = 217^{+25}_{-21}$ MeV is quoted in PDG [50]. Therefore, allowing 15% error in $\Lambda_{\rm QCD}$, the flavor-averaged branching ratios are found to be

---

[5] The sign of f_{a_1} is opposite to f_π as noticed in [63].

[6] As mentioned before, $a_2(D\pi)$ is *a priori* not calculable in the QCD factorization approach. Therefore, we choose $a_2(D\pi) \approx 0.25$ for the purpose of illustration. Nevertheless, a rough estimate of $a_2(D\pi)$ has been made in [17] by treating the charmed meson as a light meson while keeping its highly asymmetric distribution amplitude. It yields $a_2(D\pi) \approx 0.25\exp(-i40^\circ)$.

$$\begin{aligned} \mathcal{B}(\overline{B}^0 \to D^+\pi^-) &= (3.1^{+0.0}_{-0.0}) \times 10^{-3}\ (3.2 \times 10^{-3}), \\ \mathcal{B}(B^- \to D^0\pi^-) &= (5.0^{+0.1}_{-0.0}) \times 10^{-3}\ (4.9 \times 10^{-3}), \\ \mathcal{B}(\overline{B}^0 \to D^0\pi^0) &= (2.5^{+1.1}_{-0.8}) \times 10^{-4}\ (0.6 \times 10^{-4}), \end{aligned} \tag{3.42}$$

where the branching ratios for decays without FSIs are shown in parentheses. We see that the $D^0\pi^0$ mode is sensitive to the cutoff scales Λ_{D^*} and Λ_D, whereas the other two color-allowed channels are not. It is clear that the naively predicted $\mathcal{B}(\overline{B}^0 \to D^0\pi^0)$ before taking into account rescattering effects is too small compared to experiment. In contrast, $\overline{B}^0 \to D^+\pi^-$ and $B^- \to D^0\pi^-$ are almost not affected by final-state rescattering. Moreover,

$$\frac{\mathcal{C}}{\mathcal{T}}\bigg|_{D\pi} = \begin{cases} 0.28\, e^{-i48^\circ}, \\ 0.20, \end{cases} \qquad \frac{\mathcal{E}}{\mathcal{T}}\bigg|_{D\pi} = \begin{cases} 0.14\, e^{i96^\circ}, & \text{with FSI} \\ 0, & \text{without FSI} \end{cases} \tag{3.43}$$

where we have assumed negligible short-distance W-exchange and taken the central values of the cutoffs. Evidently, even if the short-distance weak annihilation vanishes, a long-distance contribution to W-exchange can be induced from rescattering. Consequently,

$$\frac{\mathcal{C}-\mathcal{E}}{\mathcal{T}+\mathcal{E}}\bigg|_{D\pi} = \begin{cases} 0.40\, e^{-i67^\circ}, \\ 0.20, \end{cases} \qquad \frac{\mathcal{C}-\mathcal{E}}{\mathcal{T}+\mathcal{C}}\bigg|_{D\pi} = \begin{cases} 0.33\, e^{-i50^\circ}, & \text{with FSI} \\ 0.17, & \text{without FSI} \end{cases} \tag{3.44}$$

Therefore, our results are consistent with experiment (3.5). This indicates that rescattering will enhance the ratios and provide the desired strong phases. That is, the enhancement of $R \equiv (\mathcal{C}-\mathcal{E})/(\mathcal{T}+\mathcal{E})$ relative to the naive expectation is ascribed to the enhancement of color-suppressed W-emission and the long-distance W-exchange, while the phase of R is accounted for by the strong phases of $\mathcal{C}$ and $\mathcal{E}$ topologies.

Because the rescattering long-distance amplitudes have the same weak phases as the short-distance factorizable ones, it is clear that there is no direct CP violation induced from rescattering FSIs.

Since the decay $\overline{B}^0 \to D_s^+K^-$ proceeds only through the topological W-exchange diagram, the above determination of $\mathcal{E}$ allows us to estimate its decay rate. From Eq. (3.43) it follows that $|\mathcal{E}/(\mathcal{T}+\mathcal{E})|^2 = 0.020$ in the presence of FSIs. Therefore, we obtain

$$\frac{\Gamma(\overline{B}^0 \to D_s^+K^-)}{\Gamma(\overline{B}^0 \to D^+\pi^-)} = 0.019\,, \tag{3.45}$$

which is indeed consistent with the experimental value of 0.014 ± 0.005 [50]. The agreement will be further improved after taking into account SU(3) breaking in the $\mathcal{E}$ amplitude of $\overline{B}^0 \to D_s^+K^-$.

IV. $B \to \pi K$ DECAYS

The penguin dominated $B \to \pi K$ decay amplitudes have the general expressions

TABLE I: Experimental data for CP averaged branching ratios (top, in units of 10^{-6}) and CP asymmetries (bottom) for $B \to \pi K$ [50, 65].

Mode	BaBar	Belle	CLEO	Average
$B^- \to \pi^- \overline{K}^0$	$26.0 \pm 1.3 \pm 1.0$	$22.0 \pm 1.9 \pm 1.1$	$18.8^{+3.7+2.1}_{-3.3-1.8}$	24.1 ± 1.3
$\overline{B}^0 \to \pi^+ K^-$	$17.9 \pm 0.9 \pm 0.7$	$18.5 \pm 1.0 \pm 0.7$	$18.0^{+2.3+1.2}_{-2.1-0.9}$	18.2 ± 0.8
$B^- \to \pi^0 K^-$	$12.0 \pm 0.7 \pm 0.6$	$12.0 \pm 1.3^{+1.3}_{-0.9}$	$12.9^{+2.4+1.2}_{-2.2-1.1}$	12.1 ± 0.8
$\overline{B}^0 \to \pi^0 \overline{K}^0$	$11.4 \pm 0.9 \pm 0.6$	$11.7 \pm 2.3^{+1.2}_{-1.3}$	$12.8^{+4.0+1.7}_{-3.3-1.4}$	11.5 ± 1.0
$\mathcal{A}_{\pi^- K_S}$	$-0.087 \pm 0.046 \pm 0.010$	$0.05 \pm 0.05 \pm 0.01$	$0.18 \pm 0.24 \pm 0.02$	-0.020 ± 0.034
$\mathcal{A}_{\pi^+ K^-}$	$-0.133 \pm 0.030 \pm 0.009$	$-0.101 \pm 0.025 \pm 0.005$	$-0.04 \pm 0.16 \pm 0.02$	-0.113 ± 0.019
$\mathcal{A}_{\pi^0 K^-}$	$0.06 \pm 0.06 \pm 0.01$	$0.04 \pm 0.05 \pm 0.02$	$-0.29 \pm 0.23 \pm 0.02$	0.04 ± 0.04
$\mathcal{A}_{\pi^0 K_S}$	$-0.06 \pm 0.18 \pm 0.06$	$-0.12 \pm 0.20 \pm 0.07$		-0.09 ± 0.14
$\mathcal{S}_{\pi^0 K_S}$	$0.35^{+0.30}_{-0.33} \pm 0.04$	$0.30 \pm 0.59 \pm 0.11$		$0.34^{+0.27}_{-0.29}$

$$
\begin{aligned}
A(\overline{B}^0 \to \pi^+ K^-) &= \mathcal{T} + \mathcal{P} + \frac{2}{3}\mathcal{P}'_{\rm EW} + \mathcal{P}_A, \\
A(\overline{B}^0 \to \pi^0 \overline{K}^0) &= \frac{1}{\sqrt{2}}(\mathcal{C} - \mathcal{P} + \mathcal{P}_{\rm EW} + \frac{1}{3}\mathcal{P}'_{\rm EW} - \mathcal{P}_A), \\
A(B^- \to \pi^- \overline{K}^0) &= \mathcal{P} - \frac{1}{3}\mathcal{P}'_{\rm EW} + \mathcal{A} + \mathcal{P}_A, \\
A(B^- \to \pi^0 K^-) &= \frac{1}{\sqrt{2}}(\mathcal{T} + \mathcal{C} + \mathcal{P} + \mathcal{P}_{\rm EW} + \frac{2}{3}\mathcal{P}'_{\rm EW} + \mathcal{A} + \mathcal{P}_A),
\end{aligned}
\tag{4.1}
$$

where $\mathcal{P}_{\rm EW}$ and $\mathcal{P}'_{\rm EW}$ are color-allowed and color-suppressed electroweak penguin amplitudes, respectively, and $\mathcal{P}_A$ is the penguin-induced weak annihilation amplitude. The decay amplitudes satisfy the isospin relation

$$
A(\overline{B}^0 \to \pi^+ K^-) + \sqrt{2}A(\overline{B}^0 \to \pi^0 \overline{K}^0) = -A(B^- \to \pi^- \overline{K}^0) + \sqrt{2}A(B^- \to \pi^0 K^-). \tag{4.2}
$$

Likewise, a similar isospin relation holds for charge conjugate fields

$$
A(B^0 \to \pi^- K^+) + \sqrt{2}A(B^0 \to \pi^0 \overline{K}^0) = -A(B^+ \to \pi^+ K^0) + \sqrt{2}A(B^+ \to \pi^0 K^+). \tag{4.3}
$$

In the factorization approach [66, 67],

$$
\begin{aligned}
\mathcal{T}_{\rm SD} &= \kappa_1 \lambda_u a_1, \qquad \mathcal{C}_{\rm SD} = \kappa_2 \lambda_u a_2, \qquad \mathcal{P}_{\rm SD} = \kappa_1 \Big[\lambda_u (a_4^u + a_6^u r_\chi^K) + \lambda_c (a_4^c + a_6^c r_\chi^K)\Big], \\
\mathcal{P}_{\rm EW}^{\rm SD} &= \frac{3}{2}\kappa_2 (\lambda_u + \lambda_c)(-a_7 + a_9), \quad \mathcal{P}'^{\rm SD}_{\rm EW} = \frac{3}{2}\kappa_1 \Big[\lambda_u (a_8^u r_\chi^K + a_{10}^u) + \lambda_c (a_8^c r_\chi^K + a_{10}^c)\Big],
\end{aligned}
\tag{4.4}
$$

with $\lambda_q \equiv V_{qs}^* V_{qb}$, $r_\chi^K = 2m_K^2/[m_b(\mu)(m_s + m_q)(\mu)]$, and

$$
\kappa_1 = i\frac{G_F}{\sqrt{2}} f_K F_0^{B\pi}(m_K^2)(m_B^2 - m_\pi^2), \qquad \kappa_2 = i\frac{G_F}{\sqrt{2}} f_\pi F_0^{BK}(m_\pi^2)(m_B^2 - m_K^2). \tag{4.5}
$$

The parameters $a_i^{u,c}$ can be calculated in the QCD factorization approach [17]. They are basically the Wilson coefficients in conjunction with short-distance nonfactorizable corrections such as vertex

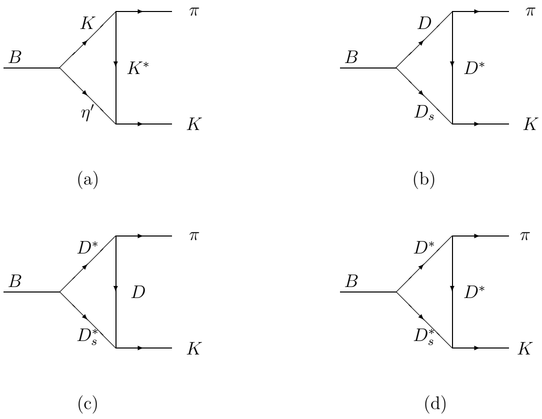

FIG. 5: Long-distance t-channel rescattering contributions to $B \to K\pi$.

corrections and hard spectator interactions. Formally, $a_i (i \neq 6, 8)$ and $a_{6,8} r_\chi^K$ should be renormalization scale and scheme independent. In practice, there exists some residual scale dependence in $a_i(\mu)$ to finite order. At the scale $\mu = 2.1$ GeV, the numerical results are

$$
\begin{aligned}
& a_1 = 0.9921 + i0.0369, \qquad a_2 = 0.1933 - i0.1130, \qquad a_3 = -0.0017 + i0.0037, \\
& a_4^u = -0.0298 - i0.0205, \qquad a_4^c = -0.0375 - i0.0079, \qquad a_5 = 0.0054 - i0.0050, \\
& a_6^u = -0.0586 - i0.0188, \qquad a_6^c = -0.0630 - i0.0056, \qquad a_7 = i5.4 \times 10^{-5}, \\
& a_8^u = (45.0 - i5.2) \times 10^{-5}, \qquad a_8^c = (44.2 + i3.1) \times 10^{-5}, \qquad a_9 = -(953.9 + i24.5) \times 10^{-5}, \\
& a_{10}^u = (-58.3 + i86.1) \times 10^{-5}, \qquad a_{10}^c = (-60.3 + i88.8) \times 10^{-5}.
\end{aligned} \tag{4.6}
$$

For current quark masses, we use $m_b(m_b) = 4.4$ GeV, $m_c(m_b) = 1.3$ GeV, $m_s(2.1\,\mathrm{GeV}) = 90$ MeV and $m_q/m_s = 0.044$.

Using the above coefficients $a_i^{u,c}$ leads to

$$
\begin{aligned}
\mathcal{B}(B^- \to \pi^- \overline{K}^0)_{\rm SD} &= 17.8 \times 10^{-6}, \qquad \mathcal{A}^{\rm SD}_{\pi^- K_S} = 0.01, \\
\mathcal{B}(\overline{B}^0 \to \pi^+ K^-)_{\rm SD} &= 13.9 \times 10^{-6}, \qquad \mathcal{A}^{\rm SD}_{\pi^+ K^-} = 0.04, \\
\mathcal{B}(B^- \to \pi^0 K^-)_{\rm SD} &= 9.7 \times 10^{-6}, \qquad \mathcal{A}^{\rm SD}_{\pi^0 K^-} = 0.08, \\
\mathcal{B}(\overline{B}^0 \to \pi^0 \overline{K}^0)_{\rm SD} &= 6.3 \times 10^{-6}, \qquad \mathcal{A}^{\rm SD}_{\pi^0 K_S} = -0.04\,,
\end{aligned} \tag{4.7}
$$

where we have used $|V_{cb}| = 0.041$, $|V_{ub}/V_{cb}| = 0.09$ and $\gamma = 60^\circ$ for quark mixing matrix elements.[7] From Table I it is clear that the predicted branching ratios are slightly smaller than experiment especially for $\overline{B}^0 \to \pi^0 \overline{K}^0$ where the prediction is about two times smaller than the data. Moreover, the predicted CP asymmetry for $\pi^+ K^-$ is opposite to the experimental measurement in sign. By now, direct CP violation in $\overline{B}^0 \to \pi^+ K^-$ has been established by both BaBar [14] and Belle [15].

---

[7] The notations (α, β, γ) and (ϕ_1, ϕ_2, ϕ_3) with $\alpha \equiv \phi_2, \beta \equiv \phi_1, \gamma \equiv \phi_3$ are in common usage for the angles of the unitarity triangle.

Leading long-distance rescattering contributions to $B \to K\pi$ are shown in Fig. 5. The absorptive amplitudes are

$$\begin{aligned}
\mathcal{A}bs\,(5a) &= -\int_{-1}^{1} \frac{|\vec{p}_1| d\cos\theta}{16\pi m_B}\, g_{K^*K\pi}\, g_{K^*K\eta'} A(\overline{B}^0 \to \overline{K}^0\eta')\, \frac{F^2(t,m_\rho)}{t-m_{K^*}^2}\, H_1,\\
\mathcal{A}bs\,(5b) &= \int_{-1}^{1} \frac{|\vec{p}_1| d\cos\theta}{16\pi m_B}\, g_{D^*D\pi}\, g_{D^*D_sK} A(\overline{B}^0 \to D^+D_s^-) \frac{F^2(t,m_{D^*})}{t-m_{D^*}^2}\, J_2,\\
\mathcal{A}bs\,(5c) &= -i\frac{G_F}{\sqrt{2}} V_{cb}V_{cs}^* f_{D_s^*} m_{D_s^*} \int_{-1}^{1} \frac{|\vec{p}_1| d\cos\theta}{16\pi m_B}\, g_{D^*D\pi}\, g_{D_s^*DK}\, \frac{F^2(t,m_D)}{t-m_D^2}\\
&\times \Big[(m_B+m_{D^*})A_1^{BD^*}(m_{D_s^*}^2)H_4 - \frac{2A_2^{BD^*}(m_{D_s^*}^2)}{m_B+m_{D^*}}H_4'\Big],\\
\mathcal{A}bs\,(5d) &= i\frac{G_F}{\sqrt{2}} V_{cb}V_{cs}^* f_{D_s^*} m_{D_s^*} \int_{-1}^{1} \frac{|\vec{p}_1| d\cos\theta}{16\pi m_B}\, g_{D^*D^*\pi}\, g_{D_s^*DK}\, \frac{F^2(t,m_{D^*})}{t-m_{D^*}^2}\\
&\times \Big[(m_B+m_{D^*})A_1^{BD^*}(m_{D_s^*}^2)J_5 - \frac{2A_2^{BD^*}(m_{D_s^*}^2)}{m_B+m_{D^*}}J_5'\Big],
\end{aligned} \tag{4.8}$$

with

$$J_2 = -p_3\cdot p_4 - \frac{(p_1\cdot p_3 - m_3^2)(p_2\cdot p_4 - m_4^2)}{m_{D^*}^2}, \tag{4.9}$$

and J_5, J_5' can be obtained from H_5 and H_5', respectively, under the replacement of $p_3 \leftrightarrow p_4$.

Hence,

$$\begin{aligned}
A(B^- \to \pi^-\overline{K}^0) &= A(B^- \to \pi^-\overline{K}^0)_{\rm SD} + i\mathcal{A}bs(5a+5b+5c+5d),\\
A(\overline{B}^0 \to \pi^+K^-) &= A(\overline{B}^0 \to \pi^+K^-)_{\rm SD} + i\mathcal{A}bs(5a+5b+5c+5d),\\
A(B^- \to \pi^0K^-) &= A(B^- \to \pi^0K^-)_{\rm SD} + \frac{i}{\sqrt{2}}\mathcal{A}bs(5a+5b+5c+5d),\\
A(\overline{B}^0 \to \pi^0\overline{K}^0) &= A(\overline{B}^0 \to \pi^0\overline{K}^0)_{\rm SD} - \frac{i}{\sqrt{2}}\mathcal{A}bs(5a+5b+5c+5d).
\end{aligned} \tag{4.10}$$

As noticed before, the rescattering diagrams 5(b)-5(d) with charm intermediate states contribute only to the topological penguin graph. Indeed, it has been long advocated that charming-penguin long-distance contributions increase significantly the $B \to K\pi$ rates and yield better agreement with experiment [33]. For a recent work along this line, see [34].

To proceed with the numerical calculation, we use the experimental value $A(\overline{B}^0 \to \overline{K}^0\eta') = (-7.8+i4.5)\times 10^{-8}$ GeV with the phase determined from the topological approach [10]. For strong couplings, $g_{K^*K\pi}$ defined for $K^{*+} \to K^0\pi^+$ is fixed to be 4.6 from the measured K^* width, and the $K^*K\eta'$ coupling is fixed to be

$$g_{K^{*+}\to K^+\eta'} = \frac{1}{\sqrt{3}} g_{K^{*+}\to K^+\pi^0} = \frac{1}{\sqrt{6}} g_{K^{*+}\to K^0\pi^+} \tag{4.11}$$

by approximating the η' wave function by $\eta' = \frac{1}{\sqrt{6}}(u\bar{u}+d\bar{d}+2s\bar{s})$. A χ^2 fit to the measured decay rates yields $\eta_{D^{(*)}} = 0.69$ for the exchanged particle D or D^*, while η_{K^*} is less constrained as the exchanged K^* particle contribution [Fig. 5(a)] is suppressed relative to the D or D^* contribution. Since the decay $B \to D\overline{D}_s$ is quark-mixing favored over $B \to D\pi$, the cutoff scale here thus should be lower than that in $B \to D\pi$ decays where $\eta_{D^{(*)}} = 2.2$ as it should be. As before, we allow 15%

TABLE II: Comparison of experimental data and fitted outputs for CP averaged branching ratios (top, in units of 10^{-6}) and the theoretical predictions of CP asymmetries (bottom) for $B \to \pi K$.

Mode	Expt.	SD	SD+LD
$\mathcal{B}(B^- \to \pi^- \overline{K}^0)$	24.1 ± 1.3	17.8	$23.3^{+4.6}_{-3.7}$
$\mathcal{B}(\overline{B}^0 \to \pi^+ K^-)$	18.2 ± 0.8	13.9	$19.3^{+5.0}_{-3.1}$
$\mathcal{B}(B^- \to \pi^0 K^-)$	12.1 ± 0.8	9.7	$12.5^{+2.6}_{-1.6}$
$\mathcal{B}(\overline{B}^0 \to \pi^0 \overline{K}^0)$	11.5 ± 1.0	6.3	$9.1^{+2.5}_{-1.6}$
$\mathcal{A}_{\pi^- K_S}$	-0.02 ± 0.03	0.01	$0.024^{+0.0}_{-0.001}$
$\mathcal{A}_{\pi^+ K^-}$	-0.11 ± 0.02	0.04	$-0.14^{+0.01}_{-0.03}$
$\mathcal{A}_{\pi^0 K^-}$	0.04 ± 0.04	0.08	$-0.11^{+0.02}_{-0.04}$
$\mathcal{A}_{\pi^0 K_S}$	-0.09 ± 0.14	-0.04	$0.031^{+0.008}_{-0.014}$
$\mathcal{S}_{\pi^0 K_S}$	0.34 ± 0.28	0.79	0.78 ± 0.01

uncertainty for the $\Lambda_{\rm QCD}$ scale and obtain the branching ratios and CP asymmetries as shown in Table II, where use has been made of $f_{D_s^*} \approx f_{D_s} = 230$ MeV and the heavy quark symmetry relations

$$g_{D^* D_s K} = \sqrt{\frac{m_{D_s}}{m_D}}\, g_{D^* D\pi}, \qquad g_{D_s^* DK} = \sqrt{\frac{m_{D_s^*}}{m_{D^*}}}\, g_{D^* D\pi}. \tag{4.12}$$

It is found that the absorptive contribution from the $K\eta'$ intermediate states is suppressed relative to $D^{(*)}\overline{D}_s^{(*)}$ as the latter are quark-mixing-angle most favored, i.e. $B \to D^{(*)}\overline{D}_s^{(*)} \gg B \to K\eta'$. Evidently, all πK modes are sensitive to the cutoffs Λ_{D^*} and Λ_D. We see that the sign of the direct CP partial rate asymmetry for $\overline{B}^0 \to \pi^+ K^-$ is flipped after the inclusion of rescattering and the predicted $\mathcal{A}_{\pi^+ K^-} = -0.14^{+0.01}_{-0.03}$ is now in good agreement with the world average of -0.11 ± 0.02. Note that the branching ratios for all πK modes are enhanced by $(30 \sim 40)\%$ via final-state rescattering.

Note that there is a sum-rule relation [28]

$$2\Delta\Gamma(\pi^0 K^-) - \Delta\Gamma(\pi^- \overline{K}^0) - \Delta\Gamma(\pi^+ K^-) + 2\Delta\Gamma(\pi^0 \overline{K}^0) = 0, \tag{4.13}$$

based on isospin symmetry. Hence, a violation of the above relation would provide an important test for the presence of electroweak penguin contributions. It is interesting to check how good the above relation works in light of the present data. We rewrite it as

$$\frac{\mathcal{A}_{\pi^+ K^-}\mathcal{B}(\pi^+ K^-) - 2\mathcal{A}_{\pi^0 \overline{K}^0}\mathcal{B}(\pi^0 \overline{K}^0)}{2\mathcal{A}_{\pi^0 K^-}\mathcal{B}(\pi^0 K^-) - \mathcal{A}_{\pi^- \overline{K}^0}\mathcal{B}(\pi^- \overline{K}^0)} = \frac{\tau_{\overline{B}^0}}{\tau_{B^-}}. \tag{4.14}$$

The left hand side of the above equation yields 0.07 ± 2.28, while the right hand side is 0.923 ± 0.014 [50]. Although the central values of the data seem to imply the need of non-vanishing electroweak penguin contributions and/or some New Physics, it is not conclusive yet with present data. For further implications of this sum-rule relation, see [28].

TABLE III: Experimental data for CP averaged branching ratios (top, in units of 10^{-6}) and CP asymmetries (bottom) for $B \to \pi\pi$ [50, 65].

Mode	BaBar	Belle	CLEO	Average
$\overline{B}^0 \to \pi^+\pi^-$	$4.7 \pm 0.6 \pm 0.2$	$4.4 \pm 0.6 \pm 0.3$	$4.5^{+1.4+0.5}_{-1.2-0.4}$	4.6 ± 0.4
$\overline{B}^0 \to \pi^0\pi^0$	$1.17 \pm 0.32 \pm 0.10$	$2.32^{+0.44+0.22}_{-0.48-0.18}$	< 4.4	1.51 ± 0.28
$B^- \to \pi^-\pi^0$	$5.8 \pm 0.6 \pm 0.4$	$5.0 \pm 1.2 \pm 0.5$	$4.6^{+1.8+0.6}_{-1.6-0.7}$	5.5 ± 0.6
$\mathcal{A}_{\pi^+\pi^-}$	$0.09 \pm 0.15 \pm 0.04$	$0.58 \pm 0.15 \pm 0.07$		0.31 ± 0.24[a]
$\mathcal{S}_{\pi^+\pi^-}$	$-0.30 \pm 0.17 \pm 0.03$	$-1.00 \pm 0.21 \pm 0.07$		-0.56 ± 0.34[a]
$\mathcal{A}_{\pi^0\pi^0}$	$0.12 \pm 0.56 \pm 0.06$	$0.43 \pm 0.51^{+0.17}_{-0.16}$		0.28 ± 0.39
$\mathcal{A}_{\pi^-\pi^0}$	$-0.01 \pm 0.10 \pm 0.02$	$-0.02 \pm 0.10 \pm 0.01$		-0.02 ± 0.07

[a] Error-bars of $\mathcal{A}_{\pi^+\pi^-}$ and $S_{\pi^+\pi^-}$ are scaled by $S = 2.2$ and 2.5, respectively. When taking into account the measured correlation between $\mathcal{A}$ and S, the averages are cited by Heavy Flavor Averaging Group [65] to be $\mathcal{A}_{\pi^+\pi^-} = 0.37 \pm 0.11$ and $S_{\pi^+\pi^-} = -0.61 \pm 0.14$ with errors not being scaled up.

V. $B \to \pi\pi$ DECAYS

A. Short-distance contributions and Experimental Status

The experimental results of CP averaged branching ratios and CP asymmetries for charmless $B \to \pi\pi$ decays are summarized in Table III. For a neutral B meson decay into a CP eigenstate f, CP asymmetry is defined by

$$\frac{\Gamma(\overline{B}(t) \to f) - \Gamma(B(t) \to f)}{\Gamma(\overline{B}(t) \to f) + \Gamma(B(t) \to f)} = \mathcal{S}_f \sin(\Delta m t) - \mathcal{C}_f \cos(\Delta m t), \tag{5.1}$$

where Δm is the mass difference of the two neutral B eigenstates, $\mathcal{S}_f$ is referred to as mixing-induced CP asymmetry and $\mathcal{A}_f = -\mathcal{C}_f$ is the direct CP asymmetry. Note that the Belle measurement [12] gives an evidence of CP violation in $B^0 \to \pi^+\pi^-$ decays at the level of 5.2 standard deviations, while this has not been confirmed by BaBar [20]. As a result, we follow Particle Data Group [50] to use a scale factor of 2.2 and 2.5, respectively, for the error-bars in $\mathcal{A}_{\pi^+\pi^-}$ and $S_{\pi^+\pi^-}$ (see Table III). The CP-violating parameters $\mathcal{C}_f$ and $\mathcal{S}_f$ can be expressed as

$$\mathcal{C}_f = \frac{1 - |\lambda_f|^2}{1 + |\lambda_f|^2}, \qquad \mathcal{S}_f = \frac{2\,\mathrm{Im}\lambda_f}{1 + |\lambda_f|^2}, \tag{5.2}$$

where

$$\lambda_f = \frac{q}{p}\,\frac{A(\overline{B}^0 \to f)}{A(B^0 \to f)}. \tag{5.3}$$

For $\pi\pi$ modes, $q/p = e^{-i2\beta}$ with $\sin 2\beta = 0.726 \pm 0.037$ [68].

The $B \to \pi\pi$ decay amplitudes have the general expressions

$$A(\overline{B}^0 \to \pi^+\pi^-) \ = \ \mathcal{T} + \mathcal{P} + \frac{2}{3}\mathcal{P}'_{\rm EW} + \mathcal{E} + \mathcal{P}_A + \mathcal{V},$$

$$
\begin{aligned}
A(\overline{B}^0 \to \pi^0\pi^0) &= -\frac{1}{\sqrt{2}}(\mathcal{C} - \mathcal{P} + \mathcal{P}_{\rm EW} + \frac{1}{3}\mathcal{P}'_{\rm EW} - \mathcal{E} - \mathcal{P}_A - \mathcal{V}), \qquad (5.4)\\
A(B^- \to \pi^-\pi^0) &= \frac{1}{\sqrt{2}}(\mathcal{T} + \mathcal{C} + \mathcal{P}_{\rm EW} + \mathcal{P}'_{\rm EW}),
\end{aligned}
$$

where $\mathcal{V}$ is the vertical W-loop topological diagram (see Sec. II). In the factorization approach, the quark diagram amplitudes are given by [66, 67]

$$
\begin{aligned}
\mathcal{T}_{\rm SD} &= \kappa\lambda_u a_1, \qquad \mathcal{C}_{\rm SD} = \kappa\lambda_u a_2, \qquad \mathcal{P}_{\rm SD} = \kappa\Big[\lambda_u(a_4^u + a_6^u r_\chi^\pi) + \lambda_c(a_4^c + a_6^c r_\chi^\pi)\Big],\\
\mathcal{P}_{\rm EW}^{\rm SD} &= \frac{3}{2}\kappa(\lambda_u + \lambda_c)(-a_7 + a_9), \quad \mathcal{P}'^{\rm SD}_{\rm EW} = \frac{3}{2}\kappa\Big[\lambda_u(a_8^u r_\chi^\pi + a_{10}^u) + \lambda_c(a_8^c r_\chi^\pi + a_{10}^c)\Big], \qquad (5.5)
\end{aligned}
$$

where $\lambda_q \equiv V_{qd}^* V_{qb}$, $\kappa \equiv i\frac{G_F}{\sqrt{2}} f_\pi F_0^{B\pi}(m_\pi^2)(m_B^2 - m_\pi^2)$ and the chiral enhancement factor $r_\chi^\pi = 2m_\pi^2/[m_b(\mu)(m_u + m_d)(\mu)]$ arises from the $(S-P)(S+P)$ part of the penguin operator Q_6. The explicit expressions of the weak annihilation amplitude $\mathcal{E}$ in QCD factorization can be found in [17]. It is easily seen that the decay amplitudes satisfy the isospin relation

$$
A(\overline{B}^0 \to \pi^+\pi^-) = \sqrt{2}\Big[A(B^- \to \pi^-\pi^0) + A(\overline{B}^0 \to \pi^0\pi^0)\Big]. \qquad (5.6)
$$

Note that there is another isospin relation for charge conjugate fields

$$
A(B^0 \to \pi^+\pi^-) = \sqrt{2}\Big[A(B^+ \to \pi^+\pi^0) + A(B^0 \to \pi^0\pi^0)\Big]. \qquad (5.7)
$$

Substituting the coefficients $a_i^{u,c}$ given in Eq. (4.6) into Eqs. (5.4) and (5.5) leads to[8]

$$
\begin{aligned}
\mathcal{B}(\overline{B}^0 \to \pi^+\pi^-)_{\rm SD} &= 7.6 \times 10^{-6}, \qquad \mathcal{A}^{\rm SD}_{\pi^+\pi^-} = -0.05,\\
\mathcal{B}(\overline{B}^0 \to \pi^0\pi^0)_{\rm SD} &= 2.7 \times 10^{-7}, \qquad \mathcal{A}^{\rm SD}_{\pi^0\pi^0} = 0.61, \qquad (5.8)\\
\mathcal{B}(B^- \to \pi^-\pi^0)_{\rm SD} &= 5.1 \times 10^{-6}, \qquad \mathcal{A}^{\rm SD}_{\pi^-\pi^0} = 5 \times 10^{-5}.
\end{aligned}
$$

To obtain the above branching ratios and CP asymmetries we have applied the form factor $F_0^{B\pi}(0) = 0.25$ as obtained from the covariant light-front approach [63] and neglected the W-annihilation contribution. Nevertheless, the numerical results are similar to that in [18] (see Tables 9 and 10 of [18]) except for $\mathcal{A}_{\pi^-\pi^0}$ for which we obtain a sign opposite to [18].

We see that the predicted $\pi^+\pi^-$ rate is too large, whereas $\pi^0\pi^0$ is too small compared to experiment (see Table III). Furthermore, the predicted value of direct CP asymmetry, $A^{SD}_{\pi^+\pi^-} = -0.05$, is in disagreement with the experimental average of 0.31 ± 0.24. [9] In the next subsection, we will study the long-distance rescattering effect to see its impact on CP violation.

In the topological analysis in [10], it is found that in order to describe $B \to \pi\pi$ and $B \to \pi K$ branching ratios and CP asymmetries, one must introduce a large value of $|\mathcal{C}/\mathcal{T}|$ and a non-trivial phase between $\mathcal{C}$ and $\mathcal{T}$. Two different fit procedures have been adopted in [10] to fit $\pi\pi$ and πK

---

[8] Charge conjugate modes are implicitly included in the flavor-averaged branching ratios throughout this paper.

[9] In the so-called perturbative QCD approach for nonleptonic B decays [69], the signs of $\pi^+\pi^-$ and $K^-\pi^+$ CP asymmetries are correctly predicted and the calculated magnitudes are compatible with experiment.

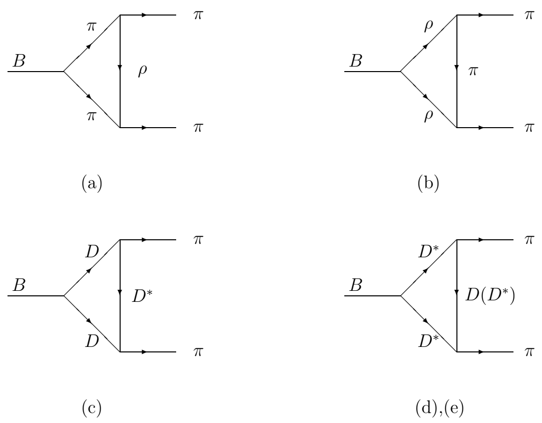

FIG. 6: Long-distance t-channel rescattering contributions to $B \to \pi\pi$. Graphs (d) and (e) correspond to the exchanged particles D and D^*, respectively.

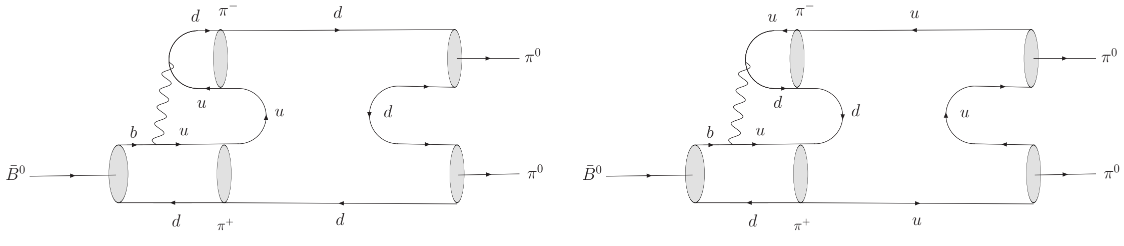

(a) (b)

FIG. 7: Contributions to $\overline{B}^0 \to \pi^0\pi^0$ from the color-allowed weak decay $\overline{B}^0 \to \pi^+\pi^-$ followed by quark annihilation processes (a) and (b). They have the same topologies as the penguin and W-exchange graphs, respectively.

data points by assuming negligible weak annihilation contributions. One of the fits yields[10]

$$\gamma = (65^{+13}_{-35})^\circ, \qquad \frac{\mathcal{C}}{\mathcal{T}}\bigg|_{\pi\pi,\pi K} = (0.46^{+0.43}_{-0.30})\exp[-i(94^{+43}_{-52})]^\circ. \tag{5.9}$$

The result for the ratio $\mathcal{C}/\mathcal{T}$ in charmless B decays is thus consistent with (3.5) extracted from $B \to D\pi$.

B. Long-distance contributions to $B \to \pi\pi$

Some leading rescattering contributions to $B \to \pi\pi$ are shown in Figs. 6(a)-6(e). While all the five diagrams contribute to $\overline{B}^0 \to \pi^+\pi^-$ and $\overline{B}^0 \to \pi^0\pi^0$, only the diagrams 6(a) and 6(b) contribute to $B^- \to \pi^-\pi^0$. Since the $\pi^-\pi^0$ final state in B^- decay must be in $I = 2$, while the intermediate $D\overline{D}$ state has $I=0$ or $I=1$, it is clear that $B^- \to \pi^-\pi^0$ cannot receive rescattering from $B^- \to D^-D^0 \to \pi^-\pi^0$. It should be stressed that all the graphs in Fig. 6 contribute to the penguin amplitude. To see this, let us consider Fig. 7 which is one of the manifestations of Fig. 6(a) at the quark level. (Rescattering diagrams with quark exchange are not shown in Fig. 7.) It is easily seen that Figs. 7(a) and 7(b) can be redrawn as the topologies $\mathcal{P}$ and $\mathcal{E}$, respectively. Likewise, Figs. 6(c)-(e) correspond to the topological $\mathcal{P}$. Consequently,

---

[10] The other fit yields $|\mathcal{C}/\mathcal{T}| = 1.43^{+0.40}_{-0.31}$ which is unreasonably too large. This ratio is substantially reduced once the up and top quark mediated penguins are taken into account [10].

$$\begin{aligned}
\mathcal{T} &= \mathcal{T}_{\rm SD}, \\
\mathcal{C} &= \mathcal{C}_{\rm SD} + i\mathcal{A}bs\,(6a+6b), \\
\mathcal{E} &= \mathcal{E}_{\rm SD} + i\mathcal{A}bs\,(6a+6b), \\
\mathcal{P} &= \mathcal{P}_{\rm SD} + i\mathcal{A}bs\,(6a+6b+6c+6d+6e).
\end{aligned} \tag{5.10}$$

Hence,[11]

$$\begin{aligned}
A(\overline{B}^0 \to \pi^+\pi^-) &= A(\overline{B}^0 \to \pi^+\pi^-)_{\rm SD} + 2i\mathcal{A}bs\,(6a+6b) + i\mathcal{A}bs(6c+6d+6e), \\
A(\overline{B}^0 \to \pi^0\pi^0) &= A(\overline{B}^0 \to \pi^0\pi^0)_{\rm SD} + \frac{1}{\sqrt{2}} i\mathcal{A}bs\,(6a+6b+6c+6d+6e), \\
A(B^- \to \pi^-\pi^0) &= A(B^- \to \pi^-\pi^0)_{\rm SD} + \frac{1}{\sqrt{2}} i\mathcal{A}bs\,(6a+6b),
\end{aligned} \tag{5.11}$$

The absorptive parts of $B \to M_1(p_1)M_2(p_2) \to \pi(p_3)\pi(p_4)$ with $M_{1,2}$ being the intermediate states in Fig. 6 are

$$\begin{aligned}
\mathcal{A}bs\,(6a) &= -\int_{-1}^{1} \frac{|\vec{p}_1| d\cos\theta}{16\pi m_B}\, g^2_{\rho\pi\pi} A(\overline{B}^0 \to \pi^+\pi^-)\, \frac{F^2(t,m_\rho)}{t-m^2_\rho+im_\rho\Gamma_\rho}\, H_1, \\
\mathcal{A}bs\,(6b) &= -i\frac{G_F}{\sqrt{2}} V_{ub}V^*_{ud} f_\rho m_\rho \int_{-1}^{1} \frac{|\vec{p}_1| d\cos\theta}{16\pi m_B}\, g^2_{\rho\pi\pi}\, \frac{F^2(t,m_\pi)}{t-m^2_\pi} \\
&\quad\times \Big[(m_B+m_\rho)A_1^{B\rho}(m^2_\pi)4H_3 - \frac{2A_2^{B\rho}(m^2_\pi)}{m_B+m_\rho}4H'_3\Big], \\
\mathcal{A}bs\,(6c) &= \int_{-1}^{1} \frac{|\vec{p}_1| d\cos\theta}{16\pi m_B}\, g^2_{D^*D\pi} A(\overline{B}^0 \to D^+D^-) \frac{F^2(t,m_{D^*})}{t-m^2_{D^*}}\, J_2, \\
\mathcal{A}bs\,(6d) &= -i\frac{G_F}{\sqrt{2}} V_{cb}V^*_{cd} f_{D^*} m_{D^*} \int_{-1}^{1} \frac{|\vec{p}_1| d\cos\theta}{16\pi m_B}\, g^2_{D^*D\pi}\, \frac{F^2(t,m_D)}{t-m^2_D} \\
&\quad\times \Big[(m_B+m_{D^*})A_1^{BD^*}(m^2_{D^*})H_4 - \frac{2A_2^{BD^*}(m^2_{D^*})}{m_B+m_{D^*}}H'_4\Big], \\
\mathcal{A}bs\,(6e) &= i\frac{G_F}{\sqrt{2}} V_{cb}V^*_{cd} f_{D^*} m_{D^*} \int_{-1}^{1} \frac{|\vec{p}_1| d\cos\theta}{16\pi m_B}\, g^2_{D^*D^*\pi}\, \frac{F^2(t,m_{D^*})}{t-m^2_{D^*}} \\
&\quad\times \Big[(m_B+m_{D^*})A_1^{BD^*}(m^2_{D^*})J_5 - \frac{2A_2^{BD^*}(m^2_{D^*})}{m_B+m_{D^*}}J'_5\Big].
\end{aligned} \tag{5.12}$$

---

[11] In a similar context, it has been argued in [31] that the analogous Figs. 6(a)-(b) do not contribute to the decay $D^0 \to \pi^0\pi^0$ owing to the cancellation between the quark annihilation and quark exchange diagrams at the quark level. However, a careful examination indicates that the quark annihilation processes gain an additional factor of 2 as noticed in [38]. Consequently, the intermediate $\pi^+\pi^-$ state does contribute to $B^0 \to \pi^0\pi^0$ and $D^0 \to \pi^0\pi^0$ via final-state rescattering.

Since in SU(3) flavor limit the final-state rescattering parts of Figs. 6(c)-(e) should be the same as that of Figs. 5(b)-(d), it means that the cutoff scales Λ_D and Λ_{D^*} appearing in the rescattering diagrams of $B \to \pi\pi$ are identical to that in $B \to \pi K$ decays in the limit of SU(3) symmetry. Allowing 20% SU(3) breaking and recalling that $\eta_{D^{(*)}} = 0.69$ in $B \to \pi K$ decays, we choose $\eta_{D^{(*)}} = \eta_\rho = 0.83$ for $B \to \pi\pi$ decays. Because the decay $\overline{B}^0 \to D^+D^-$ is Cabibbo suppressed relative to $\overline{B}^0 \to D^+D_s^-$, it is evident that the absorptive part of the charm loop diagrams, namely, Figs. 6(c)-(e), cannot enhance the $\pi^0\pi^0$ rate sizably. However, since the branching ratio of the short-distance induced $B^0 \to \pi^+\pi^-$, namely 7.6×10^{-6} [see Eq. (5.8)], already exceeds the measured value substantially, this means that a dispersive part of the long-distance rescattering amplitude must be taken into account. This dispersive part also provides the main contribution to the $\pi^0\pi^0$ rate. There is a subtle point here: If the dispersive contribution is fixed by fitting to the measured $B \to \pi\pi$ rates, the χ^2 value of order 0.2 is excellent and the predicted direct CP violation for $\pi^+\pi^-$ agrees with experiment. Unfortunately, the calculated mixing-induced CP-violating parameter S will have a wrong sign. Therefore, we need to accommodate the data of branching ratios and the parameter S simultaneously. We find (in units of GeV)

$$\mathcal{D}is\, A = 1.5 \times 10^{-6} V_{cb}V_{cd}^* - 6.7 \times 10^{-7} V_{ub}V_{ud}^*, \tag{5.13}$$

for $\eta_\pi = \eta_\rho = 1.2$. It should be stressed that these dispersive contributions cannot arise from the rescattering processes in Figs. 6(a)-(e) because they will also contribute to $B \to K\pi$ decays via SU(3) symmetry and modify all the previous predictions very significantly. As pointed out in [38], there exist $\pi\pi \to \pi\pi$ and $D\bar{D} \to \pi\pi$ meson annihilation diagrams in which the two initial quark pairs in the zero isospin configuration are destroyed and then created. Such annihilation diagrams have the same topology as the vertical W-loop diagram $\mathcal{V}$ as mentioned in Sec. II. Hence, this FSI mechanism occurs in $\pi^+\pi^-$ and $\pi^0\pi^0$ but not in the $K\pi$ modes. That is, the dispersive term given in Eq. (5.13) does not contribute to $B \to K\pi$ decays.

The resultant amplitudes are then given by (in units of GeV)[12]

$$\begin{aligned}
A(\overline{B}^0 \to \pi^+\pi^-) &= (2.03 + i2.02) \times 10^{-8} + (1.40 - i0.77) \times 10^{-8} - i1.64 \times 10^{-8}, \\
A(B^0 \to \pi^+\pi^-) &= (-2.21 + i2.04) \times 10^{-8} - (2.21 - i2.05) \times 10^{-8} - i1.64 \times 10^{-8}, \\
A(\overline{B}^0 \to \pi^0\pi^0) &= (-6.15 + i3.46) \times 10^{-9} + (7.89 - i2.73) \times 10^{-9} - i1.07 \times 10^{-8}, \\
A(B^0 \to \pi^0\pi^0) &= (3.32 + i1.11) \times 10^{-9} + (3.32 + i1.11) \times 10^{-9} - i1.07 \times 10^{-8}, \\
A(B^- \to \pi^-\pi^0) &= (2.05 + i1.08) \times 10^{-8} + (2.07 - i2.73) \times 10^{-9}, \\
A(B^+ \to \pi^+\pi^0) &= (-1.90 + i1.34) \times 10^{-8} - (1.90 - i1.34) \times 10^{-8},
\end{aligned} \tag{5.14}$$

where the numbers in the first parentheses on the right hand side are due to short-distance contributions, while the second term in parentheses and the third term arise from the absorptive and dispersive parts, respectively, of long-distance rescattering. (The dispersive contribution to $B^- \to \pi^-\pi^0$ is too small and can be neglected.) Form the above equation, it is clear that the

---

[12] Note that $B \to PP$ and $B \to VV$ decay amplitudes are accompanied by a factor of i in our phase convention [see Eq. (3.8)].

TABLE IV: Same as Table II except for $B \to \pi\pi$ decays.

Mode	Expt.	SD	SD+LD
$\mathcal{B}(\overline{B}^0 \to \pi^+\pi^-)$	4.6 ± 0.4	7.6	$4.6^{+0.2}_{-0.1}$
$\mathcal{B}(\overline{B}^0 \to \pi^0\pi^0)$	1.5 ± 0.3	0.3	$1.5^{+0.1}_{-0.0}$
$\mathcal{B}(B^- \to \pi^-\pi^0)$	5.5 ± 0.6	5.1	5.4 ± 0.0
$\mathcal{A}_{\pi^+\pi^-}$	0.31 ± 0.24	-0.05	$0.35^{+0.15}_{-0.14}$
$\mathcal{S}_{\pi^+\pi^-}$	-0.56 ± 0.34	-0.66	$-0.16^{+0.15}_{-0.16}$
$\mathcal{A}_{\pi^0\pi^0}$	0.28 ± 0.39	0.56	$-0.30^{+0.01}_{-0.04}$
$\mathcal{A}_{\pi^-\pi^0}$	-0.02 ± 0.07	5×10^{-5}	$-0.009^{+0.002}_{-0.001}$

long-distance dispersive amplitude gives the dominant contribution to $\pi^0\pi^0$ and contributes destructively with the short-distance $\pi^+\pi^-$ amplitude. The corresponding CP averaged branching ratios and direct CP asymmetries are shown in Table IV, where the ranges indicate the uncertainties of the QCD scale $\Lambda_{\rm QCD}$ by 15%. We only show the ranges due to the cut-off as numerical predictions depend sensitively on it. It is evident that the $\pi^-\pi^0$ rate is not significantly affected by FSIs, whereas the $\pi^+\pi^-$ and $\pi^0\pi^0$ modes receive sizable long-distance corrections.[13]

Since the branching ratio of $B^0 \to D^+D^-$ is about 50 times larger than that of $B^0 \to \pi^+\pi^-$, it has been proposed in [35] that a small mixing of the $\pi\pi$ and $D\overline{D}$ channels can account for the puzzling observation of $B^0 \to \pi^0\pi^0$. However, the aforementioned dispersive part of final-state rescattering was not considered in [35] and consequently the predicted branching ratio $\mathcal{B}(B^0 \to \pi^+\pi^-) \sim 11 \times 10^{-6}$ is too large compared to experiment. In the present work, we have shown that it is the dispersive part of long-distance rescattering from $D\bar{D} \to \pi\pi$ that accounts for the suppression of the $\pi^+\pi^-$ mode and the enhancement of $\pi^0\pi^0$.

As far as CP rate asymmetries are concerned, the long-distance effect will generate a sizable direct CP violation for $\pi^+\pi^-$ with a correct sign. Indeed, the signs of direct CP asymmetries in $B \to \pi\pi$ decays are all flipped by the final-state rescattering effects. It appears that FSIs lead to CP asymmetries for $\pi^+\pi^-$ and $\pi^0\pi^0$ opposite in sign. The same conclusion is also reached in the $\pi\pi$ and $D\overline{D}$ mixing model [35] and in an analysis of charmless B decay data [38] based on a quasi-elastic scattering model [57] (see also [40]). However, the perturbative QCD approach based on the k_T factorization theorem predicts the same sign for $\pi^+\pi^-$ and $\pi^0\pi^0$ CP asymmetries, namely, $\mathcal{A}_{\pi^+\pi^-} = 0.23 \pm 0.07$ and $\mathcal{A}_{\pi^0\pi^0} = 0.30 \pm 0.10$ [69]. Moreover, a global analysis of charmless $B \to PP$ decays based on the topological approach yields $\mathcal{A}_{\pi^+\pi^-} \sim 0.33$ and $\mathcal{A}_{\pi^0\pi^0} \sim 0.53$ [10] (see also [70] for the same conclusion reached in a different context). It is worth mentioning that the isospin analyses of $B \to \pi\pi$ decay data in [71] and [72] all indicate that given the allowed region of the $\pi^0\pi^0$ branching ratio, there is practically no constraints on $\pi^0\pi^0$ direct CP violation from BaBar and/or Belle data. And hence the sign of $\mathcal{A}_{\pi^0\pi^0}$ is not yet fixed. At any rate, even a sign measurement of direct CP asymmetry in $\pi^0\pi^0$ will provide a nice testing ground for discriminating between the FSI and PQCD approaches for CP violation.

---

[13] A different mechanism for understanding the $\pi\pi$ data is advocated in [38] where FSI is studied based on a simple two parameter model by considering a quasi-elastic scattering picture. A simultaneous fit to the measured rates *and* CP asymmetries indicates that $\pi^+\pi^-$ is suppressed by the dispersive part of $\pi\pi \to \pi\pi$ rescattering, while $\pi^0\pi^0$ is enhanced via the absorptive part. This requires a large SU(3) rescattering phase difference of order $90^\circ \sim 100^\circ$. The fitted $\pi^-\pi^0$ rate is somewhat below experiment. In the present work, it is the dispersive part of the rescattering from $D\bar{D}$ to $\pi\pi$ via annihilation that plays the role for the enhancement of $\pi^0\pi^0$ and suppression of $\pi^+\pi^-$.

It is interesting to notice that based on SU(3) symmetry, there are some model-independent relations for direct CP asymmetries between $\pi\pi$ and πK modes [73]

$$\Delta\Gamma(\pi^+\pi^-) = -\Delta\Gamma(\pi^+K^-), \qquad \Delta\Gamma(\pi^0\pi^0) = -\Delta\Gamma(\pi^0\overline{K}^0), \tag{5.15}$$

with $\Delta\Gamma(f_1f_2) \equiv \Gamma(\overline{B} \to f_1f_2) - \Gamma(B \to f_1f_2)$. From the measured rates, it follows that

$$\mathcal{A}_{\pi^+\pi^-} \approx -4.0\,\mathcal{A}_{\pi^+K^-}, \qquad \mathcal{A}_{\pi^0\pi^0} \approx -7.7\,\mathcal{A}_{\pi^0\overline{K}^0}. \tag{5.16}$$

It appears that the first relation is fairly satisfied by the world averages of CP asymmetries. Since direct CP violation in the π^+K^- mode is now established by B factories, the above relation implies that the $\pi^+\pi^-$ channel should have $\mathcal{A}_{\pi^+\pi^-} \sim \mathcal{O}(0.4)$ with a positive sign. For the neutral modes more data are clearly needed as the current experimental results have very large errors.

Finally we present the results for the ratios $\mathcal{C}/\mathcal{T}$, $\mathcal{E}/\mathcal{T}$ and $\mathcal{V}/\mathcal{T}$:

$$\frac{\mathcal{C}}{\mathcal{T}}\bigg|_{\pi\pi} = 0.36\,e^{-i55^\circ}, \qquad \frac{\mathcal{E}}{\mathcal{T}}\bigg|_{\pi\pi} = 0.19\,e^{-i85^\circ}, \qquad \frac{\mathcal{V}}{\mathcal{T}}\bigg|_{\pi\pi} = 0.56\,e^{i230^\circ}, \tag{5.17}$$

to be compared with the short-distance result $\mathcal{C}/\mathcal{T}|_{\pi\pi}^{\rm SD} = a_2/a_1 = 0.23\exp(-i32^\circ)$ from Eq. (4.6). Evidently, the ratio of $\mathcal{C}/\mathcal{T}$ in $B \to \pi\pi$ decays is similar to that in $B \to D\pi$ decays [see Eq. (3.43)]. To analyze the $B \to \pi\pi$ data, it is convenient to define $\mathcal{T}_{\rm eff} = \mathcal{T} + \mathcal{E} + \mathcal{V}$ and $\mathcal{C}_{\rm eff} = \mathcal{C} - \mathcal{E} - \mathcal{V}$. It follows from Eq. (5.17) that

$$\frac{\mathcal{C}_{\rm eff}}{\mathcal{T}_{\rm eff}}\bigg|_{\pi\pi} = 0.71\,e^{i72^\circ}. \tag{5.18}$$

This is consistent with Eq. (5.9) obtained from the global analysis of $B \to \pi\pi$ and πK data.

C. CP violation in $B^- \to \pi^-\pi^0$ decays

We see from Table IV that for $B^- \to \pi^-\pi^0$, even including FSIs CP-violating partial-rate asymmetry in the SM is likely to be very small; the SD contribution $\sim 5 \times 10^{-4}$ may increase to the level of one percent. Although this SM CP asymmetry is so small that it is difficult to measure experimentally, it provides a nice place for detecting New Physics. This is because the isospin of the $\pi^-\pi^0$ (also $\rho^-\rho^0$) state in the B decay is $I = 2$ and hence it does not receive QCD penguin contributions and receives only the loop contributions from electroweak penguins. Since these decays are tree dominated, SM predicts an almost null CP asymmetry. Final-state rescattering can enhance the CP-violating effect at most to one percent level. Hence, a measurement of direct CP violation in $B^- \to \pi^-\pi^0$ provides a nice test of the Standard Model and New Physics. This should be doable experimentally in the near future. If the measured partial rate asymmetry turns out to be larger than, say, 2%, this will mostly likely imply some New Physics beyond the Standard Model.

VI. $B \to \rho\pi$ DECAYS

The experimental results of CP averaged branching ratios and CP asymmetries for $B \to \rho\pi$ decays are summarized in Table V. The experimental determination of direct CP asymmetries for $\rho^+\pi^-$ and $\rho^-\pi^+$ is more complicated as $B^0 \to \rho^\pm\pi^\mp$ is not a CP eigenstate. The time-dependent CP asymmetries are given by

$$\begin{aligned} \mathcal{A}(t) &\equiv \frac{\Gamma(\overline{B}^0(t) \to \rho^\pm\pi^\mp) - \Gamma(B^0(t) \to \rho^\pm\pi^\mp)}{\Gamma(\overline{B}^0(t) \to \rho^\pm\pi^\mp) + \Gamma(B^0(t) \to \rho^\pm\pi^\mp)} \\ &= (S_{\rho\pi} \pm \Delta S_{\rho\pi})\sin(\Delta m t) - (C_{\rho\pi} \pm \Delta C_{\rho\pi})\cos(\Delta m t), \end{aligned} \tag{6.1}$$

where Δm is the mass difference of the two neutral B eigenstates, $\mathcal{S}_{\rho\pi}$ is referred to as mixing-induced CP asymmetry and $\mathcal{C}_{\rho\pi}$ is the direct CP asymmetry, while $\Delta S_{\rho\pi}$ and $\Delta C_{\rho\pi}$ are CP-conserving quantities. Next consider the time- and flavor-integrated charge asymmetry

$$\mathcal{A}_{\rho\pi} \equiv \frac{N(\rho^+\pi^-) - N(\rho^-\pi^+)}{N(\rho^+\pi^-) + N(\rho^-\pi^+)}, \tag{6.2}$$

where $N(\rho^+\pi^-)$ and $N(\rho^-\pi^+)$ are the sum of of yields for B^0 and $\overline{B}^0$ decays to $\rho^+\pi^-$ and $\rho^-\pi^+$, respectively. Then,

$$\begin{aligned} \mathcal{A}_{\rho^+\pi^-} &\equiv \frac{\Gamma(\overline{B}^0 \to \rho^+\pi^-) - \Gamma(B^0 \to \rho^-\pi^+)}{\Gamma(\overline{B}^0 \to \rho^+\pi^-) + \Gamma(B^0 \to \rho^-\pi^+)} = \frac{\mathcal{A}_{\rho\pi} - C_{\rho\pi} - \mathcal{A}_{\rho\pi}\Delta C_{\rho\pi}}{1 - \Delta C_{\rho\pi} - \mathcal{A}_{\rho\pi} C_{\rho\pi}}, \\ \mathcal{A}_{\rho^-\pi^+} &\equiv \frac{\Gamma(\overline{B}^0 \to \rho^-\pi^+) - \Gamma(B^0 \to \rho^+\pi^-)}{\Gamma(\overline{B}^0 \to \rho^-\pi^+) + \Gamma(B^0 \to \rho^+\pi^-)} = -\frac{\mathcal{A}_{\rho\pi} + C_{\rho\pi} + \mathcal{A}_{\rho\pi}\Delta C_{\rho\pi}}{1 + \Delta C_{\rho\pi} + \mathcal{A}_{\rho\pi} C_{\rho\pi}}. \end{aligned} \tag{6.3}$$

Note that the quantities $\mathcal{A}_{\rho^\pm\pi^\mp}$ here correspond to $\mathcal{A}_{\rho\pi}^{\mp\pm}$ defined in [71]. Hence, direct CP asymmetries $\mathcal{A}_{\rho^+\pi^-}$ and $\mathcal{A}_{\rho^-\pi^+}$ are determined from the above equations together with the measured correlation coefficients between the parameters in the time-dependent fit to $B^0 \to \rho^\pm\pi^\mp$. From Table V, it is evident that the combined BaBar and Belle measurements of $\overline{B}^0 \to \rho^\pm\pi^\mp$ imply a 3.6σ direct CP violation in the $\rho^+\pi^-$ mode, but not yet in $\rho^-\pi^+$.

The $B \to \rho\pi$ decay amplitudes have the general expressions

$$\begin{aligned} A(\overline{B}^0 \to \rho^+\pi^-) &= \mathcal{T}_V + \mathcal{P}_V + \frac{2}{3}\mathcal{P}_V'^{\rm EW}, \\ A(\overline{B}^0 \to \rho^-\pi^+) &= \mathcal{T}_P + \mathcal{P}_P + \frac{2}{3}\mathcal{P}_P'^{\rm EW}, \\ A(\overline{B}^0 \to \rho^0\pi^0) &= -\frac{1}{2}(\mathcal{C}_V - \mathcal{P}_V + \mathcal{P}_V^{\rm EW} + \frac{1}{3}\mathcal{P}_V'^{\rm EW} + \mathcal{C}_P - \mathcal{P}_P + \mathcal{P}_P^{\rm EW} + \frac{1}{3}\mathcal{P}_P'^{\rm EW}), \\ A(B^- \to \rho^-\pi^0) &= \frac{1}{\sqrt{2}}(\mathcal{T}_P + \mathcal{C}_V + \mathcal{P}_P - \mathcal{P}_V + \mathcal{P}_V^{\rm EW} + \frac{2}{3}\mathcal{P}_P'^{\rm EW} + \frac{1}{3}\mathcal{P}_V'^{\rm EW}), \\ A(B^- \to \rho^0\pi^-) &= \frac{1}{\sqrt{2}}(\mathcal{T}_V + \mathcal{C}_P + \mathcal{P}_V - \mathcal{P}_P + \mathcal{P}_P^{\rm EW} + \frac{2}{3}\mathcal{P}_V'^{\rm EW} + \frac{1}{3}\mathcal{P}_P'^{\rm EW}). \end{aligned} \tag{6.4}$$

They satisfy the strong isospin relation

$$\sqrt{2}\left[A(B^- \to \rho^-\pi^0) + A(B^- \to \rho^0\pi^-) + \sqrt{2}A(\overline{B}^0 \to \rho^0\pi^0)\right] = A(\overline{B}^0 \to \rho^+\pi^-) + A(\overline{B}^0 \to \rho^-\pi^+) \tag{6.5}$$

TABLE V: Experimental data for CP averaged branching ratios (top, in units of 10^{-6}) and direct CP asymmetries (bottom) for $B \to \rho\pi$ [50, 65]. Note that the direct CP-violating quantities $\mathcal{A}_{\rho^\pm\pi^\mp}$ correspond to $\mathcal{A}_{\rho\pi}^{\mp\pm}$ defined in [71].

Mode	BaBar	Belle	CLEO	Average
$\overline{B}^0 \to \rho^\pm\pi^\mp$	$22.6 \pm 1.8 \pm 2.2$	$29.1^{+5.0}_{-4.9} \pm 4.0$	$27.6^{+8.4}_{-7.4} \pm 4.2$	24.0 ± 2.5
$\overline{B}^0 \to \rho^0\pi^0$	$1.4 \pm 0.6 \pm 0.3 < 2.9$	$5.1 \pm 1.6 \pm 0.8$	< 5.5	1.9 ± 1.2[a]
$B^- \to \rho^-\pi^0$	$10.9 \pm 1.9 \pm 1.9$	$13.2 \pm 2.3^{+1.4}_{-1.9}$	< 43	12.0 ± 2.0
$B^- \to \rho^0\pi^-$	$9.5 \pm 1.1 \pm 0.9$	$8.0^{+2.3}_{-2.0} \pm 0.7$	$10.4^{+3.3}_{-3.4} \pm 2.1$	9.1 ± 1.3
$\mathcal{A}_{\rho^-\pi^+}$	$-0.21 \pm 0.11 \pm 0.04$	$-0.02 \pm 0.16^{+0.05}_{-0.02}$		-0.15 ± 0.09
$\mathcal{A}_{\rho^+\pi^-}$	$-0.47 \pm 0.15 \pm 0.06$	$-0.53 \pm 0.29^{+0.09}_{-0.04}$		$-0.47^{+0.13}_{-0.14}$
$\mathcal{A}_{\rho^-\pi^0}$	$0.24 \pm 0.16 \pm 0.06$	$0.06 \pm 0.19^{+0.04}_{-0.06}$		0.16 ± 0.13
$\mathcal{A}_{\rho^0\pi^-}$	$-0.19 \pm 0.11 \pm 0.02$			-0.19 ± 0.11

[a] The error-bar of $\mathcal{B}(\overline{B}^0 \to \rho^0\pi^0)$ is scaled by an S factor of 1.9. We have taken into account the BaBar measurement to obtain the weighted average of the branching ratio for this mode. Note that the average for $\mathcal{B}(\overline{B}^0 \to \rho^0\pi^0)$ is quoted to be < 2.9 in [65].

In the factorization approach (the subscript "SD" being dropped for convenience),

$$\begin{aligned}
&\mathcal{T}_{V,P} = \kappa_{V,P}\lambda_u a_1, \qquad \mathcal{C}_{V,P} = \kappa_{V,P}\lambda_u a_2, \qquad \mathcal{P}_P = \kappa_P\Big[\lambda_u a_4^u + \lambda_c a_4^c\Big],\\
&\mathcal{P}_V = \kappa_V\Big[\lambda_u(a_4^u + a_6^u r_\chi) + \lambda_c(a_4^c + a_6^c r_\chi)\Big], \qquad \mathcal{P}_{V,P}^{\rm EW} = \frac{3}{2}\kappa_{V,P}(\lambda_u+\lambda_c)(-a_7+a_9),\\
&\mathcal{P}_V'^{\rm EW} = \frac{3}{2}\kappa_V\Big[\lambda_u(a_8^u r_\chi + a_{10}^u) + \lambda_c(a_8^c r_\chi + a_{10}^c)\Big], \qquad \mathcal{P}_P'^{\rm EW} = \frac{3}{2}\kappa_P\Big[\lambda_u a_{10}^u + \lambda_c a_{10}^c\Big],
\end{aligned} \tag{6.6}$$

with

$$\kappa_V = \sqrt{2}G_F f_\pi A_0^{B\rho}(m_\pi^2) m_\rho(\varepsilon\cdot p_B), \qquad \kappa_P = \sqrt{2}G_F f_\rho F_1^{B\pi}(m_\rho^2) m_\rho(\varepsilon\cdot p_B), \tag{6.7}$$

Short-distance contributions yield

$$\begin{aligned}
\mathcal{B}(\overline{B}^0 \to \rho^-\pi^+)_{\rm SD} &= 18.4\times 10^{-6}, \qquad \mathcal{A}_{\rho^-\pi^+}^{\rm SD} = -0.03,\\
\mathcal{B}(\overline{B}^0 \to \rho^+\pi^-)_{\rm SD} &= 7.9\times 10^{-6}, \qquad \mathcal{A}_{\rho^+\pi^-}^{\rm SD} = -0.01,\\
\mathcal{B}(\overline{B}^0 \to \rho^0\pi^0)_{\rm SD} &= 5.9\times 10^{-7}, \qquad \mathcal{A}_{\rho^0\pi^0}^{\rm SD} = 0.01,\\
\mathcal{B}(B^- \to \rho^-\pi^0)_{\rm SD} &= 12.8\times 10^{-6}, \qquad \mathcal{A}_{\rho^-\pi^0}^{\rm SD} = -0.04,\\
\mathcal{B}(B^- \to \rho^0\pi^-)_{\rm SD} &= 6.8\times 10^{-6}, \qquad \mathcal{A}_{\rho^0\pi^-}^{\rm SD} = 0.06\,.
\end{aligned} \tag{6.8}$$

Note that the central values of the branching ratios for $\rho^-\pi^+, \rho^+\pi^-, \rho^0\pi^0, \rho^-\pi^0, \rho^0\pi^-$, respectively, are predicted to be 21.2, 15.4, 0.4, 14.0, 11.9 in units of 10^{-6} in [18], which are larger than our results by around a factor of 2 for $\rho^+\pi^-$ and 1.5 for $\rho^0\pi^-$. This is ascribed to the fact that the form factors $A_0^{B\rho}(0)$ and $F_1^{B\pi}(0)$ are 0.28 and 0.25, respectively, in our case [63], while they are chosen to be 0.37 ± 0.06 and 0.28 ± 0.05 in [18]. The central value of the predicted $\mathcal{B}(\overline{B}^0 \to \rho^\pm\pi^\mp) = (36.5^{+21.4}_{-17.6}) \times 10^{-6}$ [18] is large compared to the experimental value of $(24.0 \pm 2.5) \times 10^{-6}$, but it is accompanied by large errors.

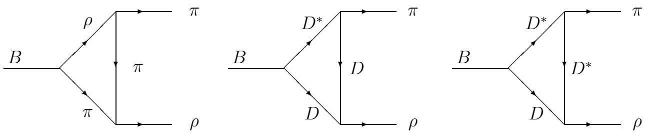

(a) (b) (c)

FIG. 8: Long-distance t-channel rescattering contributions to $B \to \rho\pi$.

The long-distance contributions are depicted in Fig. 8:

$$
\begin{aligned}
\mathcal{A}bs(8a) &= \frac{G_F}{\sqrt{2}}\lambda_u \int_{-1}^{1} \frac{|\vec{p}_1| d\cos\theta}{16\pi m_B}\, 8 g^2_{\rho\pi\pi}\, \frac{F^2(t,m_\pi)}{t-m_\pi^2} m_\rho \Big[a f_\pi A_0^{B\rho}(m_\pi^2) + b f_\rho F_1^{B\pi}(m_\rho^2)\Big] \\
&\times \left(-p_2\cdot p_3 + \frac{(p_1\cdot p_2)(p_1\cdot p_3)}{m_\rho^2}\right) \frac{E_2|\vec{p}_4| - E_4|\vec{p}_2|\cos\theta}{m_B|\vec{p}_4|}, \\
\mathcal{A}bs(8b) &= \frac{G_F}{\sqrt{2}}\lambda_u \int_{-1}^{1} \frac{|\vec{p}_1| d\cos\theta}{16\pi m_B}\, 2\sqrt{2}\, g_{D^*D\pi}\, g_V \beta\, \frac{F^2(t,m_D)}{t-m_D^2} m_{D^*} \\
&\times \Big[c f_D A_0^{BD^*}(m_D^2) + d\, f_{D^*} F_1^{BD}(m_{D^*}^2)\Big] \\
&\times \left(-p_2\cdot p_3 + \frac{(p_1\cdot p_2)(p_1\cdot p_3)}{m_\rho^2}\right) \frac{E_2|\vec{p}_4| - E_4|\vec{p}_2|\cos\theta}{m_B|\vec{p}_4|}, \\
\mathcal{A}bs(8c) &= \frac{G_F}{\sqrt{2}}\lambda_u \int_{-1}^{1} \frac{|\vec{p}_1| d\cos\theta}{16\pi m_B}\, 4\sqrt{2}\, g^2_{D^*D\pi}\, g_V \lambda\, \frac{F^2(t,m_{D^*})}{t-m_{D^*}^2} m_{D^*} \\
&\times \Big[c f_D A_0^{BD^*}(m_D^2) + d\, f_{D^*} F_1^{BD}(m_{D^*}^2)\Big] \Bigg(m_4^2 p_1\cdot p_2 - (p_2\cdot p_4)(p_1\cdot p_4) \\
&+ \frac{E_1|\vec{p}_4| + E_4|\vec{p}_1|\cos\theta}{m_B|\vec{p}_4|} \Big[(p_B\cdot p_2)(p_3\cdot p_4) - (p_B\cdot p_4)(p_2\cdot p_3)\Big]\Bigg), \qquad (6.9)
\end{aligned}
$$

where $a = b = 1/2$ for $\rho^0\pi^0$, $a = 1\,(1/\sqrt{2})$, $b = 0$ for $\rho^-\pi^+$ ($\rho^0\pi^-$), $a = 0$, $b = 1\,(1/\sqrt{2})$ for $\rho^+\pi^-$ ($\rho^-\pi^0$), $c = d = 1/2$ for $\rho^0\pi^0$, $c = d = 1/\sqrt{2}$ for $\rho^0\pi^-$, $c = d = -1/\sqrt{2}$ for $\rho^-\pi^0$, $c = 1, d = 0$ for $\rho^-\pi^+$, and $c = 0, d = 1$ for $\rho^+\pi^-$.

A χ^2 fit of the cutoff scales $\Lambda_\pi, \Lambda_{D^{(*)}}$ or the cutoff parameters η_π and $\eta_{D^{(*)}}$to the measured branching ratios of $B \to \rho\pi$ shows a flat χ^2 without a minimum for $\eta_D \lesssim 2$. Therefore, we choose the criterion that FSI contributions should accommodate the data of the $\rho^0\pi^0$ and $\rho^0\pi^-$ without affecting $\rho^\pm\pi^\mp$ and $\rho^-\pi^0$ significantly. Using $\eta_D = \eta_{D^*} = 1.6$, the branching ratios and direct CP asymmetries after taking into account long-distance rescattering effects are shown in Table VI. (The results are rather insensitive to η_π.) We see that, in contrast to the πK case, the $B \to \rho\pi$ decays are less sensitive to the cutoff scales. The $\overline{B}^0 \to \rho^0\pi^0$ rate is enhanced via rescattering by a factor of 2, which is consistent with the weighted average of $(1.9 \pm 1.2) \times 10^{-6}$. However, it is important to clarify the discrepancy between BaBar and Belle measurements for this mode. It should be remarked that direct CP violation in this mode is significantly enhanced by FSI from around 1% to 60%. Naively, this asymmetry ought to become accessible at B factories with 10^8 $B\bar{B}$ pairs. As stressed before, there is 3.6σ direct CP violation in the $\rho^+\pi^-$ mode. Our prediction

TABLE VI: Same as Table II except for $B \to \rho\pi$ decays.

Mode	Expt.	SD	SD+LD
$\mathcal{B}(\overline{B}^0 \to \rho^-\pi^+)$	$13.9^{+2.2}_{-2.1}$	18.4	$18.8^{+0.3}_{-0.2}$
$\mathcal{B}(\overline{B}^0 \to \rho^+\pi^-)$	$10.1^{+2.1}_{-1.9}$	7.9	8.4 ± 0.3
$\mathcal{B}(\overline{B}^0 \to \rho^\pm\pi^\mp)$	24.0 ± 2.5	26.3	$27.3^{+0.6}_{-0.4}$
$\mathcal{B}(\overline{B}^0 \to \rho^0\pi^0)$	1.9 ± 1.2	0.6	$1.3^{+0.4}_{-0.3}$
$\mathcal{B}(B^- \to \rho^-\pi^0)$	12.0 ± 2.0	12.9	$14.0^{+0.7}_{-0.4}$
$\mathcal{B}(B^- \to \rho^0\pi^-)$	9.1 ± 1.3	6.8	$7.5^{+0.6}_{-0.3}$
$\mathcal{A}_{\rho^-\pi^+}$	-0.15 ± 0.09	-0.03	-0.24 ± 0.6
$\mathcal{A}_{\rho^+\pi^-}$	$-0.47^{+0.13}_{-0.14}$	-0.01	-0.43 ± 0.11
$\mathcal{A}_{\rho^0\pi^0}$		0.01	$0.57^{+0.01}_{-0.03}$
$\mathcal{A}_{\rho^-\pi^0}$	0.16 ± 0.13	-0.04	0.36 ± 0.10
$\mathcal{A}_{\rho^0\pi^-}$	-0.19 ± 0.11	0.06	$-0.56^{+0.14}_{-0.15}$

of $\mathcal{A}_{\rho^+\pi^-}$ agrees with the data in both magnitude and sign, while the QCD factorization prediction $(0.6^{+11.6}_{-11.8})\%$ [18] seems not consistent with experiment.

VII. POLARIZATION IN $B \to \phi K^*,\ \rho K^*$ DECAYS

The branching ratios and polarization fractions of charmless $B \to VV$ decays have been measured for $\rho\rho$, ρK^* and ϕK^* final states. In general, it is expected that they are dominated by the longitudinal polarization states and respect the scaling law, namely [26] (see also footnote 1 on p.3)

$$1 - f_L = \mathcal{O}(m_V^2/m_B^2), \qquad f_\perp/f_\parallel = 1 + \mathcal{O}(m_V/m_B) \tag{7.1}$$

with $f_L, f_\perp$ and $f_\parallel$ being the longitudinal, perpendicular, and parallel polarization fractions, respectively. However, in sharp contrast to the $\rho\rho$ case, the large fraction of transverse polarization in $B \to \phi K^*$ decays observed by BaBar and confirmed by Belle (see Table VII) is a surprise and poses an interesting challenge for any theoretical interpretation. The aforementioned scaling law remains true even when nonfactorizable graphs are included in QCD factorization [26]. Therefore, in order to obtain a large transverse polarization in $B \to \phi K^*$, this scaling law valid at short-distance interactions must be circumvented in one way or another. One way is the Kagan's recent suggestion of sizable penguin-induced annihilation contributions [27]. Another possibility is that perhaps a sizable transverse polarization can be achieved via final-state rescattering. To be more specific, the following two FSI processes are potentially important. First, $B \to D^* D_s^*$ followed by a rescattering to ϕK^* is not subject to the scaling law and hence its large transverse polarization can be conveyed to ϕK^* via FSI. Second, the FSI effect from $\overline{B} \to D^* D_s$ or $\overline{B} \to D D_s^*$ will contribute only to the $A_\perp$ amplitude. In this section, we shall carefully examine the long-distance rescattering effects on ϕK^* polarizations.

TABLE VII: Experimental data for CP averaged branching ratios (in units of 10^{-6}) and polarization fractions for $B \to \phi K^*, \rho K^*, \rho\rho$ [50, 65, 74, 75]. The phases of the parallel and perpendicular amplitudes relative to the longitudinal one for $B \to \phi K^*$ are also included [74, 75].

Mode	BaBar	Belle	CLEO	Average
$\overline{B}^0 \to \phi \overline{K}^{*0}$	$9.2 \pm 0.9 \pm 0.5$	$10.0^{+1.6+0.7}_{-1.5-0.8}$	$11.5^{+4.5+1.8}_{-3.7-1.7}$	9.5 ± 0.9
$B^- \to \phi K^{*-}$	$12.7^{+2.2}_{-2.0} \pm 1.1$	$6.7^{+2.1+0.7}_{-1.9-1.0}$	$10.6^{+6.4+1.8}_{-4.9-1.6}$	9.7 ± 1.5
$\overline{B}^0 \to \rho^+ K^{*-}$	$16.3 \pm 5.4 \pm 2.3^{+0.0}_{-6.3} < 24$			< 24
$B^- \to \rho^0 K^{*-}$	$10.6^{+3.0}_{-2.6} \pm 2.4$		< 74	$10.6^{+3.8}_{-3.5}$
$B^- \to \rho^- \overline{K}^{*0}$	$17.0 \pm 2.9 \pm 2.0^{+0.0}_{-1.9}$	$6.6 \pm 2.2 \pm 0.8$		9.6 ± 4.7[a]
$B^- \to \rho^0 \rho^-$	$22.5^{+5.7}_{-5.4} \pm 5.8$	$31.7 \pm 7.1^{+3.8}_{-6.7}$		$26.4^{+6.1}_{-6.4}$
$\overline{B}^0 \to \rho^+ \rho^-$	$30 \pm 4 \pm 5$			30 ± 6
$B^- \to \rho^- \omega$	$12.6^{+3.7}_{-3.3} \pm 1.8$			$12.6^{+4.1}_{-3.8}$
$f_L(\phi \overline{K}^{*0})$	$0.52 \pm 0.05 \pm 0.02$	$0.52 \pm 0.07 \pm 0.05$		0.52 ± 0.05
$f_\perp(\phi \overline{K}^{*0})$	$0.22 \pm 0.05 \pm 0.02$	$0.30 \pm 0.07 \pm 0.03$		0.25 ± 0.04
$f_L(\phi K^{*-})$	$0.46 \pm 0.12 \pm 0.03$	$0.49 \pm 0.13 \pm 0.05$		0.47 ± 0.09
$f_\perp(\phi K^{*-})$		$0.12^{+0.11}_{-0.08} \pm 0.03$		$0.12^{+0.11}_{-0.09}$
$\phi_\parallel(\phi K^{*0})$ (rad)[b]	$2.34^{+0.23}_{-0.20} \pm 0.05$	$-2.30 \pm 0.28 \pm 0.04$		
$\phi_\perp(\phi K^{*0})$ (rad)[b]	$2.47 \pm 0.25 \pm 0.05$	$0.64 \pm 0.26 \pm 0.05$		
$\phi_\parallel(\phi K^{*+})$ (rad)[b]		$-2.07 \pm 0.34 \pm 0.07$		-2.07 ± 0.35
$\phi_\perp(\phi K^{*+})$ (rad)[b]		$0.93^{+0.55}_{-0.39} \pm 0.12$		$0.93^{+0.56}_{-0.41}$
$f_L(\rho^0 K^{*-})$	$0.96^{+0.04}_{-0.15} \pm 0.04$			$0.96^{+0.06}_{-0.16}$
$f_L(\rho^- \overline{K}^{*0})$	$0.79 \pm 0.08 \pm 0.04 \pm 0.02$	$0.50 \pm 0.19^{+0.05}_{-0.07}$		0.74 ± 0.08
$f_L(\rho^0 \rho^-)$	$0.97^{+0.03}_{-0.07} \pm 0.04$	$0.95 \pm 0.11 \pm 0.02$		$0.96^{+0.04}_{-0.07}$
$f_L(\rho^+ \rho^-)$	$0.99 \pm 0.03 \pm 0.04$			0.99 ± 0.05
$f_L(\rho^- \omega)$	$0.88^{+0.12}_{-0.15} \pm 0.03$			$0.88^{+0.12}_{-0.15}$

[a] The error in $\mathcal{B}(B^- \to \rho^- \overline{K}^{*0})$ is scaled by $S = 2.4$. Our average is slightly different from the value of 9.2 ± 2.0 quoted in [65].

[b] Experimental results of the relative strong phases are for $B^{(0,+)} \to \phi K^{*(0,+)}$ decays.

A. Short-distance contributions to $\overline{B} \to \phi \overline{K}^*$

In the factorization approach, the amplitude of the $\overline{B} \to \phi \overline{K}^*$ decay is given by

$$\begin{aligned} \langle \phi(\lambda_\phi) \overline{K}^*(\lambda_{K^*}) | H_{\rm eff} | \overline{B} \rangle &= \frac{G_{\rm F}}{\sqrt{2}} \sum_{q=u,c} V_{qb} V_{qs}^* \, a^q_{\phi K^*} \, \langle \phi | (\bar{s}s)_V | 0 \rangle \, \langle \overline{K}^* | (\bar{s}b)_{V-A} | \overline{B} \rangle \\ &= -i\alpha_{\phi K^*} \, \varepsilon^{*\mu}_\phi(\lambda_\phi) \varepsilon^{*\nu}_{K^*}(\lambda_{K^*}) \Big(A_1^{BK^*}(m_\phi^2) g_{\mu\nu} \\ &\quad - \frac{2A_2^{BK^*}(m_\phi^2)}{(m_B + m_{K^*})^2} p_{B\mu} p_{B\nu} - i \frac{2V^{BK^*}(m_\phi^2)}{(m_B + m_{K^*})^2} \epsilon_{\mu\nu\alpha\beta} p_B^\alpha p_{K^*}^\beta \Big), \end{aligned} \quad (7.2)$$

where λ_{ϕ,K^*} are the corresponding helicities, $a^q_{\phi K^*} \equiv a_3 + a^q_4 + a_5 - (a_7 + a_9 + a^q_{10})/2$ and $\alpha_{\phi K^*} \equiv G_{\rm F} m_\phi f_\phi (m_B + m_{K^*}) \sum_{q=u,c} V_{qb} V^*_{qs}\ a^q_{\phi K^*}/\sqrt{2}$. With A_λ defined as $\langle \phi(\lambda)\overline{K}^*(\lambda)|H_{\rm eff}|\overline{B}\rangle$, it is straightforward to obtain [76]

$$\begin{aligned} A_0 &= -i\alpha_{\phi K^*}\Big(- A_1^{BK^*}(m^2_\phi)\frac{m^2_B - m^2_\phi - m^2_{K^*}}{2m_\phi m_{K^*}} + \frac{2A_2^{BK^*}(m^2_\phi)}{(m_B + m_{K^*})^2}\frac{m^2_B p^2_c}{m_\phi m_{K^*}}\Big), \\ A_\pm &= -i\alpha_{\phi K^*}\Big(A_1^{BK^*}(m^2_\phi) \mp \frac{2V^{BK^*}(m^2_\phi)}{(m_B + m_{K^*})^2} m_B p_c\Big), \end{aligned} \tag{7.3}$$

where p_c is the center of mass momentum and we have used the phase convention $\varepsilon_\phi(\lambda) = \varepsilon_{K^*}(-\lambda)$ for $\vec{p}_{\phi,K^*} \to 0$. The longitudinal amplitude A_0 is sometimes denoted as A_L, while the transverse amplitudes are defined by

$$\begin{aligned} A_\parallel &= \frac{A_+ + A_-}{\sqrt{2}} = -i\alpha_{\phi K^*}\sqrt{2}A_1^{BK^*}(m^2_\phi), \\ A_\perp &= \frac{A_+ - A_-}{\sqrt{2}} = i\alpha_{\phi K^*}\frac{2\sqrt{2}V^{BK^*}(m^2_\phi)}{(m_B + m_{K^*})^2} m_B p_c \end{aligned} \tag{7.4}$$

in the transversity basis. The decay rate can be expressed in terms of these amplitudes as

$$\Gamma = \frac{p_c}{8\pi m^2_B}(|A_0|^2 + |A_+|^2 + |A_-|^2) = \frac{p_c}{8\pi m^2_B}(|A_L|^2 + |A_\parallel|^2 + |A_\perp|^2), \tag{7.5}$$

and the polarization fractions are defined as

$$f_\alpha \equiv \frac{\Gamma_\alpha}{\Gamma} = \frac{|A_\alpha|^2}{|A_0|^2 + |A_\parallel|^2 + |A_\perp|^2}, \tag{7.6}$$

with $\alpha = L, \parallel, \perp$.

The form factors A_1, A_2, V usually are similar in size [63]. Using above equations with a_i given in (4.6) [14] and the form factors given in [63], one immediately finds that the short-distance contributions yield (see also Table VIII)

$$f^{\rm SD}_L : f^{\rm SD}_\parallel : f^{\rm SD}_\perp = 0.88 \pm 0.06 : 0.07 \pm 0.03 : 0.05 \pm 0.03, \qquad 1 \simeq f^{\rm SD}_L \gg f^{\rm SD}_{\parallel,\perp}, \tag{7.7}$$

where the errors are estimated with 10% uncertainties in form factors. However, the above prediction is not borne out by the $B \to \phi K^*$ data (see Table VII). It is easily seen that Eq. (7.7) is closely related to the fact that $m_B \gg m_{\phi,K^*}$. We do not expect that such a relation holds in the case of $\overline{B} \to D^{(*)} D^{(*)}_s$ decays, which can rescatter to the $\phi\overline{K}^*$ final state. It is thus interesting to investigate the effect of FSI on these polarization fractions. A similar analysis was also considered recently in [78].

Another possible shortcoming of the short-distance factorization approach is that the central value of the predicted branching ratio

$$\mathcal{B}(\overline{B} \to \phi\overline{K}^*)_{\rm SD} = (4.4 \pm 2.6) \times 10^{-6} \tag{7.8}$$

---

[14] As shown explicitly in [77] within the QCD factorization approach, nonfactorizable corrections to each partial-wave or helicity amplitude are in general not the same; the effective parameters a_i can vary for different helicity amplitudes. However, since such an effect is too small to account for the large transverse polarization [26], for simplicity we shall ignore the difference of a_i in different helicity amplitudes.

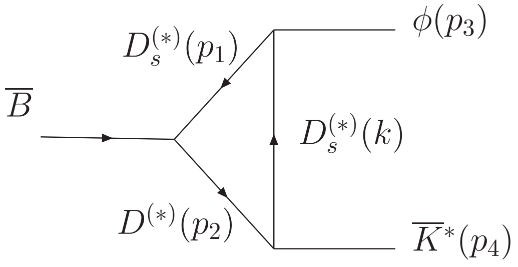

FIG. 9: Long-distance t-channel rescattering contributions to $\overline{B} \to \phi \overline{K}^*$. Note that flows in lines are along b or c quarks.

is too small by a factor of 2 compared to experiment. As pointed out in [77], in the heavy quark limit, both vector mesons in the charmless $B \to VV$ decays should have zero helicity and the corresponding amplitude is governed by the form factor A_0. Consequently, the predicted branching ratios are rather sensitive to the form factor models of A_0 and can be easily different by a factor of 2. Using the covariant light-front model for $B \to K^*$ form factors [63], we are led to the above prediction in Eq. (7.8). A similar result is also obtained in the BSW model [77]. However, a much larger branching ratio will be obtained if the form factors based on light-cone sum rules [79, 80] are employed. At any rate, if the predicted rate is too small, this is another important incentive for considering long-distance effects.

B. Long-distance contributions to $\overline{B} \to \phi \overline{K}^*$

The $D^{(*)} D_s^{(*)}$ states from $\overline{B}$ decays can rescatter to $\phi \overline{K}^*$ through the t-channel $D_s^{(*)}$ exchange in the triangle diagrams depicted in Fig. 9. The effective Lagrangian for $D^{(*)} D^{(*)} V$ vertices is given in Eq. (3.15). Note that as in Eq. (4.12), SU(3) or U(3) breaking effects in strong couplings are assumed to be taken into account by the relations

$$g_{D^{(*)} D_s^{(*)} K^*} = \sqrt{\frac{m_{D_s^{(*)}}}{m_{D^{(*)}}}} g_{D^{(*)} D^{(*)} \rho}, \qquad g_{D_s^{(*)} D_s^{(*)} \phi} = \frac{m_{D_s^{(*)}}}{m_{D^{(*)}}} g_{D^{(*)} D^{(*)} \rho}, \tag{7.9}$$

and likewise for $f_{D^{(*)} D_s^{(*)} K^*}$ and $f_{D_s^{(*)} D_s^{(*)} \phi}$.

There are totally eight different FSI diagrams in Fig. 9. The absorptive part contribution of $\overline{B} \to D_s D \to \phi \overline{K}^*$ amplitude via the D_s exchange is given by

$$\begin{aligned} \mathcal{A}bs\,(D_s D; D_s) \; &= \; \frac{1}{2} \int \frac{d^3\vec{p}_1}{(2\pi)^3 2E_1} \frac{d^3\vec{p}_2}{(2\pi)^3 2E_2} (2\pi)^4 \delta^4(p_B - p_1 - p_2) A(\overline{B}^0 \to D_s D) \\ &\quad \times (2i) g_{D_s D_s \phi} \frac{F^2(t, m_{D_s})}{t - m_{D_s}^2} (-2i) g_{D D_s K^*} (\varepsilon_3^* \cdot p_1)(\varepsilon_4^* \cdot p_2). \end{aligned} \tag{7.10}$$

We need to use some identities to recast the above amplitude into the standard expression given in Eq. (7.2). To proceed, we note that after performing the integration, the integrals

$$\int \frac{d^3\vec{p}_1}{(2\pi)^3 2E_1} \frac{d^3\vec{p}_2}{(2\pi)^3 2E_2} (2\pi)^4 \delta^4(p_B - p_1 - p_2) f(t) \times \{p_{1\mu},\, p_{1\mu} p_{1\nu},\, p_{1\mu} p_{1\nu} p_{1\alpha}\} \tag{7.11}$$

can be expressed only in terms of the external momenta p_3, p_4 with suitable Lorentz and permutation structures. Therefore, under the integration we have

$$\begin{aligned}
p_{1\mu} &\doteq P_\mu A_1^{(1)} + q_\mu A_2^{(1)}, \\
p_{1\mu}p_{1\nu} &\doteq g_{\mu\nu}A_1^{(2)} + P_\mu P_\nu A_2^{(2)} + (P_\mu q_\nu + q_\mu P_\nu)A_3^{(2)} + q_\mu q_\nu A_4^{(2)}, \\
p_{1\mu}p_{1\nu}p_{1\alpha} &\doteq (g_{\mu\nu}P_\alpha + g_{\mu\alpha}P_\nu + g_{\nu\alpha}P_\mu)A_1^{(3)} + (g_{\mu\nu}q_\alpha + g_{\mu\alpha}q_\nu + g_{\nu\alpha}q_\mu)A_2^{(3)} \\
&\quad + P_\mu P_\nu P_\alpha A_3^{(3)} + (P_\mu P_\nu q_\alpha + P_\mu q_\nu P_\alpha + q_\mu P_\nu P_\alpha)A_4^{(3)} \\
&\quad + (q_\mu q_\nu P_\alpha + q_\mu P_\nu q_\alpha + P_\mu q_\nu q_\alpha)A_5^{(3)} + q_\mu q_\nu q_\alpha A_6^{(3)},
\end{aligned} \tag{7.12}$$

where $P = p_3 + p_4$, $q = p_3 - p_4$ and $A_j^{(i)} = A_j^{(i)}(t, m_B^2, m_1^2, m_2^2, m_3^2, m_4^2)$ have the analytic forms given in Appendix A. With the aid of Eq. (7.12), we finally obtain

$$\begin{aligned}
\mathcal{A}bs\,(D_sD; D_s) &= \frac{1}{2}\int \frac{d^3\vec{p}_1}{(2\pi)^3 2E_1}\,\frac{d^3\vec{p}_2}{(2\pi)^3 2E_2}\,(2\pi)^4\delta^4(p_B - p_1 - p_2)A(\overline{B}^0 \to D_sD) \\
&\quad \times 4\; g_{D_sD_s\phi}\frac{F^2(t, m_{D_s})}{t - m_{D_s}^2} g_{DD_sK^*} \\
&\quad \times \Big\{\varepsilon_3^* \cdot \varepsilon_4^*(-A_1^{(2)}) - (\varepsilon_3^* \cdot P)(\varepsilon_4^* \cdot P)(-A_1^{(1)} + A_2^{(1)} + A_2^{(2)} - A_4^{(2)})\Big\}.
\end{aligned} \tag{7.13}$$

Likewise, the absorptive part of the $\overline{B} \to D_sD \to \phi\overline{K}^*$ amplitude via the D_s^* exchange is given by [15]

$$\begin{aligned}
\mathcal{A}bs\,(D_sD; D_s^*) &= \frac{1}{2}\int \frac{d^3\vec{p}_1}{(2\pi)^3 2E_1}\,\frac{d^3\vec{p}_2}{(2\pi)^3 2E_2}\,(2\pi)^4\delta^4(p_B - p_1 - p_2)A(\overline{B}^0 \to D_sD) \\
&\quad \times(-4) f_{D_sD_s^*\phi}\frac{F^2(t, m_{D_s})}{t - m_{D_s^*}^2}\, 4 f_{DD_s^*K^*}[p_3, \varepsilon_3^*, p_1, {}^\mu]\left(-g_{\mu\nu} + \frac{k_\mu k_\nu}{m_{D_s^*}^2}\right)[p_4, \varepsilon_4^*, p_2, {}^\nu] \\
&= \frac{1}{2}\int \frac{d^3\vec{p}_1}{(2\pi)^3 2E_1}\,\frac{d^3\vec{p}_2}{(2\pi)^3 2E_2}\,(2\pi)^4\delta^4(p_B - p_1 - p_2)A(\overline{B}^0 \to D_sD) \\
&\quad \times 16 f_{D_sD_s^*\phi}\frac{F^2(t, m_{D_s^*})}{t - m_{D_s^*}^2} f_{DD_s^*K^*} \\
&\quad \times\Bigg\{\varepsilon_3^* \cdot \varepsilon_4^*\Big\{2A_1^{(2)} p_3 \cdot p_4 - [(p_3 \cdot p_4)^2 - m_3^2 m_4^2](A_1^{(1)} - A_2^{(1)} - A_2^{(2)} + A_4^{(2)})\Big\} \\
&\quad -\varepsilon_3^* \cdot P \varepsilon_4^* \cdot P\Big[2A_1^{(2)} - p_3 \cdot p_4(A_1^{(1)} - A_2^{(1)} - A_2^{(2)} + A_4^{(2)})\Big]\Bigg\},
\end{aligned} \tag{7.14}$$

where $k = p_1 - p_3$. It can be easily seen that the FSI contribution from the $\overline{B} \to DD_s$ decay will affect both A_L and $A_\parallel$ amplitudes of the $\overline{B} \to \phi\overline{K}^*$ decay.

The absorptive part contributions of $\overline{B} \to D_s^*D \to \phi\overline{K}^*$ amplitudes via D_s and D_s^* exchanges are given by

$$\mathcal{A}bs\,(D_s^*D; D_s) = \frac{1}{2}\int \frac{d^3\vec{p}_1}{(2\pi)^3 2E_1}\,\frac{d^3\vec{p}_2}{(2\pi)^3 2E_2}\,(2\pi)^4\delta^4(p_B - p_1 - p_2)\frac{A(\overline{B}^0 \to D_s^*D)}{2\varepsilon_1^* \cdot P}$$

---

[15] To avoid using too many dummy indices, we define $[A, B, C, D] \equiv \epsilon_{\alpha\beta\gamma\delta}A^\alpha B^\beta C^\gamma D^\delta$, $[A, B, C, {}_\mu] \equiv \epsilon_{\alpha\beta\gamma\mu}A^\alpha B^\beta C^\gamma$ and so on for our convenience.

$$
\begin{aligned}
& \times \sum_{\lambda_1} 2\varepsilon_1^* \cdot P\,(-4i) f_{D_s^* D_s \phi} \frac{F^2(t, m_{D_s})}{t - m_{D_s}^2} (-2i) g_{DD_sK^*}\,[p_3, \varepsilon_3^*, p_1, \varepsilon_1] p_2 \cdot \varepsilon_4^* \\
= & \; \frac{1}{2} \int \frac{d^3\vec{p}_1}{(2\pi)^3 2E_1} \frac{d^3\vec{p}_2}{(2\pi)^3 2E_2} (2\pi)^4 \delta^4(p_B - p_1 - p_2) \frac{A(\overline{B}^0 \to D_s^* D)}{2\varepsilon_1^* \cdot P} \\
& \times (-i)[\varepsilon_3^*, \varepsilon_4^*, p_3, p_4] \Big\{ -16i\, f_{D_s^* D_s \phi} \frac{F^2(t, m_{D_s})}{t - m_{D_s}^2} g_{DD_sK^*}\, A_1^{(2)} \Big\}, \\
\mathcal{A}bs\,(D_s^* D; D_s^*) = & \; \frac{1}{2} \int \frac{d^3\vec{p}_1}{(2\pi)^3 2E_1} \frac{d^3\vec{p}_2}{(2\pi)^3 2E_2} (2\pi)^4 \delta^4(p_B - p_1 - p_2) \frac{A(\overline{B}^0 \to D_s^* D)}{2\varepsilon_1^* \cdot P} \\
& \times \sum_{\lambda_1} 2\varepsilon_1^* \cdot P\,(-4i) f_{D_s^* D_s^* \phi} \frac{F^2(t, m_{D_s^*})}{t - m_{D_s^*}^2} 4i\, f_{DD_s^*K^*} \\
& \times \varepsilon_1^\rho (\sigma g_{\rho\mu} p_1 \cdot \varepsilon_3^* + p_{3\rho} \varepsilon_{3\mu}^* - \varepsilon_{3\rho}^* p_{3\mu}) \Big(-g^{\mu\nu} + \frac{k^\mu k^\nu}{m_{D_s^*}^2} \Big) [p_4, \varepsilon_4^*, p_2, {}^\nu] \\
= & \; \frac{1}{2} \int \frac{d^3\vec{p}_1}{(2\pi)^3 2E_1} \frac{d^3\vec{p}_2}{(2\pi)^3 2E_2} (2\pi)^4 \delta^4(p_B - p_1 - p_2) \frac{A(\overline{B}^0 \to D_s^* D)}{2\varepsilon_1^* \cdot P} \\
& \times (-i)[\varepsilon_3^*, \varepsilon_4^*, p_3, p_4]\; (-32i)\, f_{D_s^* D_s^* \phi} \frac{F^2(t, m_{D_s^*})}{t - m_{D_s^*}^2} f_{DD_s^*K^*} \Big\{ A_1^{(2)} \Big[\sigma + (1 - \sigma) \frac{P \cdot p_1}{m_1^2} \Big] \\
& + (1 - A_1^{(1)} - A_2^{(1)}) \Big(P \cdot p_3 - \frac{P \cdot p_1 p_1 \cdot p_3}{m_1^2} \Big) \Big\}, \qquad (7.15)
\end{aligned}
$$

where the dependence of the polarization vector in $A(\overline{B}^0 \to D_s^* D)$ has been extracted out explicitly and $\sigma \equiv g_{D^*D^*V}/(2 f_{D^*D^*V})$.

Similarly, the absorptive parts of $\overline{B} \to D_s D^* \to \phi \overline{K}^*$ amplitudes via D_s and D_s^* exchanges are given by

$$
\begin{aligned}
\mathcal{A}bs\,(D_s D^*; D_s) = & \; \frac{1}{2} \int \frac{d^3\vec{p}_1}{(2\pi)^3 2E_1} \frac{d^3\vec{p}_2}{(2\pi)^3 2E_2} (2\pi)^4 \delta^4(p_B - p_1 - p_2) \frac{A(\overline{B}^0 \to D_s D^*)}{2\varepsilon_2^* \cdot P} \\
& \times \sum_{\lambda_2} 2\varepsilon_2^* \cdot P\, 2i g_{D_s D_s \phi} \frac{F^2(t, m_{D_s})}{t - m_{D_s}^2} (-4i) f_{D^* D_s K^*}\, [p_4, \varepsilon_4^*, p_2, \varepsilon_2] p_1 \cdot \varepsilon_3^* \\
= & \; \frac{1}{2} \int \frac{d^3\vec{p}_1}{(2\pi)^3 2E_1} \frac{d^3\vec{p}_2}{(2\pi)^3 2E_2} (2\pi)^4 \delta^4(p_B - p_1 - p_2) \frac{A(\overline{B}^0 \to D_s D^*)}{2\varepsilon_2^* \cdot P} \\
& \times (-i)[\varepsilon_3^*, \varepsilon_4^*, p_3, p_4] \Big\{ 16i\, g_{D_s D_s \phi} \frac{F^2(t, m_{D_s})}{t - m_{D_s}^2} f_{D^* D_s K^*}\, A_1^{(2)} \Big\}, \\
\mathcal{A}bs\,(D_s D^*; D_s^*) = & \; \frac{1}{2} \int \frac{d^3\vec{p}_1}{(2\pi)^3 2E_1} \frac{d^3\vec{p}_2}{(2\pi)^3 2E_2} (2\pi)^4 \delta^4(p_B - p_1 - p_2) \frac{A(\overline{B}^0 \to D_s D^*)}{2\varepsilon_2^* \cdot P} \\
& \times \sum_{\lambda_2} 2\varepsilon_2^* \cdot P\, 4i\, f_{D_s D_s^* \phi} \frac{F^2(t, m_{D_s^*})}{t - m_{D_s^*}^2} (4i) f_{D^* D_s^* K^*} \\
& \times [p_3, \varepsilon_3^*, p_1, {}_\mu] \Big(-g^{\mu\nu} + \frac{k^\mu k^\nu}{m_{D_s^*}^2} \Big) (\sigma g_{\nu\alpha} p_2 \cdot \varepsilon_4^* - p_{4\nu} \varepsilon_{4\alpha}^* + \varepsilon_{4\nu}^* p_{4\alpha}) \varepsilon_2^\alpha \\
= & \; \frac{1}{2} \int \frac{d^3\vec{p}_1}{(2\pi)^3 2E_1} \frac{d^3\vec{p}_2}{(2\pi)^3 2E_2} (2\pi)^4 \delta^4(p_B - p_1 - p_2) \frac{A(\overline{B}^0 \to D_s D^*)}{2\varepsilon_2^* \cdot P}
\end{aligned}
$$

$$
\begin{aligned}
&\times(-i)[\varepsilon_3^*, \varepsilon_4^*, p_3, p_4]\; 32i\, f_{D_s D_s^* \phi} \frac{F^2(t, m_{D_s^*})}{t - m_{D_s^*}^2} f_{D^* D_s^* K^*} \Big\{ A_1^{(2)} \Big[\sigma + (1-\sigma) \frac{P \cdot p_2}{m_2^2} \Big] \\
&+ (A_1^{(1)} - A_2^{(1)}) \Big(P \cdot p_4 - \frac{P \cdot p_2 p_2 \cdot p_4}{m_2^2} \Big) \Big\},
\end{aligned} \tag{7.16}
$$

where again the dependence of the polarization vector in $A(\overline{B}^0 \to D_s D^*)$ has been extracted out explicitly. Note that through rescattering FSI, both $\overline{B} \to D_s^* D$ and $\overline{B} \to D_s D^*$ will affect only the $A_\perp$ term of the $\overline{B} \to \phi \overline{K}^*$ decay amplitude.

To consider the FSI effect from the decay $\overline{B} \to D_s^* D^*$, we denote the decay amplitude as

$$
A(\overline{B} \to D_s^*(p_1, \lambda_1) D^*(p_2, \lambda_2)) = \varepsilon_1^{*\mu} \varepsilon_2^{*\nu} (a\, g_{\mu\nu} + b P_\mu P_\nu + ic\, [_\mu, _\nu, P, p_2]). \tag{7.17}
$$

The absorptive part of the $\overline{B} \to D_s^* D^* \to \phi \overline{K}^*$ amplitude via a t-channel D_s exchange has the expression

$$
\begin{aligned}
\mathcal{A}bs\,(D_s^* D^*; D_s) \;=\;& \frac{1}{2} \int \frac{d^3\vec{p}_1}{(2\pi)^3 2E_1} \frac{d^3\vec{p}_2}{(2\pi)^3 2E_2} (2\pi)^4 \delta^4(p_B - p_1 - p_2)(a\, g_{\mu\nu} + b P_\mu P_\nu + ic[_\mu, _\nu, P, p_2]) \\
&\times \sum_{\lambda_1, \lambda_2} \varepsilon_1^{*\mu} \varepsilon_2^{*\nu} (-4i) f_{D_s^* D_s \phi} \frac{F^2(t, m_{D_s})}{t - m_{D_s}^2} (-4i) f_{D^* D_s K^*} [p_3, \varepsilon_3^*, p_1, \varepsilon_1][p_4, \varepsilon_4^*, p_2, \varepsilon_2] \\
=\;& \frac{1}{2} \int \frac{d^3\vec{p}_1}{(2\pi)^3 2E_1} \frac{d^3\vec{p}_2}{(2\pi)^3 2E_2} (2\pi)^4 \delta^4(p_B - p_1 - p_2) 16 f_{D_s^* D_s \phi} \frac{F^2(t, m_{D_s})}{t - m_{D_s}^2} f_{D^* D_s K^*} \\
&\times \Big\{ \varepsilon_3^* \cdot \varepsilon_4^* \{ 2a\, p_3 \cdot p_4 A_1^{(2)} - [(p_3 \cdot p_4)^2 - m_3^2 m_4^2][a(A_1^{(1)} - A_2^{(1)} - A_2^{(2)} + A_4^{(2)}) + b A_1^{(2)}] \} \\
&- \varepsilon_3^* \cdot P \varepsilon_4^* \cdot P \{ 2a\, A_1^{(2)} - p_3 \cdot p_4 [a(A_1^{(1)} - A_2^{(1)} - A_2^{(2)} + A_4^{(2)}) + b A_1^{(2)}] \} \\
&- i[\varepsilon_3^*, \varepsilon_4^*, p_3, p_4]\, 2c \Big\{ P \cdot p_3 (A_1^{(2)} - A_1^{(3)} - A_2^{(3)}) + P \cdot p_4 (A_1^{(3)} - A_2^{(3)}) - p_3 \cdot p_4 A_2^{(3)} \\
&+ [(p_3 \cdot p_4)^2 - m_3^2 m_4^2](A_3^{(2)} - A_4^{(2)} - A_4^{(3)} + A_6^{(3)}) \Big\} \Big\}.
\end{aligned} \tag{7.18}
$$

We see that the above FSI contributes to all three polarization components. The contribution from the D_s^* exchange is

$$
\begin{aligned}
\mathcal{A}bs\,(D_s^* D^*; D_s^*) \;=\;& \frac{1}{2} \int \frac{d^3\vec{p}_1}{(2\pi)^3 2E_1} \frac{d^3\vec{p}_2}{(2\pi)^3 2E_2} (2\pi)^4 \delta^4(p_B - p_1 - p_2)(a\, g_{\delta\beta} + b P_\delta P_\beta + ic[_\delta, _\beta, P, p_2]) \\
&\times \sum_{\lambda_1, \lambda_2} \varepsilon_1^{*\delta} \varepsilon_2^{*\beta} (-4i) f_{D_s^* D_s^* \phi} \frac{F^2(t, m_{D_s^*})}{t - m_{D_s^*}^2} (4i) f_{D^* D_s^* K^*}\, \varepsilon_1^\rho (\sigma g_{\rho\mu} p_1 \cdot \varepsilon_3^* + p_{3\rho} \varepsilon_{3\mu}^* - \varepsilon_{3\rho}^* p_{3\mu}) \\
&\times \Big(-g^{\mu\nu} + \frac{k^\mu k^\nu}{m_{D_s^*}^2} \Big) (\sigma g_{\nu\alpha} p_2 \cdot \varepsilon_4^* - p_{4\nu} \varepsilon_{4\alpha}^* + \varepsilon_{3\nu}^* p_{3\alpha}) \varepsilon_2^\alpha \\
=\;& \frac{1}{2} \int \frac{d^3\vec{p}_1}{(2\pi)^3 2E_1} \frac{d^3\vec{p}_2}{(2\pi)^3 2E_2} (2\pi)^4 \delta^4(p_B - p_1 - p_2)\, 16 f_{D_s^* D_s^* \phi} \frac{F^2(t, m_{D_s^*})}{t - m_{D_s^*}^2} f_{D^* D_s^* K^*} \\
&\times \Big\{ \varepsilon_3^* \cdot \varepsilon_4^* \Big\{ \Big[-1 + \frac{(1-\sigma)^2}{m_{D_s^*}^2} A_1^{(2)} \Big] \Big[a\, p_3 \cdot p_4 + b p_3 \cdot p_2 p_1 \cdot p_4 \\
&+ \frac{a + b p_1 \cdot p_2}{m_1^2 m_2^2} (-m_2^2 p_3 \cdot p_1 p_1 \cdot p_4 - m_1^2 p_3 \cdot p_2 p_2 \cdot p_4 + p_3 \cdot p_1 p_1 \cdot p_2 p_2 \cdot p_4) \Big] \\
&+ a \Big(-p_3 \cdot p_4 + \frac{p_3 \cdot k k \cdot p_4}{m_{D_s^*}^2} \Big) + A_1^{(2)} \Big\{ \sigma^2 \Big[2a - b p_1 \cdot p_2 + \frac{a + b p_1 \cdot p_2}{m_1^2 m_2^2} (p_1 \cdot p_2)^2 \Big]
\end{aligned}
$$

$$
\begin{aligned}
&+\sigma\bigg[b-\frac{a+bp_1\cdot p_2}{m_1^2m_2^2}p_1\cdot p_2\bigg]P^2 \\
&+(\sigma-1)\frac{p_4\cdot k}{m_{D_s^*}^2}\bigg[bp_2\cdot p_3+\frac{a+bp_1\cdot p_2}{m_1^2m_2^2}(m_1^2p_2\cdot p_3-m_2^2p_1\cdot p_3-p_2\cdot p_1p_1\cdot p_3)\bigg] \\
&+(\sigma-1)\frac{p_3\cdot k}{m_{D_s^*}^2}\bigg[-bp_1\cdot p_4+\frac{a+bp_1\cdot p_2}{m_1^2m_2^2}(m_1^2p_2\cdot p_4-m_2^2p_1\cdot p_4+p_1\cdot p_2p_2\cdot p_4)\bigg] \\
&+\bigg(p_3\cdot p_4-\frac{p_3\cdot kk\cdot p_4}{m_{D_s^*}^2}\bigg)\bigg[b+\frac{a+bp_1\cdot p_2}{m_1^2m_2^2}(m_1^2+m_2^2+p_1\cdot p_2)\bigg]\bigg\}\bigg\} \\
&-\varepsilon_3^*\cdot P\varepsilon_4^*\cdot P\bigg\{\frac{(1-\sigma)^2}{m_{D_s^*}^2}(A_1^{(1)}-A_2^{(1)}-A_2^{(2)}+A_4^{(2)})\bigg[a\,p_3\cdot p_4+bp_3\cdot p_2p_1\cdot p_4 \\
&+\frac{a+bp_1\cdot p_2}{m_1^2m_2^2}(-m_2^2p_3\cdot p_1p_1\cdot p_4-m_1^2p_3\cdot p_2p_2\cdot p_4+p_3\cdot p_1p_1\cdot p_2p_2\cdot p_4)\bigg] \\
&+\sigma^2(A_1^{(1)}-A_2^{(1)}-A_2^{(2)}+A_4^{(2)})\bigg[2a-bp_1\cdot p_2+\frac{(p_1\cdot p_2)^2}{m_1^2m_2^2}(a+bp_1\cdot p_2)\bigg] \\
&-\sigma\bigg[b-\frac{a+bp_1\cdot p_2}{m_1^2m_2^2}p_1\cdot p_2\bigg][(A_2^{(2)}-A_4^{(2)})P^2+(1-2A_1^{(1)})p_1\cdot p_3 \\
&-(A_1^{(1)}-A_2^{(1)})(p_1\cdot p_4+p_2\cdot p_3)]-\bigg[1-(1-\sigma)(A_1^{(1)}-A_2^{(1)})\frac{p_4\cdot k}{m_{D_s^*}^2}\bigg] \\
&\times\bigg[a+\frac{a+bp_1\cdot p_2}{m_1^2m_2^2}(-m_1^2p_2\cdot p_3+p_2\cdot p_1p_1\cdot p_3)\bigg] \\
&-\bigg[1+(1-\sigma)(1-A_1^{(1)}-A_2^{(1)})\frac{p_3\cdot k}{m_{D_s^*}^2}\bigg]\bigg(a+bp_1\cdot p_4-\frac{a+bp_1\cdot p_2}{m_2^2}p_2\cdot p_4\bigg) \\
&-\bigg[A_1^{(1)}+A_2^{(1)}-(1-\sigma)(A_2^{(2)}-A_4^{(2)})\frac{p_4\cdot k}{m_{D_s^*}^2}\bigg] \\
&\times\bigg[bp_2\cdot p_3+\frac{a+bp_1\cdot p_2}{m_1^2m_2^2}(m_1^2p_2\cdot p_3-m_2^2p_1\cdot p_3-p_2\cdot p_1p_1\cdot p_3)\bigg] \\
&+\bigg[A_1^{(1)}-A_2^{(1)}+(1-\sigma)\frac{p_3\cdot k}{m_{D_s^*}^2}(A_1^{(1)}-A_2^{(1)}-A_2^{(2)}+A_4^{(2)})\bigg) \\
&\times\bigg[bp_1\cdot p_4-\frac{a+bp_1\cdot p_2}{m_1^2m_2^2}(m_1^2p_2\cdot p_4-m_2^2p_1\cdot p_4+p_1\cdot p_2p_2\cdot p_4)\bigg] \\
&+\bigg(p_3\cdot p_4-\frac{p_3\cdot kk\cdot p_4}{m_{D_s^*}^2}\bigg)\bigg\{b(A_1^{(1)}+A_2^{(1)}-A_2^{(2)}+A_4^{(2)}) \\
&+\frac{a+bp_1\cdot p_2}{m_1^2m_2^2}[p_1\cdot p_2(A_1^{(1)}-A_2^{(1)}-A_2^{(2)}+A_4^{(2)})-m_1^2(1-2A_1^{(1)}+A_2^{(2)}-A_4^{(2)}) \\
&-m_2^2(A_2^{(2)}-A_4^{(2)})]\bigg\}\bigg\}-i[\varepsilon_3^*,\varepsilon_4^*,p_3,p_4]\,2c\bigg\{\bigg(p_3\cdot p_4-\frac{p_3\cdot kk\cdot p_4}{m_{D_s^*}^2}\bigg)A_2^{(1)} \\
&-\bigg[2\sigma-(1-\sigma)\frac{q\cdot k}{2m_{D_s^*}^2}\bigg]A_1^{(2)}\bigg\}\bigg\},
\end{aligned}
\tag{7.19}
$$

with $P=p_3+p_4$, $q=p_3-p_4$ and $k=p_1-p_3=p_4-p_2$ as before. Clearly the above rescattering amplitude contributes to all three polarization components $A_{L,\|,\perp}$.

C. Numerical results

In order to perform a numerical study of the analytic results obtained in the previous subsection, we need to specify the short-distance $A(\overline{B}\to D_s^{(*)}D^{(*)})$ amplitudes. In the factorization approach, we have

$$\begin{aligned}
A(\overline{B}\to D_sD)_{SD} &= i\frac{G_{\rm F}}{\sqrt{2}}V_{cb}V_{cs}^*a_1f_{D_s}(m_B^2-m_D^2)F_0^{BD}(m_{D_s}^2),\\
A(\overline{B}\to D_s^*D)_{SD} &= \frac{G_{\rm F}}{\sqrt{2}}V_{cb}V_{cs}^*a_1f_{D_s^*}m_{D_s^*}F_1^{BD}(m_{D_s^*}^2)(2\varepsilon_{D_s^*}^*\cdot p_B),\\
A(\overline{B}\to D_sD^*)_{SD} &= \frac{G_{\rm F}}{\sqrt{2}}V_{cb}V_{cs}^*a_1f_{D_s}m_{D^*}A_0^{BD^*}(m_{D_s}^2)(2\varepsilon_{D^*}^*\cdot p_B),\\
A(\overline{B}\to D_s^*D^*)_{SD} &= -i\frac{G_{\rm F}}{\sqrt{2}}V_{cb}V_{cs}^*a_1f_{D_s^*}m_{D_s^*}(m_B+m_{D^*})\varepsilon_{D_s^*}^{*\mu}\varepsilon_{D^*}^{*\nu}\Bigg[A_1^{BD^*}(m_{D_s^*}^2)g_{\mu\nu}\\
&\quad -\frac{2A_2^{BD^*}(m_{D_s^*}^2)}{(m_B+m_{D^*})^2}p_{B\mu}p_{B\nu}-i\frac{2V^{BD^*}(m_{D_s^*}^2)}{(m_B+m_{D^*})^2}\epsilon_{\mu\nu\alpha\beta}p_B^\alpha p_{D^*}^\beta\Bigg].
\end{aligned} \tag{7.20}$$

Writing $A=A^{SD}+i\mathcal{A}bsA^{LD}$ with $\mathcal{A}bsA^{LD}$ being given in the previous subsection and using the form factors given in [63], we obtain the numerical results for $B\to\phi K^*$ amplitudes as exhibited in Table VIII. The branching ratio after the inclusion of FSIs is

$$\mathcal{B}(B\to\phi K^*)=(9.2^{+4.3}_{-2.7})\times10^{-6} \tag{7.21}$$

for $\Lambda_{D_s,D_s^*}=m_{D_s,D_s^*}+\eta\,\Lambda_{\rm QCD}$ with $\eta=0.80$ and 15% error in $\Lambda_{\rm QCD}$. Several remarks are in order. (i) The polarization amplitudes are very sensitive to the cutoffs Λ_{D_s,D_s^*}. (ii) We have assumed a monopole behavior [i.e. $n=1$ in Eq. (3.22)] for the form factor $F(t,m_{D_s})$ and a dipole form (i.e. $n=2$) for $F(t,m_{D_s^*})$.[16] If the monopole form for $F(t,m_{D_s^*})$ is utilized, the parameter η will become unnaturally small in order to avoid too large FSI contributions. (iii) the interference between short-distance and long-distance contributions is mild. This is because $B\to\phi K^*$ and $B\to D_s^{(*)}D^{(*)}$ amplitudes should have the similar weak phase as $|V_{cb}V_{cs}^*|\gg|V_{ub}V_{us}^*|$. [17] As a result, the long-distance contribution is essentially "orthogonal" to the short-distance one. (iv) The calculated strong phases shown in Table VIII are in agreement with experiment for $\phi_\parallel$ but not

---

[16] For $B\to D\pi$, $K\pi,\pi\pi$ decays, assuming a dipole form for the form factor appearing in the $V_{\rm exc}VP$ or $V_{\rm exc}VV$ vertex with $V_{\rm exc}$ being the exchanged vector particle [see e.g. Figs. 4(e), 4(f), 5(d) and 6(e)] and a monopole behavior for all other form factors, we found that the best χ^2 fit to the measured decay rates is very similar to the one with the monopole form for all the form factors. Only the cutoff Λ or the parameter η appearing in Eq. (3.40) is slightly modified. The resultant branching ratios and CP asymmetries remain almost the same. The same exercise also indicates that if the dipole behavior is assumed for all the form factors, then the χ^2 value becomes too poor to be acceptable. This is the another good reason why we usually choose $n=1$ in Eq. (3.22) for the form factors except for the one appearing in $V_{\rm exc}VP$ or $V_{\rm exc}VV$ vertex.

[17] The weak phase of SD $\overline{B}\to\phi\overline{K}^*$ and $\overline{B}\to D_s^{(*)}D^{(*)}$ is not exactly the same. Moreover, our $\overline{B}\to\phi\overline{K}^*$ SD amplitude is not purely imaginary. It carries a phase as shown in Table VIII mainly because of the phase difference in a_4^u and a_4^c in our case [cf. Eq. (4.6)].

TABLE VIII: Short-distance (SD) and long-distance (LD) contributions to the decay amplitudes (in unit of 10^{-8} GeV) and the polarization fractions for $\overline{B} \to \phi \overline{K}^*$. LD contributions are calculated with $\Lambda_{D_s,D_s^*} = m_{D_s,D_s^*} + \eta\Lambda_{\rm QCD}$, where $\eta = 0.8$ and errors come from a 15% variation on $\Lambda_{\rm QCD}$.

	longitudinal (L)	parallel ($\parallel$)	perpendicular ($\perp$)
A^{SD}	$0.63 - 1.98i$	$-0.18 + 0.55i$	$0.15 - 0.46i$
A^{SD+LD}	$-0.57^{+0.33}_{-0.39} - (2.03 \pm 0.01)i$	$2.28^{+0.77}_{-0.67} + (0.64 \pm 0.03)i$	$0.32 \pm 0.05 - (0.44 \pm 0.00)i$
$A(D_sD; D_s)$	$-1.10^{+0.30}_{-0.34} - (0.04 \pm 0.01)i$	$0.07 \pm 0.02 + 0.00i$	0
$A(D_sD; D_s^*)$	0.00	$-0.02 \pm 0.01 - 0.00i$	0
$A(D_s^*D; D_s)$	0	0	$-0.19 \pm 0.05 - 0.01i$
$A(D_s^*D; D_s^*)$	0	0	$-0.01 - 0.00i$
$A(D_sD^*; D_s)$	0	0	$0.17 \pm 0.05 + 0.01i$
$A(D_sD^*; D_s^*)$	0	0	$0.01 + 0.00i$
$A(D_s^*D^*; D_s)$	$-0.06 \pm 0.02 - 0.00i$	$2.35^{+0.73}_{-0.63} + (0.09^{+0.03}_{-0.02})i$	$0.21^{+0.07}_{-0.06} + 0.01i$
$A(D_s^*D^*; D_s^*)$	$-0.04^{+0.02}_{-0.03} - 0.00i$	$0.06^{+0.04}_{-0.03} + 0.00i$	$-0.01 \pm 0.01 - 0.00i$
f^{SD}	0.88	0.07	0.05
f^{SD+LD}	$0.43^{+0.13}_{-0.09}$	$0.54^{+0.10}_{-0.14}$	0.03 ± 0.01
$f^{\rm expt}$	0.51 ± 0.04 [a]	0.27 ± 0.06 [a]	0.22 ± 0.04 [a]
$\arg(A_iA_L^*)^{SD}$	–	π	0
$\arg(A_iA_L^*)^{SD+LD}$	–	$2.12^{+0.11}_{-0.07}$	$0.89^{+0.21}_{-0.24}$
$\arg(A_iA_L^*)^{\rm BaBar}$	–	$2.34^{+0.23}_{-0.20} \pm 0.05$	$-0.67 \pm 0.25 \pm 0.05$ [b]
$\arg(A_iA_L^*)^{\rm Belle}$	–	$2.21 \pm 0.22 \pm 0.05$ [b]	$-0.72 \pm 0.21 \pm 0.06$ [b]

[a] $f^{\rm expt}$ is the experimental average of polarization fractions for $B^- \to \phi K^{*-}$ and $\overline{B}^0 \to \phi \overline{K}^{*0}$.

[b] See footnote 18 for details.

for $\phi_\perp$.[18] (v) There are large cancellations among various long-distance contributions, e.g. between $A(D_s^*D; D_s^{(*)})$ and $A(D_sD^*; D_s^{(*)})$.

The cancellation in $\overline{B} \to D_s^*D \to \phi K^*$ and $\overline{B} \to D_sD^* \to \phi K^*$ contributions can be understood from SU(3) symmetry, CP conjugation [19] and the similarity in the size of source amplitudes. To see this, let $\langle \phi(\bar{s}s)K^*(\bar{q}s)|T_{\rm st}|D_s^*(\bar{c}s)D(\bar{q}c)\rangle$ be the $D_s^*D \to \phi K^*$ rescattering matrix element, which is represented in the right-hand part of Fig. 9. After changing $s \to q$ in $D_s^*(\bar{c}s)$ and $\phi(\bar{s}s)$ (on the upper right part of Fig. 9), and $\bar{q} \to \bar{s}$ in $D(\bar{q}c)$ and $K^*(\bar{q}s)$ (on the lower right part of of the same figure) under the SU(3) symmetry transformation, the above matrix element becomes $\langle K^*(\bar{s}q)\phi(\bar{s}s)|T_{\rm st}|D^*(\bar{c}q)D_s(\bar{s}c)\rangle$. Applying charge conjugation after the SU(3) transformation, we are led to

---

[18] In Table VII, the experimental results of $\phi_\parallel$ and $\phi_\perp$ are for $B \to \phi K^*$ decays. The Belle results for $(\phi_\parallel, \phi_\perp)$ should be transformed to $(-\phi_\parallel, \pi - \phi_\perp)$. This phase transformation will not modify the experimentally measured distributions (see [81] for details) but it will flip the relative sign between $\phi_\parallel$, $\phi_\perp$ and lead to $|A_+| > |A_-|$ for $B \to \phi K^*$ as expected from the factorization approach. Since our calculations are for $\overline{B} \to \phi \overline{K}^*$ decays, in Table VIII we have transformed BaBar and Belle results from $\phi_\perp$ to $\phi_\perp - \pi$ so that $|A_+| < |A_-|$ in $\overline{B} \to \phi \overline{K}^*$. Note that in the absence of FSIs, $\phi_\parallel = \phi_\perp = \pi$ for $B \to \phi K^*$ and $\phi_\parallel = \pi$, $\phi_\perp = 0$ for $\overline{B} \to \phi \overline{K}^*$.

[19] The combined symmetry is reminiscent of CPS symmetry which is used extensively in kaon decay matrix elements on the lattice [82, 83].

$$\langle \phi(\bar{s}s)K^*(\bar{q}s)|T_{\rm st}|D_s^*(\bar{c}s)D(\bar{q}c)\rangle = -\langle K^*(\bar{q}s)\phi(\bar{s}s)|T_{\rm st}|D^*(\bar{q}c)D_s(\bar{c}s)\rangle, \tag{7.22}$$

where the overall negative sign arises from the transformation of vector particles under charge conjugation. In the $\overline{B} \to D_s^* D \to \phi K^*$ rescattering amplitude, the above matrix element is sandwiched by $\varepsilon^*(p_1,\lambda)\cdot p_B$ from $\overline{B} \to D_s^* D$ amplitudes and $\epsilon_{\mu\nu\rho\sigma}\varepsilon^\mu(p_3,\lambda')\varepsilon^\nu(p_4,\lambda'')p_3^\rho p_4^\sigma$ to project out the $A_\perp$ term. These factors bring the initial and final states into p-wave configurations. Applying parity transformation will interchange the particle momentum in the B rest frame. Such an interchange does not yield a further sign flip as the initial and final states are both in the p-wave configuration. To be more specific, we have

$$\mathbf{P}\sum_\lambda |D^*(p_1,\lambda)D(p_2)\rangle\ \varepsilon(p_1,\lambda)^\mu p_{B\mu} = \sum_\lambda |D^*(p_2,-\lambda)D(p_1)\rangle\ [-\varepsilon_\mu(p_2,-\lambda)p_B^\mu], \tag{7.23}$$

where the identity $\varepsilon_\mu(\vec{p},\lambda) = -\varepsilon^\mu(-\vec{p},-\lambda)$ with $p_1^\mu = (E,\vec{p}) = p_{2\mu}$ in the B rest frame for the $m_1 = m_2$ case and $p_1 \leftrightarrow p_2$ under the parity transformation ($\mathbf{P}$) on initial state particles have been used. For the parity transformation of the final state, we have

$$\begin{aligned}
&\mathbf{P}\sum_{\lambda',\lambda''} |K^*(p_3,\lambda')\phi(p_4,\lambda'')\rangle\ \epsilon_{\mu\nu\rho\sigma}\varepsilon^\mu(p_3,\lambda')\varepsilon^\nu(p_4,\lambda'')p_3^\rho p_4^\sigma \\
&= \sum_{\lambda',\lambda''} |K^*(p_4,-\lambda')\phi(p_3,-\lambda'')\rangle\ \epsilon_{\mu\nu\rho\sigma}(-)^2\varepsilon_\mu(p_4,-\lambda')\varepsilon_\nu(p_3,-\lambda'')p_{4\rho}p_{3\sigma} \\
&= -\sum_{\lambda',\lambda''} |K^*(p_4,\lambda'')\phi(p_3,\lambda')\rangle\ \epsilon_{\mu\nu\rho\sigma}\varepsilon^\mu(p_3,\lambda')\varepsilon^\nu(p_4,\lambda'')p_3^\rho p_4^\sigma,
\end{aligned} \tag{7.24}$$

where similar identities and indices relabelling have been used. We thus have

$$\begin{aligned}
&\sum_{\lambda,\lambda'\lambda''} \epsilon_{\mu\nu\rho\sigma}\varepsilon^\mu(p_3,\lambda')\varepsilon^\nu(p_4,\lambda'')p_3^\rho p_4^\sigma\ \langle\phi(p_3,\lambda')K^*(p_4,\lambda'')|T_{\rm st}|D_s^*(p_1,\lambda)D(p_2)\rangle\ \varepsilon^*(p_1,\lambda)\cdot p_B \\
&= -\sum_{\lambda,\lambda'\lambda''} \epsilon_{\mu\nu\rho\sigma}\varepsilon^\mu(p_3,\lambda')\varepsilon^\nu(p_4,\lambda'')p_3^\rho p_4^\sigma\ \langle K^*(p_4,\lambda'')\phi(p_3,\lambda')|T_{\rm st}|D^*(p_2,\lambda)D_s(p_1)\rangle\ \varepsilon^*(p_2,\lambda)\cdot p_B
\end{aligned} \tag{7.25}$$

from SU(3) [U(3)] symmetry and CP conjugation. The right-hand side of the above equation is proportional to the $\overline{B} \to D_s D^* \to \phi K^*$ rescattering matrix element with an additional negative sign, which is the source of cancellation. This cancellation turns out to be quite effective as the $\overline{B} \to D_s^* D$ and $\overline{B} \to D_s D^*$ amplitudes are numerically similar, i.e. $f_{D_s^*} m_{D_s^*} F_1^{BD}(m_{D_s^*}^2) \simeq f_{D_s} m_{D^*} A_0^{BD^*}(m_{D_s}^2)$. Note that SU(3) breaking does not really help avoid the cancellation. Since the number of s quarks involved in $\overline{B} \to D_s^* D \to \phi\overline{K}^*$ and $\overline{B} \to D_s D^* \to \phi\overline{K}^*$ is the same, SU(3) breaking affects both amplitudes in a similar manner and the net effect cancels.

Because of the above-mentioned cancellation and the fact that $\bar{B} \to D_s^* D^*$ does not give rise to a large $A_\perp$, we cannot obtain large $f_\perp(\overline{B} \to \phi\overline{K}^*)$ through FSI. The latter point can be seen from the fact that the polarization fraction of $\overline{B} \to D_s^* D^*$ is $f_L : f_\parallel : f_\perp \simeq 0.51 : 0.41 : 0.08$. Although the $D_s^*D^*$ intermediate state has a smaller A_L, it does not have a large $A_\perp$. The suppression in $A_\perp$ can be understood from the smallness of the p_c/m_B factor as shown in Eq. (7.4). In principle, one could obtain a larger $A_\perp^{LD}(B \to \phi K^*)$ by applying a larger $\Lambda_{D_s^*}$ to get a larger $A(D_s^*D^*; D_s^*)$. However, such a large $A(D_s^*D^*; D_s^*)$ will also enhance A_L^{LD}, giving a too large $\overline{B} \to \phi \overline{K}^*$ decay rate and does not really bring up $f_\perp$.

D. $B^- \to K^{*-}\rho^0$ decays

In the factorization approach, the amplitude of the $\overline{B} \to K^{*-}\rho^0$ decay is given by

$$\begin{aligned}
\langle K^{*-}(\lambda_{K^*})\rho^0(\lambda_\rho)|H_{\rm eff}|B^-\rangle &= \frac{G_{\rm F}}{\sqrt{2}}\sum_{q=u,c} V_{qb}V_{qs}^*\ a^q_{K^*\rho}\ \langle\rho|(\bar u u)_V|0\rangle\,\langle K^{*-}|(\bar s b)_{V-A}|B^-\rangle \\
&\quad +\frac{G_{\rm F}}{\sqrt{2}}\sum_{q=u,c} V_{qb}V_{qs}^*\ b^q_{K^*\rho}\ \langle K^{*-}|(\bar s u)_V|0\rangle\,\langle\rho^0|(\bar u b)_{V-A}|B^-\rangle \\
&= -i\ \varepsilon^{*\mu}_{K^*}(\lambda_{K^*})\varepsilon^{*\nu}_{\rho}(\lambda_\rho)\Big\{[\alpha_{K^*\rho}A_1^{BK^*}(m_\rho^2)+\beta_{K^*\rho}A_1^{B\rho}(m_{K^*}^2)]g_{\mu\nu} \\
&\quad -2\Big[\alpha_{K^*\rho}\frac{A_2^{BK^*}(m_\rho^2)}{(m_B+m_{K^*})^2}+\beta_{K^*\rho}\frac{A_2^{B\rho}(m_{K^*}^2)}{(m_B+m_\rho)^2}\Big]p_{B\mu}p_{B\nu} \\
&\quad -2i\Big[-\alpha_{K^*\rho}\frac{V^{BK^*}(m_\phi^2)}{(m_B+m_{K^*})^2}+\beta_{K^*\rho}\frac{V^{B\rho}(m_{K^*}^2)}{(m_B+m_\rho)^2}\Big]\epsilon_{\mu\nu\alpha\beta}p_B^\alpha p_\rho^\beta\Big\}, \\
\langle \overline{K}^{*0}(\lambda_{K^*})\rho^-(\lambda_\rho)|H_{\rm eff}|B^-\rangle &= \frac{G_{\rm F}}{\sqrt{2}}\sum_{q=u,c} V_{qb}V_{qs}^*\ c^q_{K^*\rho}\ \langle\overline{K}^{*0}|(\bar s d)_V|0\rangle\,\langle\rho^-|(\bar d b)_{V-A}|B^-\rangle \\
&= -i\ \gamma_{K^*\rho}\varepsilon^{*\mu}_{K^*}(\lambda_{K^*})\varepsilon^{*\nu}_{\rho}(\lambda_\rho)\Big\{A_1^{B\rho}(m_{K^*}^2)g_{\mu\nu} \\
&\quad -2\frac{A_2^{B\rho}(m_{K^*}^2)}{(m_B+m_\rho)^2}p_{B\mu}p_{B\nu}-2i\frac{V^{B\rho}(m_{K^*}^2)}{(m_B+m_\rho)^2}\epsilon_{\mu\nu\alpha\beta}p_B^\alpha p_\rho^\beta\Big\}, \qquad (7.26)
\end{aligned}$$

where

$$\begin{aligned}
a^u_{K^*\rho} &= a_2+\frac{3}{2}(a_7+a_9), \quad a^c_{K^*\rho}=\frac{3}{2}(a_7+a_9), \quad b^u_{K^*\rho}=a_1+a_4^u+a_{10}^u, \quad b^c_{K^*\rho}=a_4^c+a_{10}^c, \\
c^u_{K^*\rho} &= a_4^u-\frac{1}{2}a_{10}^u, \quad c^c_{K^*\rho}=a_4^c-\frac{1}{2}a_{10}^c, \\
\alpha_{K^*\rho} &= \frac{G_{\rm F}}{2}f_\rho m_\rho(m_B+m_{K^*})\sum_{q=u,c}V_{qb}V_{qs}^*\ a^q_{K^*\rho}, \quad \beta_{K^*\rho}=\frac{G_{\rm F}}{2}f_{K^*}m_{K^*}(m_B+m_\rho)\sum_{q=u,c}V_{qb}V_{qs}^*\ b^q_{K^*\rho}, \\
\gamma_{K^*\rho} &= \frac{G_{\rm F}}{\sqrt{2}}f_{K^*}m_{K^*}(m_B+m_\rho)\sum_{q=u,c}V_{qb}V_{qs}^*\ c^q_{K^*\rho}.
\end{aligned}$$

Likewise, we have

$$\begin{aligned}
A_0(K^{*-}\rho^0) &= -i\Big(-[\alpha_{K^*\rho}A_1^{BK^*}(m_\rho^2)+\beta_{K^*\rho}A_1^{B\rho}(m_{K^*}^2)]\frac{m_B^2-m_{K^*}^2-m_\rho^2}{2m_{K^*}m_\rho} \\
&\quad +2\Big[\alpha_{K^*\rho}\frac{A_2^{BK^*}(m_\rho^2)}{(m_B+m_{K^*})^2}+\beta_{K^*\rho}\frac{A_2^{B\rho}(m_{K^*}^2)}{(m_B+m_\rho)^2}\Big]\frac{m_B^2p_c^2}{m_{K^*}m_\rho}\Big), \\
A_\parallel(K^{*-}\rho^0) &= -i\sqrt{2}[\alpha_{K^*\rho}A_1^{BK^*}(m_\rho^2)+\beta_{K^*\rho}A_1^{B\rho}(m_{K^*}^2)],
\end{aligned}$$

TABLE IX: Same as Table VIII except for $B^-\to K^{*-}\rho^0$ and $\Lambda_{D,D^*}=m_{D,D^*}+\eta\Lambda_{\rm QCD}$.

	longitudinal (L)	parallel ($\parallel$)	perpendicular ($\perp$)
A^{SD}	$1.18-1.69i$	$-0.26+0.37i$	$0.16-0.10i$
A^{SD+LD}	$0.11^{+0.30}_{-0.35}-(1.73^{+0.02}_{-0.01})i$	$1.43^{+0.53}_{-0.46}+(0.43\pm0.02)i$	$0.25\pm0.03-0.10i$
$A(D_sD;D)$	$-1.01^{+0.27}_{-0.31}-(0.04\pm0.01)i$	$0.04\pm0.01+0.00i$	0
$A(D_sD;D^*)$	0.00	$-0.01\pm0.01-0.00i$	0
$A(D_s^*D;D)$	0	0	$-0.13^{+0.03}_{-0.04}-0.00i$
$A(D_s^*D;D^*)$	0	0	0.00
$A(D_sD^*;D)$	0	0	$0.11\pm0.03+0.00i$
$A(D_sD^*;D^*)$	0	0	0.00
$A(D_s^*D^*;D)$	$-0.03\pm0.01-0.00i$	$1.62^{+0.50}_{-0.44}+(0.06\pm0.02)i$	$0.12^{+0.04}_{-0.03}+0.00i$
$A(D_s^*D^*;D^*)$	$-0.04\pm0.02-0.00i$	$0.04^{+0.03}_{-0.02}+0.00i$	$-0.01^{+0.00}_{-0.01}-0.00i$
f^{SD}	0.95	0.04	0.01
f^{SD+LD}	$0.57^{+0.16}_{-0.14}$	$0.42^{+0.14}_{-0.16}$	0.01
$f^{\rm expt}$	$0.96^{+0.04}_{-0.16}$		

$$
\begin{aligned}
A_\perp(K^{*-}\rho^0) &= 2\sqrt{2}i\Big[-\alpha_{K^*\rho}\frac{V^{BK^*}(m_\phi^2)}{(m_B+m_{K^*})^2}+\beta_{K^*\rho}\frac{V^{B\rho}(m_{K^*}^2)}{(m_B+m_\rho)^2}\Big]m_Bp_c,\\
A_0(\overline{K}^{*0}\rho^-) &= -i\gamma_{K^*\rho}\Big(-A_1^{B\rho}(m_{K^*}^2)\frac{m_B^2-m_{K^*}^2-m_\rho^2}{2m_{K^*}m_\rho}+\frac{2A_2^{B\rho}(m_{K^*}^2)}{(m_B+m_\rho)^2}\frac{m_B^2p_c^2}{m_{K^*}m_\rho}\Big),\\
A_\parallel(\overline{K}^{*0}\rho^-) &= -i\gamma_{K^*\rho}\sqrt{2}A_1^{B\rho}(m_{K^*}^2),\quad A_\perp(\overline{K}^{*0}\rho^-)=i\gamma_{K^*\rho}\frac{2\sqrt{2}V^{B\rho}(m_{K^*}^2)}{(m_B+m_\rho)^2}m_Bp_c. \qquad (7.27)
\end{aligned}
$$

Similar to the calculation for $B\to\phi K^*$, we obtain

$$
\begin{aligned}
\mathcal{B}^{SD}(B^-\to K^{*-}\rho^0) &= (4.1\pm2.2)\times10^{-6},\\
\mathcal{B}^{SD}(B^-\to \overline{K}^{*0}\rho^-) &= (4.3\pm2.9)\times10^{-6},\\
f_L^{\rm SD}:f_\parallel^{\rm SD}:f_\perp^{\rm SD}(K^{*-}\rho^0) &= 0.95\pm0.02:0.04\pm0.02:0.01\pm0.00,\\
f_L^{\rm SD}:f_\parallel^{\rm SD}:f_\perp^{\rm SD}(\overline{K}^{*0}\rho^-) &= 0.92\pm0.05:0.04\pm0.02:0.04\pm0.01, \qquad (7.28)
\end{aligned}
$$

where the errors are estimated from 10% uncertainties in form factors.

The formulae for long-distance contributions to $B^-\to K^{*-}\rho^0$ decays are similar to that in $B\to\phi K^*$ with the intermediate state $D_s^{(*)}$ and strong couplings $f(g)_{D_s^{(*)}D_s^{(*)}\phi}$ and $f(g)_{D^{(*)}D_s^{(*)}K^*}$ replaced by $D^{(*)}$, $f(g)_{D_s^{(*)}D^{(*)}K^*}$ and $f(g)_{D^{(*)}D^{(*)}\rho}/\sqrt{2}$, respectively. Likewise, the $B^-\to\overline{K}^{*0}\rho^-$ rescattering amplitudes can be obtained by a similar replacement except for an additional factor of $1/\sqrt{2}$ associated with $f(g)_{D^{(*)}D^{(*)}\rho}$.

Numerical results for $B^-\to K^{*-}\rho^0$ and $B^-\to K^{*0}\rho^-$ are shown in Tables IX and X, respectively. Using $\Lambda_{D^{(*)}}=m_{D^{(*)}}+\eta\Lambda_{\rm QCD}$ with $\eta=0.8$, we obtain

$$
\begin{aligned}
&\mathcal{B}^{SD+LD}(K^{*-}\rho^0)=(4.8^{+1.8}_{-0.9})\times10^{-6}, &&\mathcal{B}^{SD+LD}(\overline{K}^{*0}\rho^-)=(10.3^{+4.9}_{-3.1})\times10^{-6},\\
&\mathcal{A}^{SD}(K^{*-}\rho^0)=0.30, &&\mathcal{A}^{SD}(\overline{K}^{*0}\rho^-)=0.11,\\
&\mathcal{A}^{SD+LD}(K^{*-}\rho^0)=0.02^{+0.05}_{-0.02}, &&\mathcal{A}^{SD+LD}(\overline{K}^{*0}\rho^-)\simeq0.00\,. \qquad (7.29)
\end{aligned}
$$

TABLE X: Same as Table VIII except for $B^- \to \overline{K}^{*0}\rho^-$.

	longitudinal (L)	parallel ($\parallel$)	perpendicular ($\perp$)
A^{SD}	$0.43 - 2.04i$	$-0.10 + 0.45i$	$0.09 - 0.41i$
A^{SD+LD}	$-1.09^{+0.42}_{-0.49} - (2.09 \pm 0.02)i$	$2.29^{+0.75}_{-0.65} + (0.54^{+0.03}_{-0.02})i$	$0.22 \pm 0.04 - 0.41i$
$A(D_s D; D)$	$-1.42^{+0.39}_{-0.44} - (0.05 \pm 0.02)i$	$0.06 \pm 0.02 + 0.00i$	0
$A(D_s D; D^*)$	0.00	$-0.02 \pm 0.01 - 0.00i$	0
$A(D_s^* D; D)$	0	0	$-0.18 \pm 0.05 - 0.00i$
$A(D_s^* D; D^*)$	0	0	$-0.01 - 0.00i$
$A(D_s D^*; D)$	0	0	$0.16^{+0.05}_{-0.04} + 0.00i$
$A(D_s D^*; D^*)$	0	0	$0.01 + 0.00i$
$A(D_s^* D^*; D)$	$-0.04 \pm 0.01 - 0.00i$	$2.29^{+0.70}_{-0.62} + (0.09^{+0.03}_{-0.02})i$	$0.17^{+0.06}_{-0.05} + 0.01i$
$A(D_s^* D^*; D^*)$	$-0.05^{+0.02}_{-0.04} - 0.00i$	$0.06^{+0.04}_{-0.03} + 0.00i$	$-0.01 \pm 0.01 - 0.00i$
f^{SD}	0.92	0.04	0.04
f^{SD+LD}	$0.49^{+0.11}_{-0.08}$	$0.49^{+0.08}_{-0.12}$	0.02 ± 0.01
$f^{\rm expt}$	0.74 ± 0.08		

Note that the long-distance contributions are similar to that of the $\phi\overline{K}^*$ case up to some SU(3) breaking and the LD contributions to $K^{*-}\rho^0$ and $\overline{K}^{*0}\rho^-$ are related through the above-mentioned factor of $\sqrt{2}$ from the $D^{(*)}D^{(*)}\rho$ vertices. Before the inclusion of FSIs, $K^{*-}\rho^0$ and $\overline{K}^{*0}\rho^-$ have similar rates as the former receives additional tree contributions from $\mathcal{T}$ and $\mathcal{C}$ topologies. However, the LD contribution to the former is suppressed at the amplitude level by a factor of $\sqrt{2}$ and this accounts for the disparity in rates between these two modes. The cancellation between $\overline{B} \to PV \to VV$ and $\overline{B} \to VP \to VV$ amplitudes remains. Since the short distance $B^- \to K^{*-}\rho^0$ amplitude has a non-vanishing weak phase, we have interferences between SD and LD contributions resulting in quite sensitive direct CP. Comparing to the data shown in Table VII, we note that (i) the $K^{*-}\rho^0$ and $\overline{K}^{*0}\rho^-$ rates are consistent with the data within errors and (ii) the predicted $f_L(\overline{K}^{*0}\rho^-)$ agrees well with experiment, while $f_L(K^{*-}\rho^0)$ is lower than the BaBar data. This should be clarified by future improved experiments.

E. FSI contributions from other channels

For LD contributions to the $\overline{B} \to \phi\overline{K}^{(*)}$ decay, it is also possible to have $B \to J/\psi K^{(*)} \to \phi K^*$ via a t-channel η_s (a pseudoscalar with the $s\bar{s}$ quark content) exchange and $B \to K^{(*)}J/\psi \to \phi K^*$ via a t-channel K exchange. However, it does not seem that it can fully explain the polarization anomaly for two reasons: (i) The CP and SU(3) [CPS] symmetry argument also leads to the cancellation in the $B \to J/\psi K \to \phi K^*$ via a t-channel η_s exchange and $B \to K J/\psi \to \phi K^*$ via a t-channel K exchange contribution. (ii) The $B \to J/\psi K^*$ decay does not generate a large enough $A_\perp$ source. The polarization fractions of $B \to J/\psi K^*$ are $f_L : f_\parallel : f_\perp \simeq 0.47 : 0.35 : 0.17$, which differ not much from that of $\overline{B} \to D_s^* D^*$. On the other hand, it is known that SU(3) breaking and the electromagnetic interaction take place in J/ψ decays (in particular, in the case of $J/\psi \to \overline{K}^* K$, $K^*\overline{K}$ and $\phi\eta^{(\prime)}$ decays of interest) at the level of $\sim 20\%$ and $\sim 10\%$ [84], respectively. The above-mentioned cancellation may not be very effective. Hence, we should look at the FSI contributions from this channel more carefully.

The Lagrangian relevant for $J/\psi \to PV$ and $\phi \to PP$ decays is given by

$$\mathcal{L} = i g_{VPP} \mathrm{Tr}(V^\mu P \overset{\leftrightarrow}{\partial}_\mu P) + \frac{g_{J/\psi VP}}{\sqrt{2}} \epsilon^{\mu\nu\alpha\beta} \partial_\mu (J/\psi)_\nu \mathrm{Tr}(\partial_\alpha V_\beta P), \tag{7.30}$$

where $V(P)$ is the vector (pseudoscalar) nonet matrix. We have $g_{\phi KK} = 4.8$ and $g_{J/\psi K^* K} = 2.6 \times 10^{-3}$ GeV^{-1} fitted from the data [50]. The $g_{J\psi\phi\eta_s}$ coupling is estimated to be $0.4\, g_{J/\psi K^* K}$, where the deviation comes from SU(3) breaking and the contribution of electromagnetic interactions [84], and we estimate $g_{K^* K \eta_s} \simeq g_{\phi KK}$.

It is straightforward to obtain

$$\begin{aligned}
\mathcal{A}bs\,(J/\psi\overline{K};\eta_s) \;&=\; \frac{1}{2}\int \frac{d^3\vec{p}_1}{(2\pi)^3 2E_1}\,\frac{d^3\vec{p}_2}{(2\pi)^3 2E_2}\,(2\pi)^4\delta^4(p_B-p_1-p_2)\frac{A(\overline{B}^0\to J/\psi\overline{K})}{2\varepsilon_1^*\cdot P}\\
&\quad\times(-i)[\varepsilon_3^*,\varepsilon_4^*,p_3,p_4]\Big\{-2\sqrt{2}i\,g_{J/\psi\phi\eta_s}\frac{F^2(t,m_{\eta_s})}{t-m_{\eta_s}^2}g_{K^*K\eta}\,A_1^{(2)}\Big\},\\
\mathcal{A}bs\,(\overline{K}/J\psi;K) \;&=\; \frac{1}{2}\int \frac{d^3\vec{p}_1}{(2\pi)^3 2E_1}\,\frac{d^3\vec{p}_2}{(2\pi)^3 2E_2}\,(2\pi)^4\delta^4(p_B-p_1-p_2)\frac{A(\overline{B}^0\to \overline{K}J/\psi)}{2\varepsilon_2^*\cdot P}\\
&\quad\times(-i)[\varepsilon_3^*,\varepsilon_4^*,p_3,p_4]\Big\{2\sqrt{2}i\,g_{\phi KK}\frac{F^2(t,m_K)}{t-m_K^2}f_{J/\psi K^*K}\,A_1^{(2)}\Big\},
\end{aligned} \tag{7.31}$$

with

$$A(\overline{B}\to J/\psi\overline{K}) \;=\; \frac{G_\mathrm{F}}{\sqrt{2}}V_{cb}V_{cs}^* a_2 f_{J/\psi} m_{J/\psi} F_1^{BK}(m_{J/\psi}^2)(2\varepsilon_{J/\psi}^*\cdot p_B). \tag{7.32}$$

We obtain

$$A_\perp^{LD}(J/\psi\overline{K};\eta_s) = 2.4\times 10^{-11}\,\mathrm{GeV}, \quad A_\perp^{LD}(J/\psi\overline{K};K) = -6.9\times 10^{-11}\,\mathrm{GeV}, \tag{7.33}$$

where use of $a_2 = 0.28$, $f_{J/\psi} = 405$ MeV, $m_{\eta_s} \simeq 800$ MeV and $F(t, m_{K,\eta_s}) = 1$ has been made. Although the cancellation is incomplete as expected, the FSI contributions (even without the form factor suppression) from the $\overline{B} \to J/\psi\overline{K}$ decay are too small to explain the data (see Tables VII and VIII). The smallness of these contributions is due to the smallness of the OZI suppressed $g_{J/\psi PV}$ coupling.

One possibility of having a large $f_\perp$ is to circumvent the cancellation in $\overline{B} \to VP \to VV$ and $\overline{B} \to PV \to VV$ rescatterings. For example, we may consider $B \to SA \to \phi K^*$ contributions, where S and A denotes scalar and axial vector mesons, respectively. We need SA instead of VS, PA intermediate states to match the $(\phi K^*)_{p-wave}$ quantum numbers. The $B \to SA$ and $B \to AS$ amplitudes may not be similar (note that $f_{D_{s0}^*} \ll f_{D_0^*}$) and the charge conjugation properties of $A(^1P_1)$ and $A(^3P_1)$ are different.

To show this, we consider the FSI contributions to $f_\perp(VV)$ from the even-parity charmed meson (denoted by D^{**}) intermediate states. The Lagrangian ($\mathcal{L}_{D^{**}D^{**}V}$) for the interactions of

TABLE XI: Short-distance (SD) and long-distance (LD) contributions from $D_s^{**}D^{**}$ intermediate states to the decay amplitudes (in unit of 10^{-8} GeV) and the polarization fractions for $B \to \phi K^*$. LD contributions are calculated with $\Lambda_{D_{s0}^*, D_{s1}} = m_{D_{s0}^*, D_{s1}} + \eta\Lambda_{\rm QCD}$ and $\eta = 1.5$.

	longitudinal (L)	parallel ($\parallel$)	perpendicular ($\perp$)
A^{SD}	$0.63 - 1.98i$	$-0.18 + 0.55i$	$0.15 - 0.46i$
A^{SD+LD}	$-1.65 - 2.07i$	$0.50 + 0.58i$	$1.29 - 0.42i$
$A(D_{s0}^* D_0^*; D_{s0}^*)$	$-0.33 - 0.01i$	$0.00 + 0.00i$	0
$A(D_{s0}^* D_0^*; D_{s1})$	$0.03 + 0.00i$	$-1.99 - 0.07i$	0
$A(D_{s1} D_0^*; D_{s0}^*)$	0	0	$0.07 + 0.00i$
$A(D_{s1} D_0^*; D_{s1})$	0	0	$1.15 + 0.04i$
$A(D_{s0}^* D_1; D_{s0})$	0	0	$0.02 + 0.00i$
$A(D_{s0}^* D_1; D_{s1})$	0	0	$0.26 + 0.01i$
$A(D_{s1} D_1; D_{s0}^*)$	$-0.01 - 0.00i$	$0.83 + 0.03i$	$0.14 + 0.01i$
$A(D_{s1} D_1; D_{s1})$	$-1.97 - 0.07i$	$1.83 + 0.07i$	$-0.50 - 0.02i$
f^{SD}	0.88	0.07	0.05
f^{SD+LD}	0.74	0.06	0.19
$f^{\rm expt}$	0.52 ± 0.05	0.23 ± 0.06	0.25 ± 0.04

the charmed meson $J_j^P = (0^+, 1^+)_{1/2}$ multiplets and vector mesons is similar to (3.15) for the s-wave charm meson case. In chiral and heavy quark limits, the effective Lagrangian can be expressed compactly in terms of superfields [60]

$$\mathcal{L}_{D^{**}D^{**}V} = \quad i\beta_1 \langle S_b v^\mu (V_\mu - \rho_\mu)_{ba} \overline{S}_a \rangle + i\overline{\lambda}_1 \langle S_b \sigma^{\mu\nu} F_{\mu\nu}(\rho)_{ba} \overline{S}_a \rangle, \tag{7.34}$$

with the superfield $S = \frac{1+\not{v}}{2}(D_1^\mu \gamma_\mu \gamma_5 - D_0^*)$, which is similar to the superfield H except for the γ_5 factor and the phase in front of D_0^*. Hence, the Lagrangian in terms of the component fields can be obtained from Eq. (3.15) with g_{DDV}, f_{D^*DV}, $f_{D^*D^*V}$, $g_{D^*D^*V}$, β, λ, D^*-field and D-field replaced by $g_{D_0^*D_0^*V}$, $f_{D_1D_0^*V}$, $f_{D_1D_1V}$, $g_{D_1D_1V}$, β_1, $\overline{\lambda}_1$, D_1-field and $-iD_0^*$-field, respectively, and with an overall negative sign on $\mathcal{L}$.

The absorptive part contributions of $\overline{B} \to D_s^{**}D^{**} \to \phi\overline{K}^*$ via D_{s0}^* and D_{s1} exchanges are given by

$$\begin{aligned}
\mathcal{A}bs\,(D_{s0}^* D_0^*; D_{s0}^* \text{ or } D_{s1}) &= \mathcal{A}bs\,(D_s D; D_s \text{ or } D_s^*) \quad \text{with } D_{(s)}^* \to D_{(s)1} \text{ and } D_{(s)} \to D_{(s)0}^*, \\
\mathcal{A}bs\,(D_{s1} D_0^*; D_{s0}^* \text{ or } D_{s1}) &= -i\mathcal{A}bs\,(D_s^* D; D_s \text{ or } D_s^*) \quad \text{with } D_{(s)}^* \to D_{(s)1} \text{ and } D_{(s)} \to D_{(s)0}^*, \\
\mathcal{A}bs\,(D_{s0}^* D_1; D_{s0}^* \text{ or } D_{s1}) &= i\mathcal{A}bs\,(D_s D^*; D_s \text{ or } D_s^*) \quad \text{with } D_{(s)}^* \to D_{(s)1} \text{ and } D_{(s)} \to D_{(s)0}^*, \\
\mathcal{A}bs\,(D_{s1} D_1; D_{s0}^* \text{ or } D_{s1}) &= \mathcal{A}bs\,(D_s^* D^*; D_s \text{ or } D_s^*) \quad \text{with } D_{(s)}^* \to D_{(s)1} \text{ and } D_{(s)} \to D_{(s)0}^*,
\end{aligned} \tag{7.35}$$

and the $\overline{B} \to D_s^{**}D^{**}$ factorization amplitudes are

$$A(\overline{B} \to D_{s0}^* D_0^*) \;=\; i\frac{G_{\rm F}}{\sqrt{2}} V_{cb} V_{cs}^* a_1 f_{D_{s0}^*} (m_B^2 - m_{D_0^*}^2) F_0^{BD_0^*}(m_{D_{s0}^*}^2),$$

$$\begin{aligned}
A(\overline{B}\to D_{s1}D_0^*) &= -i\frac{G_{\rm F}}{\sqrt{2}}V_{cb}V_{cs}^*a_1 f_{D_{s1}}m_{D_{s1}}F_1^{BD_0^*}(m_{D_{s1}}^2)(2\varepsilon^*_{D_{s1}}\cdot p_B),\\
A(\overline{B}\to D_{s0}^*D_1) &= -i\frac{G_{\rm F}}{\sqrt{2}}V_{cb}V_{cs}^*a_1 f_{D_{s0}^*}m_{D_1}V_0^{BD_1}(m_{D_{s0}^*}^2)(2\varepsilon^*_{D_1}\cdot p_B),\\
A(\overline{B}\to D_s^*D^*) &= i\frac{G_{\rm F}}{\sqrt{2}}V_{cb}V_{cs}^*a_1 f_{D_{s1}}m_{D_{s1}}(m_B-m_{D_1})\varepsilon^{*\mu}_{D_{s1}}\varepsilon^{*\nu}_{D_1}\Big[V_1^{BD_1}(m_{D_{s1}}^2)g_{\mu\nu}\\
&\quad -\frac{2V_2^{BD_1}(m_{D_{s1}}^2)}{(m_B-m_{D^*})^2}p_{B\mu}p_{B\nu}-i\frac{2A^{BD_1}(m_{D_{s1}}^2)}{(m_B-m_{D^*})^2}\epsilon_{\mu\nu\alpha\beta}p_B^\alpha p_{D_1}^\beta\Big]. \qquad (7.36)
\end{aligned}$$

with decay constants and form factors given in [63]. Note that the $-i$ and i factors appearing in (7.35) originate from the phases differences of $D^*_{(s)0}$ and $D_{(s)}$ in the superfields S and H, respectively. From these equations, it is now evident that the contributions from $\overline{B}\to D_{s1}D_0^*\to\phi\overline{K}^*$ and $\overline{B}\to D_{s0}^*D_1\to\phi\overline{K}^*$ rescatterings add up instead of cancellation as noticed before. To estimate the numerical significance of these contributions, we shall use $\beta_1=1(\simeq\beta)$, $\overline{\lambda}_1=1\,\mathrm{GeV}^{-1}(\simeq\lambda)$ and $\Lambda_{D_{s0}^*,D_{s1}}=m_{D_{s0}^*,D_{s1}}+\eta\Lambda_{\rm QCD}$ with $\eta=1.5$ and the monopole form for the form factors $F(t,m_{D_s^*})$ and $F(t,m_{D_{s1}})$. Numerical results are shown in Table XI. The branching ratio is $\mathcal{B}^{SD+LD}(B\to\phi K^*)=8.4\times10^{-6}$. It is interesting to notice that most of the FSI contributions from the intermediate $D_s^{**}D^{**}$ states add up in $A_\perp$ giving $f_\perp\simeq0.2$, which is close to data. Note that we only consider the contribution from $D_{s1/2}D_{1/2}$ intermediate states. A more detailed study including other multiplets such as $D_{3/2}$ along this line is worth pursuing.

F. Comparison with other works

Although the analysis of the ϕK^* polarization anomaly by Colangelo, De Fazio and Pham (CDP) [78] is very similar to ours, their results are quite different form ours in some respects (see also [85] for a different analysis based on the Regge theory). First, in our case, the interference between short-distance and long-distance contributions is mild because the absorptive long-distance contribution is essentially "orthogonal" to the short-distance one (see Table IX). By fixing $\Lambda=2.3$ GeV, to be compared with our choice of $\Lambda_{D_s,D_s^*}=m_{D_s,D_s^*}+\eta\Lambda_{\rm QCD}$ with $\eta=0.8$, CDP introduced a parameter r so that $A=A_{SD}+rA_{LD}$ with $r=0$ corresponding to the absence of rescattering. It appears from Fig. 3 of [78] that there is a drastic SD and LD interference behavior in the CDP calculation, namely, the resulting branching ratio is not symmetric with respect to the reflection of r: $r\to-r$. It is not clear to us why the absorptive LD contribution obtained by CDP is not orthogonal to the SD one at all. Second, instead of employing a small r factor of order 0.08 to reduce the FSI contribution, we use the form factors with different momentum dependence for the exchanged particles D_s and D_s^*. As a result, $f_L\approx1/2$ can be accommodated in our work with a reasonable cutoff. Third, we have shown large cancellations occurring in the processes $\overline{B}\to D_s^*D\to\phi\overline{K}^*$ and $\overline{B}\to D_sD^*\to\phi\overline{K}^*$ and this can be understood as a consequence of CP and SU(3) [CPS] symmetry. We are not able to check the aforementioned cancellation in the CDP work as no details are offered to the individual LD amplitudes. Anyway, $f_\perp$ is very small (of order 3%) in our case, while CDP obtained $f_\perp\approx0.15$. Fourth, CDP adapt a different phase convention for pseudoscalar mesons. Considerable efforts have been made in keeping the consistency of phase conventions and reminders on phase subtleties (see, for example, footnote 2 on p.11) are given in this work. On the other hand, as far as the analytic expressions are concerned we do not find any inconsistency in the phase convention chosen in the CDP work. Fifth, we apply the $U(3)$ symmetry for the ϕ meson, while CDP seem to consider only the ω_8 component of it. Since in both approaches ϕ always couples to a $D_s^{(*)} D_s^{(*)}$ pair (see Fig. 9 in this work and Fig. 2 in [78]), only the $s\bar{s}$ component of ϕ is relevant. Hence, the FSI amplitudes in CDP should be identical to ours up to an overall factor of the Clebsch-Gordan coefficient, $-2/\sqrt{6}$. We do not expect any qualitative difference arising from the different treatments of the ϕ wave function. In particular, the cancellation argument presented in Sec. VII.C should be also applicable to their case.

Working in the context of QCD factorization, Kagan [26] has recently argued that the lower value of the longitudinal polarization fraction can be accommodated in the Standard Model provided that the penguin-induced annihilation contributions are taken into account. In general, the annihilation amplitudes induced by the $(V-A)(V-A)$ operators are subject to helicity suppression. Indeed, they are formally power suppressed by order $(\Lambda_{\rm QCD}/m_b)^2$ [17]. However, the $(S-P)(S+P)$ penguin operator induced annihilation is no longer subject to helicity suppression and could be substantially enhanced. In QCD factorization, the penguin-induced annihilation amplitude contains some infrared divergent integral, say X_A, arising from the logarithmic endpoint divergence, and the logarithmic divergence squared X_A^2. Modelling the logarithmic divergence by [17]

$$X_A = (1 + \rho_A e^{i\phi_A}) \ln \frac{m_B}{\Lambda_h}, \tag{7.37}$$

with Λ_h being a hadron scale of order 500 MeV and $\rho_A \leq 1$, Kagan has shown that the ϕK^* polarization measurements can be accommodated by fitting to the annihilation parameter ρ_A (see Fig. 4 of [26]). Note that the penguin-induced annihilation terms being formally of order $1/m_b^2$ do respect the scaling law stated in Eq. (7.1), but they can be $\mathcal{O}(1)$ numerically.

Assuming Kagan's reasoning [27] is correct, it means that although QCD factorization does not predict a lower value of the ϕK^* longitudinal polarization, one may be able to find a value for ρ_A within an acceptable range to be able to accommodate the data.

It is worth mentioning also that the annihilation amplitudes in VV modes are calculable in the so-called perturbative QCD approach for hadronic B decays where the end-point divergence is regulated by the parton's transverse momentum. In particular, the $\overline{B} \to \phi \bar{K}^*$ decay is studied in [86], giving $f_L : f_\parallel : f_\perp = 0.75 : 0.13 : 0.11$ and $\mathcal{B}(B^- \to \phi K^{*-}) = 16.0 \times 10^{-6}$. Although f_L is reduced after the inclusion of nonfactorizable and annihilation contributions, $f_{\parallel,\perp}$ are only of order 10%. The annihilation contribution indeed helps but it is not sufficient.

A common feature of the final-state rescattering or a large penguin-induced annihilation contribution as a mechanism for explaining the observed ϕK^* anomaly is that the same mechanism will also lead to a large transverse polarization in the ρK^* modes, which is borne out by experiment in the decay $B^- \to \rho^- \overline{K}^{*0}$ but not in $B^- \to \rho^0 K^{*-}$ (see Table VII). This has to be clarified experimentally.

An alternative suggestion for the solution of the ϕK^* anomaly was advocated in [87] that a energetic transverse gluon from the $b \to sg$ chromodipole operator keeps most of its quantum numbers except color when it somehow penetrates through the B meson surface and descends to a transversely polarized ϕ meson. Sizable transverse components of the $\overline{B} \to \phi \bar{K}^*$ decay can be accommodated by having $f_{\parallel} > f_{\perp}$ (see also Table VIII). Since the gluon is a flavor singlet, this mechanism can distinguish ϕ from ρ, hence it affects $\overline{B} \to \phi \overline{K}^*, \omega \overline{K}^*$ but not $\overline{B} \to \overline{K}^* \rho$. The $\overline{B} \to \omega \overline{K}^*$ is predicted to be of order 4×10^{-6} with large transverse components. On the other hand, a recent estimation based on PQCD [88] seems to indicate the above-mentioned contribution is too small to explain the $\phi \overline{K}^*$ anomaly. Moreover, the predicted absence of the transverse polarization in $B \to \rho K^*$ is not consistent with experiment at least for $\rho^- \overline{K}^{*0}$ and $\rho^+ K^{*-}$ modes.

VIII. DISCUSSION AND CONCLUSION

In this work we have studied the effects of final-state interactions on the hadronic B decay rates and their impact on direct CP violation. Such effects are modelled as soft final-state rescattering of some leading intermediate two-body channels and can be classified according to the topological quark diagrams. It amounts to considering the one-particle-exchange processes at the hadron level for long-distance rescattering effects. Our main results are as follows:

1. The color-suppressed neutral modes such as $B^0 \to D^0 \pi^0, \pi^0 \pi^0, \rho^0 \pi^0, K^0 \pi^0$ can be substantially enhanced by long-distance rescattering effects, whereas the color-allowed modes are not significantly affected by FSIs.

2. All measured color-suppressed charmful decays of $\overline{B}^0$ into $D^{(*)0} \pi^0, D^0 \eta, D^0 \omega$ and $D^0 \rho^0$ are significantly larger than theoretical expectations based on naive factorization. The rescattering from $B \to \{D\pi, D^* \rho\} \to D\pi$ contributes to the color-suppressed W-emission and W-exchange topologies and accounts for the observed enhancement of the $D^0 \pi^0$ mode without arbitrarily assigning the ratio of a_2/a_1 a large magnitude and strong phase as done in many previous works.

3. The branching ratios of all penguin-dominated $B \to \pi K$ decays are enhanced via final-state rescattering effects by (30-40)%. CP asymmetry in the $K^- \pi^+$ mode is predicted by the short-distance approach to be $\sim 4\%$. It is modified by final-state rescattering to the level of 14% with a sign flip, in good agreement with the world average of -0.11 ± 0.02. Given the establishment of direct CP violation in $\overline{B}^0 \to K^- \pi^+$, a model-independent relation assuming SU(3) implies that the $\pi^+ \pi^-$ mode has direct CP asymmetry of order 40% with a positive sign. An isospin sum-rule relation involving the branching ratios and CP asymmetries of the four $B \to K\pi$ modes indicates the presence of electroweak contributions and/or some New Physics. Better measurements are needed to put this on a firmer footing.

4. If only the absorptive part of final-state rescattering is considered, it cannot explain the observed enhancement of the $\pi^0 \pi^0$ rate, whereas the predicted $\pi^+ \pi^-$ will be too large by a factor of 2 compared to experiment. The dispersive part of rescattering from $D\bar{D} \to \pi\pi$ and $\pi\pi \to \pi\pi$ via meson annihilation (i.e. the so-called vertical W-loop diagram $\mathcal{V}$) which interferes destructively with the short-distance amplitude of $B^0 \to \pi^+ \pi^-$ can reduce $\pi^+ \pi^-$ and enhance $\pi^0 \pi^0$ substantially.

5. For tree-dominated $B \to \pi\pi$ decays, it is known that the predicted direct CP asymmetry in the $\pi^+\pi^-$ mode by the short-distance approach is small with a negative sign. We have shown that its sign is flipped by final-state rescattering and its magnitude is substantially enhanced. Direct CP violation in $B \to \pi^0\pi^0$ is predicted to have a sign opposite to that of $\pi^+\pi^-$, in contrast to the predictions based on perturbative QCD (PQCD). Hence, even a sign measurement of direct CP asymmetry in $\pi^0\pi^0$ can be used to discriminate between the FSI and PQCD approaches for CP violation.

6. CP partial rate asymmetry in $B^\pm \to \pi^\pm\pi^0$ is very small in the SM and remains so even after the inclusion of FSIs, with a magnitude less than 1 percent. Since CP asymmetry is caused by the electroweak penguin but not the QCD penguin (up to isospin violation), this is a good mode for searching New Physics.

7. For tree-dominated $B \to \rho\pi$ decays, we showed that (i) the color-suppressed $\rho^0\pi^0$ mode is slightly enhanced by rescattering effects to the order of 1.3×10^{-6}, which is consistent with the weighted average of the experimental values. However, the discrepancy between BaBar and Belle for this mode should be clarified soon. It should be stressed that direct CP violation in this mode is significantly enhanced by FSI from around 1% to 60%. (ii) Direct CP violation in the $\rho^+\pi^-$ mode is greatly enhanced by FSI from the naive expectation of ~ -0.01 from the short-distance approach to the level of -0.42, in agreement with BaBar and Belle.

8. As for the intriguing $B \to \phi K^*$ polarization anomaly, the longitudinal polarization fraction can be significantly reduced by the rescattering contribution from the intermediate DD_s states. However, no sizable perpendicular polarization is found owing mainly to the large cancellations among various contributions from intermediate D_sD^* and D_s^*D states. Consequently, our result for the perpendicular polarization fraction is different from a recent similar analysis in [78]. Final-state rescattering effects from this particular set of states seem not be able to fully account for the polarization anomaly observed in $B \to \phi K^*$ and FSI from other intermediate states and/or some other mechanism e.g. the penguin-induced annihilation [27], may have to be invoked. Given the fact that both Belle and BaBar observe large phases in various polarization amplitudes (see Table VII), FSI may still provide a plausible explanation. In any case, our conclusion is that the small value of the longitudinal polarization in VV modes cannot be regarded as a clean signal for New Physics.

Needless to say, the calculation of final-state rescattering effects in hadronic B decays is rather complicated and very much involved and hence it suffers from several possible theoretical uncertainties. Though most of them have been discussed before, it is useful to make a summary here:

(i) The strong form factor $F(t)$ for the off-shell effects of the exchanged particle. It is parameterized as in Eq. (3.22) by introducing a cutoff scale Λ. Moreover, we write $\Lambda = m_{\rm exc} + \eta\Lambda_{\rm QCD}$ [cf. Eq. (3.40)], where the parameter η is expected to be of order unity and can be determined from the measured rates. For a given exchanged particle, the cutoff varies from process to process. For example, $\eta_D = 2.1,\ 0.69,\ 1.6$ for $B \to D\pi, K\pi, \rho\pi$ decays, respectively. To see the sensitivity on the cutoff, we have allowed 15% error in the QCD scale $\Lambda_{\rm QCD}$. Another important uncertainty arises from the momentum dependence of the form factor $F(t)$. Normally it is assumed to be of the monopole form. However, the analysis of the ϕK^* decays prefers to a dipole behavior for the form factor $F(t, m_{D_s^*})$ appearing in the $V_{\rm exc}VP$ or $V_{\rm exc}VV$ vertex with the exchanged vector particle $V_{\rm exc}$ and a monopole dependence for other form factors. A more rigorous study of the momentum dependence of the strong form factor is needed. It turns out that CP asymmetries and the decay rates especially for the color-suppressed modes are in general sensitive to the cutoff scale. This constitutes the major theoretical uncertainties for long-distance rescattering effects.

(ii) Form factors and decay constants. Model predictions for the form factors can vary as much as 30% which in turn imply large uncertainties in the branching ratios. In particular, the $B \to VV$ decays are fairly sensitive to the *difference* between the form factors A_1 and A_2. For form factor transitions in this work we rely on the covariant light-front model which is favored by the current data.

(iii) Strong couplings of heavy mesons and their SU(3) breaking. We have applied chiral and heavy quark symmetries to relate various strong couplings of heavy mesons with the light pseudoscalar or vector mesons. It is not clear how important are the chiral and $1/m_Q$ corrections. For SU(3) breaking effects, we have assumed that they are taken into account in the relations given in Eqs. (4.12) and (7.9).

(iv) The real part of the long-distance contribution which can be obtained from the dispersion relation (3.39). Unlike the absorptive part, the dispersive contribution suffers from the large uncertainties due to some possible subtractions and the complication from integrations. For this reason, we have ignored it so far. However, in order to resolve the discrepancy between theory and experiment for $B^0 \to \pi^+\pi^-$ and $B^0 \to \pi^0\pi^0$, we have argued that it is the dispersive part of long-distance rescattering of $D\bar{D} \to \pi\pi$ and $\pi\pi \to \pi\pi$ via meson annihilation that accounts for the suppression of the $\pi^+\pi^-$ mode and the enhancement of $\pi^0\pi^0$.

(v) CKM matrix elements and γ. Direct CP asymmetry is proportional to $\sin\gamma$. All numbers in the present work are generated by using $\gamma = 60^\circ$.

(vi) Intermediate multi-body contributions which have not been considered thus far and may have cancellations with the contributions from two-body channels.

Finally, it is worth remarking that the final-state rescattering effects from intermediate charmed mesons as elaborated in the present work has some similarity to the long-distance "charming penguin" effects advocated in the literature [32, 33, 34]. The relevance of this long-distance effect has been conjectured to be justified in the so-called soft collinear effective theory [89]. Indeed, we have pointed out that some of the charmed meson loop diagrams in the decays e.g. $B \to \pi\pi, \pi K, \phi K^*$ will manifest as the long-distance $c\bar{c}$ penguins. However, we have also considered FSIs free of charming penguins. For example, long-distance rescattering effects in $B \to D\pi$ and in $B^- \to \pi^-\pi^0$ (also $\rho^-\rho^0$) decays have nothing to do with the charming penguin effects. In other words, our systematic approach for FSIs goes beyond the long-distance charming penguin mechanism.

Acknowledgments

We are grateful to Andrei V. Gritsan for helpful discussions on B to VV data. This research was supported in part by the National Science Council of R.O.C. under Grant Nos. NSC93-2112-M-001-043, NSC93-2112-M-001-053 and by the U.S. DOE contract No. DE-AC02-98CH10886(BNL).

APPENDIX A: USEFUL FORMULA

Under the integration, the covariant integrals

$$\int \frac{d^3\vec{p}_1}{(2\pi)^3 2E_1}\,\frac{d^3\vec{p}_2}{(2\pi)^3 2E_2}\,(2\pi)^4\delta^4(p_B-p_1-p_2)f(t)\times\{p_{1\mu},\,p_{1\mu}p_{1\nu},\,p_{1\mu}p_{1\nu}p_{1\alpha}\} \tag{A1}$$

can only be expressed by external momenta p_3, p_4 with suitable Lorentz and permutation structures. Hence we can express these $p_{1\mu}$, $p_{1\mu}p_{1\nu}$, $p_{1\mu}p_{1\nu}p_{1\alpha}$ in terms for $P = p_3 + p_4$ and $q = p_3 - p_4$ as in Eq. (7.12) within the integration. By contracting the left-hand side of Eq. (7.12) with P_μ, q_μ and $g_{\mu\nu}$, we are able to solve for these $A_j^{(i)}$ and obtain

$$\begin{pmatrix} A_1^{(1)} \\ A_2^{(1)} \end{pmatrix} = \begin{pmatrix} P^2 & P\cdot q \\ P\cdot q & q^2 \end{pmatrix}^{-1}\cdot\begin{pmatrix} P\cdot p_1 \\ q\cdot p_1 \end{pmatrix},$$

$$\begin{pmatrix} A_1^{(2)} \\ A_2^{(2)} \\ A_3^{(2)} \\ A_4^{(2)} \end{pmatrix} = \begin{pmatrix} 4 & P^2 & 2P\cdot q & q^2 \\ P^2 & (P^2)^2 & 2P^2 P\cdot q & (P\cdot q)^2 \\ 2P\cdot q & 2P^2 P\cdot q & 2P^2q^2+(P\cdot q)^2 & 2P\cdot q q^2 \\ q^2 & (P\cdot q)^2 & 2P\cdot q q^2 & q^2 \end{pmatrix}^{-1}\cdot\begin{pmatrix} p_1^2 \\ (P\cdot p_1)^2 \\ 2P\cdot p_1 p_1\cdot q \\ (q\cdot p_1)^2 \end{pmatrix},$$

$$\begin{pmatrix} A_1^{(3)} \\ A_2^{(3)} \\ A_3^{(3)} \\ A_4^{(3)} \\ A_5^{(3)} \\ A_6^{(3)} \end{pmatrix} = \begin{pmatrix} 18P^2 & 18P\cdot q & 3(P^2)^2 & 9P^2P\cdot q & 3q^2P^2+6(P\cdot q)^2 & 3q^2P\cdot q \\ & 18q^2 & 3P^2P\cdot q & 3P^2q^2+6(P\cdot q)^2 & 9q^2P\cdot q & 3(q^2)^2 \\ & & (P^2)^3 & 3(P^2)^2P\cdot q & 3(P\cdot q)^2P^2 & (P\cdot q)^3 \\ & & & 3(P^2)^2q^2+6P^2(P\cdot q)^2 & 3(P\cdot q)^3+6P^2q^2P\cdot q & 3(P\cdot q)^2q^2 \\ & & & & 3(q^2)^2P^2+6q^2(P\cdot q)^2 & 3(q^2)^2P\cdot q \\ & & & & & (q^2)^3 \end{pmatrix}^{-1}$$

$$\cdot\begin{pmatrix} 3m_1^2 P\cdot p_1 \\ 3m_1^2 q\cdot p_1 \\ (P\cdot p_1)^3 \\ 3(P\cdot p_1)^2 p_1\cdot q \\ 3(q\cdot p_1)^2 p_1\cdot P \\ (q\cdot p_1)^3 \end{pmatrix}, \tag{A2}$$

where the lower left part of the symmetric inverse matrix for the $A_j^{(3)}$ case is not shown explicitly. Note that the t dependence of $A_j^{(i)}$ is in the column matrices in the right-hand side of the above equations and t always appears in the numerators of $A_j^{(i)}$ in a polynomial form.

APPENDIX B: THEORETICAL INPUT PARAMETERS

In this Appendix we summarize the input parameters used in the present paper. For decay constants we use

$$f_\pi = 132\,\text{MeV},\quad f_K = 160\,\text{MeV},\quad f_D = 200\,\text{MeV},\quad f_{D^*} = 230\,\text{MeV},\quad f_{a_1} = -205\,\text{MeV}. \tag{B1}$$

Note that a preliminary CLEO measurement of the semileptonic decay $D^+ \to \mu^+\nu$ yields $f_{D^+} = (202 \pm 41 \pm 17)$ MeV [90]. For form factors we follow the covariant light-front approach [63]. For purpose of comparison, we list some of the form factors at $q^2 = 0$ used in the main text:

$$F_0^{B\pi}(0) = 0.25, \quad F_0^{BK}(0) = 0.35, \quad A_0^{B\rho}(0) = 0.28, \quad A_0^{BK^*}(0) = 0.31 \tag{B2}$$

to be compared with

$$F_0^{B\pi}(0) = 0.28 \pm 0.05, \quad F_0^{BK}(0) = 0.34 \pm 0.05, \quad A_0^{B\rho}(0) = 0.37 \pm 0.06, \quad A_0^{BK^*}(0) = 0.45 \pm 0.07 \tag{B3}$$

employed in [18] and

$$F_0^{B\pi}(0) = 0.33, \quad F_0^{BK}(0) = 0.38, \quad A_0^{B\rho}(0) = 0.28, \quad A_0^{BK^*}(0) = 0.32 \tag{B4}$$

used by Bauer, Stech and Wirbel [91]. The most recent light-cone sum rule analysis yields [92]

$$F_0^{B\pi}(0) = 0.258 \pm 0.031, \qquad F_0^{BK}(0) = 0.331 + 0.041 + 0.025\delta_{a_1} \tag{B5}$$

with δ_{a_1} being defined in [92]. The $B^- \to \pi^-\pi^0$ data favors a smaller $F^{B\pi}(0)$ of order 0.25, while $B \to \rho\pi$ measurement prefers to small form factors for $B \to \rho$ transition.

For the quark mixing matrix elements, we use $A = 0.801$ and $\lambda = 0.2265$ [71] in the Wolfenstein parametrization of the quark mixing angles [93]. The other two Wolfenstein parameters ρ and η obey the relations $\bar{\eta} = R\sin\gamma$ and $\bar{\rho} = R\cos\gamma$, where $R = |V_{ud}V_{ub}^*/(V_{cd}V_{cb}^*)|$, $\bar{\rho} = (1-\lambda^2/2)\rho$ and $\bar{\eta} = (1-\lambda^2/2)\eta$. We take $\gamma = 60^\circ$ and $R = 0.39$ in this work for calculations. For current quark masses, we use $m_b(m_b) = 4.4$ GeV, $m_c(m_b) = 1.3$ GeV, $m_s(2.1\,\mathrm{GeV}) = 90$ MeV and $m_q/m_s = 0.044$.

The physical strong coupling constants are

$$\begin{aligned} g_{\rho\pi\pi} &= 6.05 \pm 0.02, \qquad g_{K^*K\pi} = 4.6, \qquad g_{D^*D\pi} = 17.9 \pm 0.3 \pm 1.9, \\ g_V &= 5.8, \qquad \beta = 0.9, \qquad \lambda = 0.56\,\mathrm{GeV}^{-1}, \end{aligned} \tag{B6}$$

where g_V, β and λ (not to be confused with the parameter λ appearing in the parametrization of quark mixing angles) are the parameters in the effective chiral Lagrangian describing the interactions of heavy mesons with low momentum light vector mesons.

---

[1] Belle Collaboration, K. Abe *et al.,* Phys. Rev. Lett. **88**, 031802 (2002).

[2] BaBar Collaboration, B. Aubert *et al.,* hep-ex/0207066.

[3] B. Melić, hep-ph/0404003.

[4] Z.G. Wang, L. Li, and T. Huang, hep-ph/0311296.

[5] P. Colangelo, F. De Fazio, and T. N. Pham, Phys. Lett. B **542**, 71 (2002); Phys. Rev. D **69**, 054023.

[6] Belle Collaboration, K. Abe *et al.,* hep-ex/0409004.

[7] CLEO Collaboration, T.E. Coan *et al.,* Phys. Rev. Lett. **88**, 062001 (2002).

[8] BaBar Collaboration, B. Aubert *et al.,* Phys. Rev. D **69**, 032004 (2004).

[9] H.Y. Cheng, Phys. Rev. D **65**, 094012 (2002).

[10] C.W. Chiang, M. Gronau, J.L. Rosner, and D. Suprun, Phys. Rev. D **70**, 034020 (2004).

[11] BaBar Collaboration, B. Aubert *et al.,* Phys. Rev. Lett. **91**, 241801 (2003).

[12] Belle Collaboration, S.H. Lee *et al.,* Phys. Rev. Lett. **91**, 261801 (2003).

[13] C.D. Lü and M.Z. Yang, Eur. Phys. J. C **23** 275 (2002).

[14] BaBar Collaboration, B. Aubert *et al.,* hep-ex/0407057.

[15] Belle Collaboration, Y. Chao *et al.,* hep-ex/0407025.

[16] Belle Collaboration, Y. Chao *et al.,* hep-ex/0408100.

[17] M. Beneke, G. Buchalla, M. Neubert, and C.T. Sachrajda, Phys. Rev. Lett. **83**, 1914 (1999); Nucl. Phys. B **591**, 313 (2000); *ibid.* **B606**, 245 (2001).

[18] M. Beneke and M. Neubert, Nucl. Phys. B **675**, 333 (2003).

[19] Belle Collaboration, K. Abe *et al.,* Phys. Rev. Lett. **93**, 021601 (2004).

[20] BaBar Collaboration, B. Aubert *et al.,* hep-ex/0408089.

[21] Belle Collaboration, Y. Sakai , plenery talk at 32nd International Conference on High Energy Physics, August, 2004, Beijing, China; BaBar Collaboration, M. Giorgi , plenery talk at 32nd International Conference on High Energy Physics, August, 2004, Beijing, China.

[22] Belle Collaboration, P. Krokovny *et al.*, Phys. Rev. Lett. **89**, 231804 (2002).

[23] BaBar Collaboration, B. Aubert *et al.,* Phys. Rev. Lett. **90**, 181803 (2003).

[24] BaBar Collaboration, B. Aubert *et al.,* Phys. Rev. Lett. **91**, 171802 (2003); hep-ex/0303020.

[25] Belle Collaboration, K.F. Chen *et al.,* Phys. Rev. Lett. **91**, 201801 (2003).

[26] A.L. Kagan, Phys. Lett. B **601**, 151 (2004).

[27] A.L. Kagan, hep-ph/0407076.

[28] D. Atwood and A. Soni, Phys. Rev. D **58**, 036005 (1998).

[29] M. Bander, D. Silverman, and A. Soni, Phys. Rev. Lett. **43**, 242 (1979).

[30] Y. Lu, B.S. Zou, and M.P. Locher, Z. Phys. A **345**, 207 (1993); M.P. Locher, Y. Lu, and B.S. Zou, *ibid* **347**, 281 (1994); X.Q. Li and B.S. Zou, Phys. Lett. B **399**, 297 (1997); Y.S. Dai, D.S. Du, X.Q. Li, Z.T. Wei, and B.S. Zou, Phys. Rev. D **60**, 014014 (1999).

[31] M. Ablikim, D.S. Du, and M.Z. Yang, Phys. Lett. B **536**, 34 (2002); J.W. Li, M.Z. Yang, and D.S. Du, hep-ph/0206154.

[32] M. Ciuchini *et al.,* Nucl. Phys. B **501**, 271 (1997); *ibid.* **512**, 3 (1998); hep-ph/0407073.

[33] P. Colangelo, G. Nardulli, N. Paver, and Riazuddin, Z. Phys. C **45**, 575 (1990); G. Isola, M. Ladisa, G. Nardulli, T.N. Pham, and P. Santorelli, Phys. Rev. D **64**, 014029 (2001); *ibid.* **65**, 094005 (2002).

[34] G. Isola, M. Ladisa, G. Nardulli, and P. Santorelli, Phys. Rev. D **68**, 114001 (2003).

[35] S. Barshay, L.M. Sehgal, and J. van Leusen, Phys. Lett. B **591**, 97 (2004).

[36] S. Barshay, G. Kreyerhoff, and L.M. Sehgal, Phys. Lett. B **595**, 318 (2004).

[37] J.F. Donoghue, E. Golowich, A.A. Petrov, and J.M. Soares, Phys. Rev. Lett. **77**, 2178 (1996); H. Lipkin, Phys. Lett. B **415**, 186 (1997); D. Delépine, J.M. Gérard, J. Pestieau, and J. Weyers, Phys. Lett. B **429**, 106 (1998); A.F. Falk, A.L. Kagan, Y. Nir, and A.A. Petrov, Phys. Rev. D **57**, 4290 (1998); M. Suzuki and L. Wolfenstein, *ibid.* **60**, 074019 (1999); A.N. Kamal, *ibid.* **60**, 094018 (1999); D.S. Du, X.Q. Li, Z.T. Wei, and B.S. Zou, Eur. Phys. J. A **4**, 91 (1999); N.G. Deshpande, X.G. He, W.S. Hou, and S. Pavasa, Phys. Rev. Lett. **82**, 2240 (1999); W.S. Hou and K.C. Yang, *ibid.* **84**, 4806 (2000).

[38] C.K. Chua, W.S. Hou, and K.C. Yang, Mod. Phys. Lett. A **18**, 1763 (2003).

[39] M. Beneke, G. Buchalla, M. Neubert, and C.T. Sachrajda, Nucl. Phys. B **606**, 245 (2001).

[40] C. Smith, Eur. Phys. J. C **33**, 523 (2004).

[41] G. t' Hooft, Nucl. Phys. B **72**, 461 (1974); A.J. Buras, J.-M. Gérard, amd R. Ruckl, *ibid.* **268**, 16 (1986).

[42] L.L. Chau and H.Y. Cheng, Phys. Rev. D **36**, 137 (1987); Phys. Lett. B **222**, 285 (1989).

[43] L.L. Chau, Phys. Rep. **95**, 1 (1983).

[44] L.L. Chau and H.Y. Cheng, Phys. Rev. Lett. **56**, 1655 (1986).

[45] J.F. Donoghue, Phys. Rev. D **33**, 1516 (1986).

[46] El hassan El aaoud and A.N. Kamal, Int. J. Mod. Phys. A **15**, 4163 (2000).

[47] P. Żenczykowski, Acta Phys. Polon. B **28**, 1605 (1997) [hep-ph/9601265].

[48] S. Weinberg, *The Quantum Theory of Fields, Volume I* (Cambridge, 1995), Sec. 3.8.

[49] H.Y. Cheng, Eur. Phys. J. C **26**, 551 (2003).

[50] Particle Data Group, S. Eidelman *et al.,* Phys. Lett. B **592**, 1 (2004).

[51] C.W. Chiang and J.L. Rosner, Phys. Rev. D **67**, 074013 (2003).

[52] J.L. Rosner, Phys. Rev. D **60**, 114026 (1999).

[53] H.Y. Cheng and K.C. Yang, Phys. Rev. D **59**, 092004 (1999).

[54] Z.Z. Xing, hep-ph/0107257.

[55] M. Neubert and A.A. Petrov, Phys. Lett. B **519**, 50 (2001).

[56] J.P. Lee, hep-ph/0109101.

[57] C.K. Chua, W.S. Hou, and K.C. Yang, Phys. Rev. D **65**, 096007 (2002).

[58] Y.Y. Keum, T. Kurimoto, H.n. Li, C.D. Lü, and A.I. Sanda, Phys. Rev. D **69**, 094018 (2004).

[59] S. Mantry, D. Pirjol, and I.W. Stewart, Phys. Rev. D **68**, 114009 (2003).

[60] R. Casalbuoni, A. Deandrea, N. Di Bartolomeo, R. Gatto, F. Feruglio, and G. Nardulli, Phys. Rep. **281**, 145 (1997).

[61] T. M. Yan, H. Y. Cheng, C. Y. Cheung, G. L. Lin, Y. C. Lin, and H. L. Yu, Phys. Rev. D **46**, 1148 (1992); **55**, 5851(E) (1997); M. B. Wise, Phys. Rev. D **45**, R2188 (1992); G. Burdman

and J. Donoghue, Phys. Lett. B **280**, 287 (1992).

[62] O. Gortchakov, M.P. Locher, V.E. Markushin, and S. von Rotz, Z. Phys. A **353**, 447 (1996).

[63] H. Y. Cheng, C. K. Chua, and C. W. Hwang, Phys. Rev. D **69**, 074025 (2004).

[64] CLEO Collaboration, S. Ahmed *et al.,* Phys. Rev. Lett. **87**, 251801 (2001).

[65] Heavy Flavor Averaging Group, http://www.slac.stanford.edu/xorg/hfag.

[66] A. Ali and C. Greub, Phys. Rev. D **57**, 2996 (1998); A. Ali, G. Kramer, and C.D. Lü, *ibid.* **58**, 094009 (1998).

[67] Y.H. Chen, H.Y. Cheng, B. Tseng, and K.C. Yang, Phys. Rev. D **60**, 094014 (1999).

[68] Z. Ligeti, hep-ph/0408267.

[69] Y.Y. Keum, H.n. Li, and A.I. Sanda, Phys. Rev. D **63**, 054008 (2001); Y.Y. Keum, talk presented at WHEPP-8 Workshop, Mumbai, India, January 2004.

[70] A.J. Buras, R. Fleischer, S. Recksiegel, and F. Schwab, Nucl. Phys. B **697**, 133 (2004).

[71] CKMfitter Group, J. Charles *et al.,* hep-ph/0406184.

[72] M. Pivk and F.R. Le Diberder, hep-ph/0406263.

[73] N.G. Deshpande and X.G. He, Phys. Rev. Lett. **75**, 1703 (1995).

[74] BaBar Collaboration, B. Aubert *et al.,* Phys. Rev. D **69**, 031102 (2004); hep-ex/0408017; hep-ex/0408063; hep-ex/0408093; hep-ex/0411054; A. Gritsan, hep-ex/0409059.

[75] Belle Collaboration, J. Zhang *et al., ibid.* **91**, 221801 (2003); K. Abe *et al.,* hep-ex/0408141.

[76] A.S. Dighe, M. Gronau, and J.L. Rosner, Phys. Rev. Lett. **79**, 4333 (1997).

[77] H.Y. Cheng and K.C. Yang, Phys. Lett. B **511**, 40 (2001).

[78] P. Colangelo, F. De Fazio and T. N. Pham, Phys. Lett. B **597**, 291 (2004).

[79] P. Ball and V.M. Braun, Phys. Rev. D **58**, 094016 (1998); P. Ball, J. High Energy Phys. **09**, 005 (1998).

[80] P. Ball, hep-ph/0306251.

[81] BaBar Collaboration, B. Aubert *et al.,* hep-ex/0408017.

[82] C.W. Bernard, T. Draper, A. Soni, H.D. Politzer, and M.B. Wise, Phys. Rev. D **32**, 2343 (1985); C.W. Bernard, T. Draper, G. Hockney, and A. Soni, Nucl. Phys. Proc. Suppl. **4**, 483 (1988); C. Dawson, G. Martinelli, G.C. Rossi, C.T. Sachrajda, S.R. Sharpe, M. Talevi, and M. Testa, Nucl. Phys. B **514**, 313 (1998).

[83] See also X.G. He, X.Q. Li, and J.P. Ma, hep-ph/0407083.

[84] A. Seiden, H. F. W. Sadrozinski, and H. E. Haber, Phys. Rev. D **38**, 824 (1988); L. Kopke and N. Wermes, Phys. Rep. **174**, 67 (1989).

[85] M. Ladisa, V. Laporta, G. Nardulli, and P. Santorelli, hep-ph/0409286.

[86] C.H. Chen, Y.Y. Keum, and H-n. Li, Phys. Rev. D **66**, 054013 (2002).

[87] W.S. Hou and M. Nagashima, hep-ph/0408007.

[88] H-n. Li, hep-ph/0408232.

[89] C.W. Bauer, D. Pirjol, I.Z. Rothstein, and I.W. Stewart, hep-ph/0401188.

[90] CLEO Collaboration, G. Bonvicini *et al.,* hep-ex/0411050; D. Besson *et al.,* hep-ex/0408071.

[91] M. Wirbel, B. Stech, and M. Bauer, Z. Phys. C **29**, 637 (1985); M. Bauer, B. Stech, and M. Wirbel, *ibid.* **34**, 103 (1987).

[92] P. Ball and R. Zwicky, hep-ph/0406232.

[93] L. Wolfenstein, Phys. Rev. Lett. **51**, 1945 (1983).